

In presenting this thesis in partial fulfillment of the requirements for an advanced degree at Idaho State University, I agree that the Library shall make it freely available for inspection. I further state that permission for extensive copying of my thesis for scholarly purposes may be granted by the Dean of the Graduate School, Dean of my academic division, or by the University Librarian. It is understood that any copying or publication of this thesis for financial gain shall not be allowed without my written permission.

Signature _____

Date _____

A balanced cross section and kinematic model for the Early Cretaceous fold-thrust belt
of central Idaho

by

Edwin C. Porter

A thesis

submitted in partial fulfillment

of the requirements for the degree of

Master of Science in the Department of Geosciences

Idaho State University

Fall 2021

To the Graduate Faculty:

The members of the committee appointed to examine the thesis of Edwin C. Porter find it satisfactory and recommend that it be accepted.

David M. Pearson
Major Advisor

Ryan B. Anderson
Committee Member

Zachary Gershberg
Graduate Faculty Representative

DEDICATION

I dedicate this thesis to my mother and father. They have always supported my decisions without judgement, have helped me celebrate the highs, and have helped carry me through the lows. Without their encouragement and emotional support, I wouldn't be where I am today.

ACKNOWLEDGEMENTS

I would like to extend my deepest gratitude to my advisor, Dr. David Pearson. Dave, you are among the most brilliant people I've ever had the pleasure of interacting with, and your propensity for developing novel solutions to complex geological problems is a thing of wonder. I have great admiration for your kind heart and immense patience (especially at those times when I was undeserving of it), and I'm so grateful for how much you have enriched my life by guiding me these past few years.

I'd also like to thank my committee member, Dr. Ryan Anderson. Ryan, I greatly enjoyed working alongside you and learning about central Idaho together. I appreciate your flexibility and enthusiasm for engaging with my research. I'd also like to thank Dr. Kendra Murray for her willingness to guide me through the early stages of my project, as well as Dr. Zac Gershberg for serving as my GFR.

Third, I'd like to thank Dr. Joel Hudley and Dr. Kevin Stewart, two professors at the University of North Carolina at Chapel Hill, for cultivating an appreciation for field geology in me. I also thank Joel for pushing me to pursue a graduate education at those times when my self-doubt may have otherwise prevented me from doing so.

Finally, I'd like to thank my friends at ISU for their support through the years. I thank Stuart Parker for his mentoring and keying me into the subtle intricacies of some of the background literature, as well as for being someone I could vent to about software frustrations. I thank Emma Gregory for her contribution as my technical support for ArcGIS on a moment's notice, which saved me more than once. I thank Logan Mahoney, Jenn Souza, and Emma Collins for the warmth and camaraderie that we shared. Having other "indoor" geologists to connect with was a real blessing at times!

Funding for this research was provided by the National Science Foundation (NSF) award EAR-1728563. I thank Petroleum Experts for donating their MOVE software to the Idaho State University Geosciences department, Richard Allmendinger for his free-use stereonet software (Stereonet 10), and Kurt Sundell and the Arizona LaserChron Center for analyzing my zircon samples.

TABLE OF CONTENTS

LIST OF FIGURES.....	vii
Abstract.....	viii
CHAPTER 1: INTRODUCTION.....	1
CHAPTER 2: GEOLOGIC BACKGROUND	8
Crystalline basement rock beneath central Idahos.....	8
Neoproterozoic rift-related and passive margin strata	10
Neoproterozoic to late Paleozoic strata.....	11
Mississippian to Permian strata of the Lost River Range and White Knob Mountains ..	19
Mesozoic crustal shortening.....	29
Critical Taper theory	31
Idaho batholith emplacement	35
Eocene volcanism and extension, and Miocene Basin and Range extension.....	36
CHAPTER 3: METHODS	38
STRUCTURAL ANALYSIS	39
U-Pb ZIRCON DATING.....	39
Background.....	39
Sample preparation and LA-ICP-MS.....	40
Zircon sample data analysis.....	45
ARCGIS MAP COMPILATION	45
2D MOVE CROSS-SECTION CONSTRUCTION AND BALANCING	45
CHAPTER 4: RESULTS.....	48

RECONNAISSANCE MAPPING OF TYPE SECTION OF THE WHITE KNOB LIMESTONE, CARBONATE BANK SUCCESSION, AND COPPER BASIN GROUP IN CENTRAL IDAHO.....	48
GEOLOGIC MAP OF BROKEN WAGON CANYON, ID	50
STRUCTURAL ANALYSIS WITHIN BROKEN WAGON CANYON, ID	52
Extensional Structures	53
Stereonet Analysis at Broken Wagon area.....	53
STEREONET ANALYSIS (WHOLE SECTION).....	63
CHAPTER 5: DISCUSSION.....	65
REVISED STRATIGRAPHY AND STRUCTURE OF BROKEN WAGON CANYON, ID	65
Revised stratigraphic relationship between Mississippian White Knob Limestone and Mississippian carbonate bank of the Lost River Range, ID	65
Structure of Broken Wagon Canyon, ID	69
Shortening direction in Broken Wagon Canyon.....	70
STRUCTURE AND STRATIGRAPHY ALONG THE MAJOR CROSS-SECTION TRANSECT	70
Additional support for revised stratigraphic relationships across the Pioneer fault.....	70
Contractional structures	71
Shortening direction in east-central Idaho.....	76
Age constraints on shortening.....	76
Current results in the context of other workers' ongoing studies in the Idaho-Montana fold-thrust belt regarding the transition in structural style	78
Extensional structures	80
CHAPTER 6: CONCLUSIONS.....	81
WORKS CITED.....	83

LIST OF FIGURES

Figure 1 “Thin-skinned” vs. “thick-skinned” structural style	2
Figure 2 Flat slab subduction model	3
Figure 3 Flat slab subduction extent	5
Figure 4 Map of basement blocks	10
Figure 5 Index map of Idaho mountain ranges.....	13
Figure 6 Correlation of map units	28
Figure 7 Critical taper model	35
Figure 8 20CP14 laser ablation spots	43
Figure 9 20CP16 laser ablation spots	44
Figure 10 Revised interpretation of Mwl and Ms contact.....	52
Figure 11 Broken Wagon Canyon stereonet	54
Figure 12 Weighted mean age plot for 20CP14	55
Figure 13 Weighted mean age plot for 20CP16	56
Figure 14 Kinematic model.....	62
Figure 15 Whole section stereonet.....	64
Figure 16 20CP14 Laser ablation targeting data.....	95
Figure 17 20CP16 Laser ablation targeting data.....	96

A balanced cross section and kinematic model for the Early Cretaceous fold-thrust belt
of central Idaho

Thesis Abstract--Idaho State University (2021)

Mesozoic contractional structures within central Idaho haven't been previously described and synthesized at a regional scale. This warranted the new analysis and geologic modeling, which constrains the kinematics, magnitude of shortening, structural style, and timing of significant shortening-related structures within central Idaho. Balanced and sequentially-restorable-cross-sectional modeling suggest that major thrust faults along the transect were rooted within décollements that exploited mechanically weak sedimentary rocks. This shortening, which was accommodated by thrust faults and folds with a WSW-ENE shortening direction, only involved Neoproterozoic and younger strata. Additionally, deformation within the region was finished by the end of Early Cretaceous time given that two plutons—dated to 95.7 ± 2.7 and 91.4 ± 2.4 Ma—cross-cut contractional structures. Integrated with recent work in southwestern Montana, results from central Idaho suggest that the northeastward transition to a thick-skinned structural style occurred as a consequence of the pre-shortening stratigraphic architecture of the overlying plate.

Key Words: fold-thrust belt, structural style, thin-skinned, thick-skinned, geologic modeling, central Idaho.

CHAPTER 1: INTRODUCTION

The Sevier fold-thrust belt of western North America accommodated horizontal shortening from Late Jurassic to early Cenozoic time (Armstrong and Oriel, 1965; Armstrong, 1968) during east-dipping subduction off the western coast of North America (Hamilton, 1969; Dickinson, 1970; Burchfiel and Davis, 1972). The Sevier fold-thrust belt forms a portion of the North American Cordillera orogenic belt, which occurs from Central America through Canada for more than 6,000 km. Shortening within the Sevier belt was accommodated primarily by bedding-parallel thrusts (“thin-skinned” structural style) that deformed pre-orogenic sedimentary rocks (Figure 1). Many of these strata were deposited during Neoproterozoic to Cambrian rifting and development of a passive margin (Stewart, 1972). The Laramide fold-thrust belt occurs east of the Sevier fold-thrust belt, and generally accommodated shortening during the later stages of activity of and after deformation within the Sevier belt (Armstrong, 1968; DeCelles, 2004). During Laramide tectonism, horizontal shortening was accommodated through thrusting with relatively deep detachments within basement rock (“thick-skinned” structural style) (Erslev, 1993). This style of thrusting generally does not accommodate as much horizontal shortening as the “thin-skinned” style (Figure 1). Today, it is thought that structural style in continental fold-thrust belts exists as a continuum, with each fold-thrust belt being more characteristically akin to the “thin-skinned” or “thick-skinned” end-members (McClelland and Oldow, 2004; Pfiffner, 2017; Parker and Pearson, 2021). In North America, the spatial transition from the Sevier to Laramide belts coincides with an eastward thinning of pre-orogenic sedimentary strata toward the interior of the North American continent.

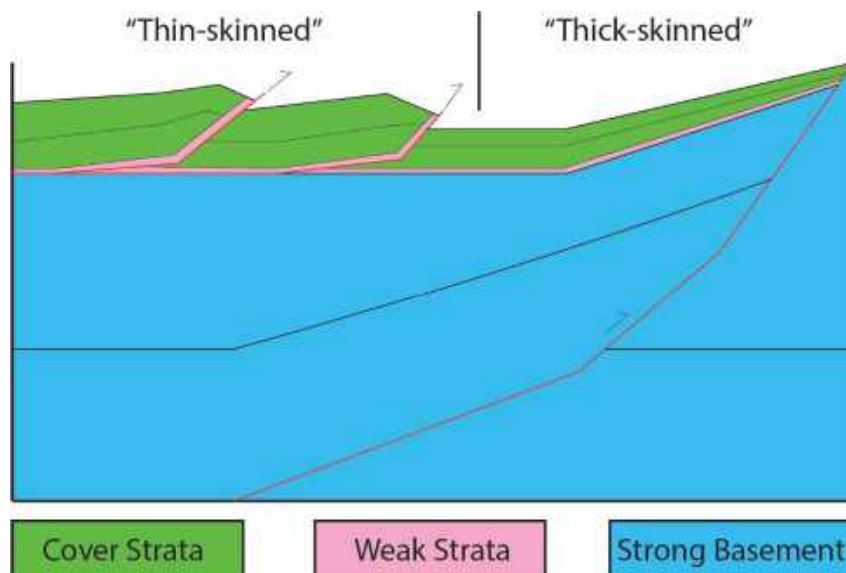


Figure 1 - Schematic diagram illustrating the difference between “thin-skinned” and “thick-skinned” thrusting. In the “thin-skinned” style, faults exploit mechanically weak strata to propagate through, allowing them to accommodate significantly more shortening.

At ca. 85 Ma, approximately 10 Ma prior to Laramide belt deformation toward the continental interior, magmatism within the southern Sierra Nevada magmatic arc ceased, followed by a continent-ward shift in the location of the magmatic belt (Coney and Reynolds, 1977; Ducea and Saleeby, 1998). Prior workers generally agree that this episode in Late Cretaceous through early Cenozoic time—what many workers consider the Laramide “orogeny” (Armstrong, 1974)—signals the beginning of the time that the subducting Farallon plate began to dip more shallowly than it had previously during the Sevier orogeny (Dickinson and Snyder, 1978). This interpretation was based upon the apparent inboard migration of the magmatic arc, the spatial and temporal transition from “thin-skinned” to “thick-skinned” thrusting, as well as underthrusting of trench sediments beneath the southwestern USA (Saleeby, 2003). Prior workers have proposed that when the subducting slab’s dip angle shallowed to sub-horizontal, the subducted plate may have scraped on the underside of the upper plate’s lithosphere, resulting in basal traction and formation of the Laramide fold-thrust belt (Bird, 1984) (Figure 2). This

paradigm model has been refined in recent decades. Today, most researchers generally agree that a region of shallowly dipping slab was geographically focused beneath southern California and was the result of the subduction of a buoyant oceanic plateau (Dickinson and Snyder, 1978; Livaccari et al., 1981; Saleeby, 2003; Liu and Currie, 2016; Yonkee and Weil, 2015; Copeland et al., 2017).

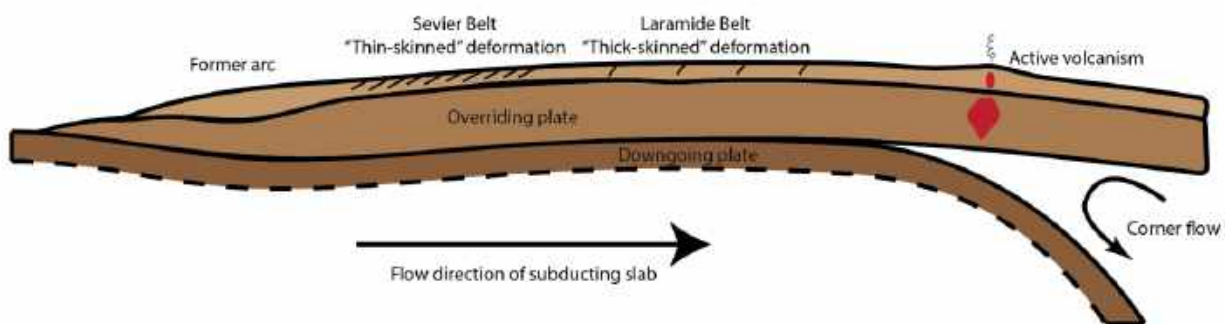


Figure 2 – Schematic diagram of a shallowing slab. In the shallowing slab model for controls on structural style, the shallowing dip angle of the subducting plate results in the two plates scraping together. This basal traction on the upper plate alters the stress field and initiates “Laramide style” deformation. Modified from Bird, 1984.

Though southwestern Montana was the locus of basement-involved, thick-skinned thrusting during Cretaceous and early Cenozoic time and thus is part of the broadly defined “Laramide province,” recent work has revealed inconsistencies in applying the model to the entire region of thick-skinned deformation within the Laramide belt (Kulik and Schmidt, 1988). For example, both thin-skinned and thick-skinned thrusts developed concurrently in the same region of southwestern Montana (McDowell, 1997; Parker and Pearson, 2021). This is problematic because the model predicts that thin-skinned deformation should have preceded thick-skinned shortening prior to slab shallowing. Another problem with the model that thick-skinned structures initiated as a result of slab shallowing is that recent work has found that the thick-skinned structures in this area began to develop long before the roughly 80 Ma proposed transition to flat-

slab subduction (Nichols et al., 1985; DeCelles, 1986; Garber et al., 2020). Therefore, this basement involvement had to have begun before flat slab subduction, which is inconsistent with the model.

Additionally, recent models of flat-slab subduction suggest that the region of shallow subduction was localized in a narrow corridor from southern California to eastern Wyoming (Saleeby, 2003; Yonkee and Weil, 2015; Copeland et al., 2017; Axen et al., 2018), and therefore was not present beneath east-central Idaho and southwestern Montana (Figure 3). This result further challenges the model. Finally, continued magmatism within the Idaho batholith (in contrast to the shut-off of magmatism within Sierra Nevada) during thick-skinned thrusting in the region (approximately 80-70 Ma) is in contrast to magmatism in the Sierra Nevada batholith, which ended after approximately 80 Ma (Dumitru et al., 1991; Gaschnig et al., 2010). The paradigm model predicts that there should be no active magmatism during shallow-slab subduction, and has been attributed to causing the cessation of magmatism in the Sierra Nevada batholith. Therefore, it is inconsistent that magmatism could continue within the Idaho batholith while subduction in the area would have been shallowly dipping in the model.

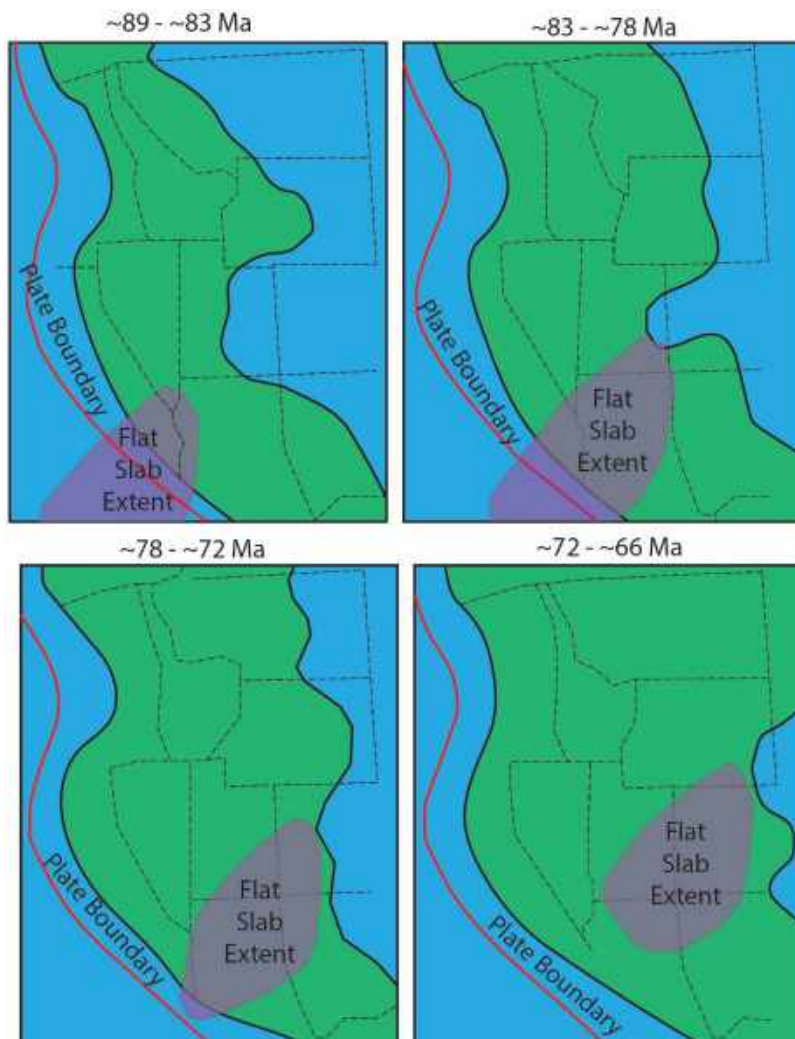


Figure 3 - Geographical extent of flat slab subduction underneath western North America throughout Cretaceous time ("subducted plateau" is purple, land is green, and water is blue). Palinspastically restored approximate modern state lines are drawn onto the figure to give a reference point for the extent of flat slab subduction. Notice that the flat slab was hypothesized to never have reached underneath central Idaho. Modified from Yonkee and Weil, 2015.

Some researchers have proposed an alternative model for what drove the transition in structural style in consideration of these observations. The alternative model suggests that structural style exists as a continuum, and the transition in style is instead primarily influenced by the uneven distribution of pre-orogenic strata and prior deformation within the upper plate (Allmendinger et al., 1983; Pearson et al., 2013; Lacombe and Bellahsen, 2016; Parker and Pearson, 2021). It is well documented that the geometry of the pre-orogenic strata varies significantly within east-central Idaho and

southeastern Idaho, specifically in the context of rift and passive margin successions (Link et al., 2017a; Brennan et al., 2020a). For example, the relatively thick package of weak (easily deformed) Neoproterozoic and Cambrian rocks prevalent throughout southern Idaho are completely absent in east-central Idaho near the Lemhi arch, which is located in the central and northern Lemhi Range and Beaverhead Mountains. The Lemhi arch is defined as the region in which Ordovician Kinnikinic Quartzite unconformably overlies Mesoproterozoic strata of the Belt Supergroup (Scholten, 1957; Link et al., 2017a).

To investigate this alternative model to explain the transition in structural style, other collaborators have focused their efforts on constraining the temporal evolution of thrust timing using foreland basin strata as a proxy (Garber et al., 2020; Finzel and Rosenblume, 2021; Rosenblume et al., 2021; Gardner, 2021); mapping and structural analysis of the fold-thrust belt in east-central Idaho and southwestern Montana, where shortening styles similar to the “thick-skinned” end member are mapped (Parker, 2021; Parker and Pearson, 2021); and evaluating thrust timing using low-temperature thermochronology (Kaempfer et al., 2021). However, an important constraint on evaluating possible causes for the transition in structural style is to document the pre-thrusting stratigraphic framework and the structural style west of the Lemhi arch. Therefore, this study intends to complement the prior work by Montoya (2019) and Parker (2021) by focusing on this region west of the Lemhi arch, spanning from the central Smoky Mountains through the Lost River Range (Plate 2). Specifically, I intend to: improve the constraints on décollement depths and positions within the region; characterize the structural style of contractional structures in central Idaho; contribute U-

Pb zircon age dates for igneous rocks that cut structures that accommodated shortening in the region to ascertain minimum end-of-shortening ages; and propose a balanced and sequentially restorable cross-sectional model for the subsurface geology of the region. In working to accomplish these goals, we also developed new interpretations for some stratigraphic relationships and structural geometries in the region.

CHAPTER 2: GEOLOGIC BACKGROUND

A primary hypothesis of this study is that the pre-thrusting rock type and cumulative geologic history of the rocks involved in thrusting determines the style of contractional deformation. As such, the field area for this project encompasses multiple stratigraphic domains along the major transect in central and east-central Idaho (Plate 2). Relevant information has been summarized in generally chronological order.

Crystalline basement rock beneath central Idaho

The depth and character of crystalline basement rocks along the transect is important to test the primary hypothesis because basement rocks are mechanically strong at temperatures below ~350°C; when these basement rocks are deformed during thrusting, their mechanical behavior exerts a prominent influence on the deformation styles of continental fold-thrust belts (Lacombe and Bellahsen, 2016). Crystalline basement rocks in the region are only intermittently exposed within the Pioneer and Albion-Raft River-Grouse Creek metamorphic core complexes (Strickland et al., 2011; Lewis et al., 2012; Link et al., 2017b), but have been inferred in the subsurface using isotopic data from younger igneous rocks (Gaschnig et al., 2013). In general, these basement rocks consist of metamorphic and plutonic rocks that formed in Archean or Paleo- to Mesoproterozoic time (Gaschnig et al., 2013; Link et al., 2017b). These rocks likely constitute part of the Grouse Creek block, which is a crystalline basement domain that likely represents a former piece of the Wyoming craton (Foster et al., 2006; Mueller et al., 2011; Gaschnig et al., 2013) (Figure 4). Structurally interlayered with Paleoproterozoic Archean basement rocks exposed within the Pioneer metamorphic core complex, Link et al. (2017b) also identified likely Mesoproterozoic metasedimentary Belt Supergroup rocks (Link et al., 2007). Taken as a whole, Link et

al. (2017b) interpreted these results to suggest that metamorphosed Belt Supergroup overlies the Grouse Creek Block in central Idaho. Northeast of the inferred boundary of the Grouse Creek Block, in east-central Idaho, prior workers noted a lack of evidence for Paleoproterozoic or Archean basement rocks in the subsurface (Foster et al., 2006; Gaschnig et al., 2013; Vervoort et al., 2016). Though originally called the Selway terrane by Foster et al. (2006), this basement domain coincides spatially with the >15 km thick Belt Supergroup and—because of the likely large-magnitude of vertical thinning expected for such a deep basin—likely does not preserve significant Archean or Paleoproterozoic crystalline basement rocks in the subsurface (Doughty and Chamberlain, 1996; Gaschnig et al., 2013; Link et al., 2017a).

Thus, basement rocks underlying the field area are assumed to be Archean/Paleoproterozoic Grouse Creek Block with some overlying, possibly metamorphosed Mesoproterozoic Belt Supergroup. To the northeast of the study area in east-central Idaho, the Grouse Creek Block was likely substantially thinned and thus probably consists of Mesoproterozoic basement rocks (Doughty and Chamberlain, 1996; Link et al., 2017a), with a thick section of Belt Supergroup overlying it. Because these rocks are partially metamorphosed and crystalline in character, they exhibit a relatively strong mechanical stratigraphy. This strength gives them a resistance to supporting laterally extensive décollements during shortening, and as such they are thought to be unlikely to host detachments.

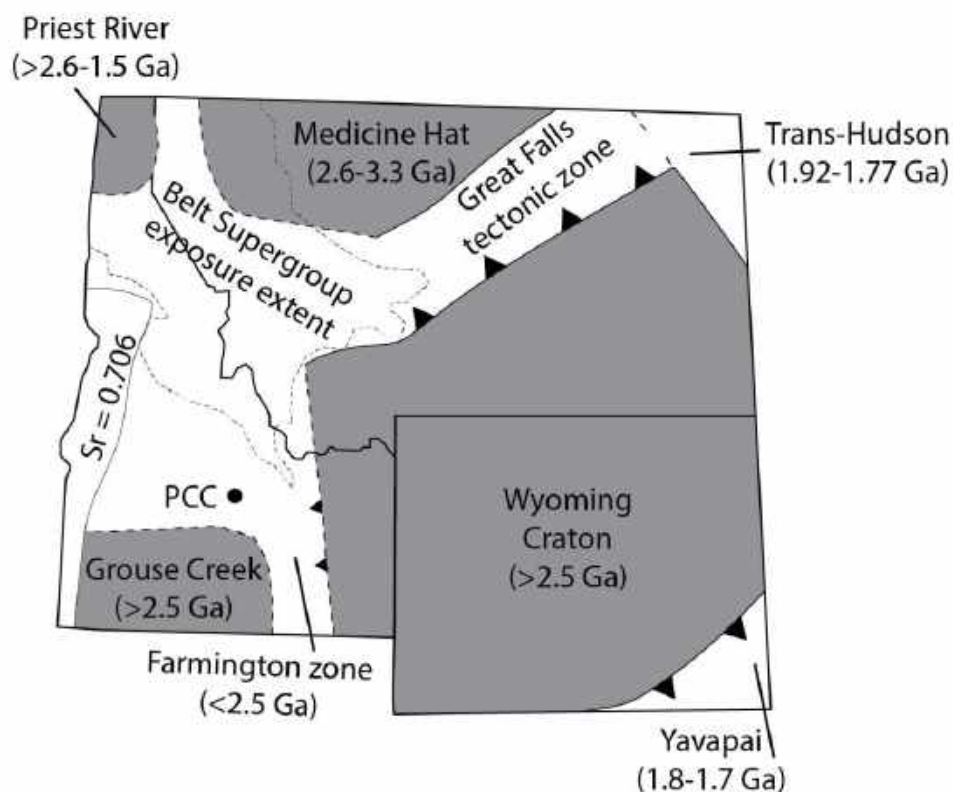


Figure 4 – Basement blocks that underlie Idaho and the approximate ages of the rocks that compose the blocks. The central black dot is the location of the Pioneer metamorphic core complex. Modified from Gashnig et al., 2013, and Vervoort et al., 2016.

To the west of these basement blocks in western Idaho, eastern Washington, and Oregon, basement rocks are flanked by terranes that were accreted primarily during Mesozoic and early Cenozoic Cordilleran subduction (Coney et al., 1980); the boundary between these terranes and the basement blocks is roughly coincident with the $^{87}\text{Sr}/^{86}\text{Sr}$ 0.706 line. West of here, the basement was rifted away during the Neoproterozoic to middle Cambrian breakup of Rodinia (Yonkee et al., 2014).

Neoproterozoic rift-related and passive margin strata

The thickness and mechanical character of sedimentary rocks that overlie crystalline basement rocks are important influences on the style of contractional structures that utilized the rift and passive margin succession (Kley et al., 1999). Thus, a

brief description of these pre-thrusting strata is necessary. In western North America, these rocks were largely deposited during rifting and passive margin formation following the breakup of Rodinia between 750 Ma and 520 Ma (Li et al., 2008; Yonkee et al., 2014). These rift events would lay the foundation for the development of a long-lived passive margin on the western margin (in modern coordinates) of Laurentia. In Yonkee et al.'s (2014) model, the early phases of rifting formed large intra-cratonic basins with variable orientations. Early rift-related Neoproterozoic strata mapped in the northern Rocky Mountains, such as the Cryogenian Uinta Mountain Group, were deposited in these basins during early stages of rifting, followed by deposition of the Cryogenian to Ediacaran Pocatello Formation and correlatives of southeastern Idaho and northern Utah as the basins grew larger (Yonkee et al., 2014). Following rifting, the margin became passive, and the remains of the old rift basin would form a continental slope and rise (Yonkee et al., 2014).

Along the transect, there are several map domains that contain major facies changes within Neoproterozoic and Paleozoic strata: (1) the Boulder Mountains and Smoky Mountains within the southwestern part of the study area; (2) the Pioneer Mountains within the central part of the study area; and (3) the Lost River Range and White Knob Mountains within the northeastern portion of the current study area. The below descriptions describe the regional, pre-thrusting stratigraphy in an older-to-younger manner and generally proceed from northeast to southwest, away from the Lemhi arch. See Figure 5 below for a reference map.

Neoproterozoic to late Paleozoic strata

Southeastern Idaho contains a relatively thick stratigraphic section of

Neoproterozoic and Cambrian rock that is interpreted to have formed in a rift margin to passive margin succession associated with the break-up of Rodinia and Pannotia (Yonkee et al., 2014). Generally fine-grained Neoproterozoic and Cambrian strata that constitute this succession in southeastern Idaho, western Wyoming, and Utah formed the primary basal décollement horizons for the Wyoming salient of the Sevier fold-thrust belt (Royse et al., 1975; Coogan and Royse, 1990; Yonkee and Weil, 2015). However, these rocks are not present atop the Lemhi arch in east-central Idaho, where Middle Ordovician Kinnikinic Quartzite lies unconformably on Mesoproterozoic quartzite (Sloss, 1950; Scholten, 1957). The absence of Neoproterozoic and Cambrian strata on the Lemhi arch may be the result of the presence of a paleotopographic high during the time of deposition (concurrent with Rodinian rifting) (Link et al., 2017a; Pearson and Link, 2017; Brennan et al., 2020a). Previous workers believed that the early Paleozoic section of southeastern Idaho was also not present in central Idaho (Umpleby, 1917; Ross, 1934). However, more recent work has identified some correlative Neoproterozoic to Middle Ordovician rocks in central Idaho, about 50 km west of the Lemhi arch (McCandless, 1982; Ruppel, 1986; Skipp and Link, 1992; Brennan et al., 2020b; Milton, 2020). Because these strata contain substantial fine-grained intervals, they may have formed important zones of mechanical weakness during Mesozoic thrusting in central Idaho.

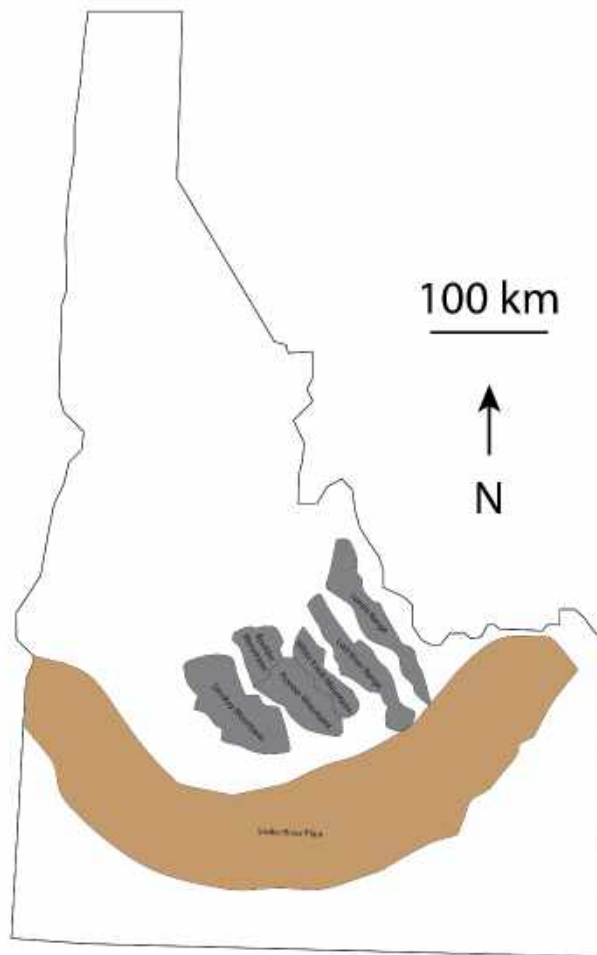


Figure 5 - Reference map of names of Idaho mountain ranges.

Northeast of the current study area, within the Lemhi Range and Beaverhead Mountains of east-central Idaho, Middle Ordovician Kinnikinic Quartzite overlies Belt strata and defines the Lemhi arch unconformity. However, west of the Lemhi arch, within the Lost River Range, Milton (2020) measured, defined the provenance of, and proposed a regional correlation for a section of Neoproterozoic to Cambrian rock that is approximately 1400 m thick and crops out within the Borah Peak horst, roughly 30 km south of the major transect for this investigation. This exposed sub-Kinnikinic stratigraphic succession here consists of three formations: the Neoproterozoic to

Cambrian Wilbert Formation (which is divided further into four members), the overlying Cambrian Tyler Peak Formation and the overlying Cambrian to Ordovician Summerhouse Formation. Within the Lost River Range and southern Lemhi Range (Fig. 5), Milton (2020) defined four units of the Wilbert Formation from bottom to top: a lower, shallow marine quartzose sandstone, an overlying shallow marine siltstone within intervals of phyllite, a fluvial sandstone, and an upper quartz arenite. Intervals of phyllite within the lower Wilbert Formation may have formed a relatively mechanically weak interval. Above the Wilbert Formation, the Tyler Peak Formation comprises quartz arenite and mechanically weaker overlying dolomitic siltstone. This mechanically weaker layer may have served as an important zone of weakness for the propagation of décollements during Mesozoic shortening, given the relatively strong mechanical stratigraphy in the underlying rock.

Southwest of the Lost River Range, Neoproterozoic and Cambrian rocks are sparsely exposed except for in the western Pioneer Mountains (Plate 2). There, the Clayton Mine Quartzite—considered to be Neoproterozoic to Cambrian in age—is exposed to the south of the current transect in the Pioneer metamorphic core complex (Dover, 1980; Brennan et al., 2020a). Northwest of the current study area near Challis, the Clayton Mine Quartzite lies in gradational contact atop the Neoproterozoic Ramshorn Slate (Brennan et al., 2020b); therefore, the Ramshorn Slate is assumed to be present at depth below the Clayton Mine Quartzite. It is unclear if these units or their metamorphosed equivalents continue into the western Pioneer Mountains or Smoky Mountains at depth (see section: *Discussion*). The Clayton Mine Quartzite is age-correlative to the members 1-3 of the Wilbert Formation, whereas the Ramshorn Slate is

older than the oldest exposed unit of Milton's (2020) section (Brennan et al., in review).

In the Lost River Range, stratigraphically atop the Tyler Peak Formation is the Cambrian to Ordovician Summerhouse Formation, which consists of a crystalline dolostone in the lower part and a quartz arenite in the upper part. The lack of fine-grained material within the unit makes it relatively strong when compared to the rest of this section. The Ella Dolomite/marble, which is a presumed Cambrian to Ordovician correlative of the Summerhouse Formation, is exposed in the western Pioneer Mountains, south of the central portion of the current study area. There, it consists of forsterite-bearing marble, calc-silicate, and quartzite (Vogl et al., 2021) and is presumed to have stratigraphically overlain the Clayton Mine Quartzite prior to faulting.

Given the limited exposure of Neoproterozoic and Cambrian rocks along the transect, equivalents of Milton's (2020) section are tentatively assumed to exist at depth southwest of the Lost River Range, which would have been a more outboard segment of the Rodinian rift margin with a presumed thick stratigraphic succession.

Though the thickness of this presumed section is poorly constrained, a more complete Neoproterozoic and Cambrian section was recently studied 25 km to the north of the current transect near Bayhorse, Idaho (Brennan et al., 2020a, 2020b). These strata were correlated by Milton (2020) and Brennan et al. (in review) to a section that is older than the Ordovician to Cambrian Summerhouse Formation and Cambrian Tyler Peak Formation within the Lost River Range. The Wilbert Formation is tentatively correlative with the uppermost Clayton Mine Quartzite at Bayhorse. Strata interpreted to underlie Milton's (2020) section that have been documented at Bayhorse are >2.4 km thick and include—from top/younger to bottom/older—a deeper, unexposed part of the

Cambrian to Neoproterozoic Clayton Mine Quartzite, an unnamed Neoproterozoic siltite, the Neoproterozoic Ramshorn Slate, the Neoproterozoic Bayhorse Dolomite, the Neoproterozoic Garden Creek Phyllite, the basal dolomite of Bayhorse Creek, and the tuff of Daugherty Gulch (Brennan et al., 2020a, 2020b). The Garden Creek Phyllite and Ramshorn Slate are fine-grained, mechanically weak rocks that may have formed important zones of mechanical weakness during Mesozoic shortening. Together with Milton's (2020) strata that total >1.2 km in thickness, this >2.4 km thick Neoproterozoic and Cambrian section results in a cumulative thickness of >3.6 km. Previous workers within the region have placed these units at depth below the northern Lost River Range and the northern Pioneer Mountains, based upon exposures of some of the units (such as the Clayton Mine Quartzite) in the area (Montoya, 2019). Because not much is known about the Cambrian to Neoproterozoic strata underneath my transect, I extended the aforementioned units southward along strike to underlie Milton's (2020) section along the transect. This is a reasonable assumption given that the Clayton Mine Quartzite is exposed to both the north and south of my transect, and that the strata south of the transect are "compositionally similar" to the Bayhorse section northeast of the transect (Brennan et al., 2020a).

Ordovician to Devonian strata

One of the most regionally continuous stratigraphic units in the study area is the Ordovician Kinnikinic Quartzite (Plate 2). This consists of up to 200 m of thick-bedded, medium-grained and silica-cemented quartz arenites interpreted to have been deposited in a shallow marine setting atop the continental shelf in Middle Ordovician time (James and Oaks, 1977).

In contrast to these mechanically strong rocks, southwest of the Lost River Range within the current transect area, the Phi Kappa Formation (Dover, 1983) consists of graptolite-bearing shales that constrain a well-defined age of Lower Ordovician (Arenigian time; 478.6 ± 1.7 Ma) through the Wenlock epoch of the Silurian Period (427.4 ± 0.8 Ma) (Maletz et al., 2005). Therefore, the Phi Kappa Formation is age-correlative to the Ordovician Kinnikinic Quartzite and Ordovician to Silurian Saturday Mountain Formation to the east (Churkin, 1963). Previous workers interpreted these rocks to represent a continental slope succession (James and Oaks, 1977) that was thrust onto the Laurentian platform in Mesozoic time (see section: *Mesozoic crustal shortening*) (Dover, 1980; Maletz et al., 2005). Because of both the fine-grained composition of the rock and the oceanic graptolite fossils, the graptolite succession and therefore all rocks of Ordovician through Devonian age in the area west of the White Knob Mountains are interpreted to have been deposited within deep water off of the continental shelf. This fine-grained material may have made the Phi Kappa Formation an ideal unit for the propagation of laterally extensive detachments during Mesozoic shortening, given the relatively weak mechanical stratigraphy that it exhibits.

Within the northeastern part of the transect within the Lost River Range and White Knob Mountains, the Ordovician to Silurian Saturday Mountain Formation conformably overlies the Kinnikinic Quartzite and consists of a dolostone with siliceous interbeds that becomes more siliceous toward the east, near the Lemhi Range. Its upper contact is defined by an unconformity with overlying dolostones of the Silurian Laketown Dolomite, which is, in turn, overlain unconformably by the Devonian Jefferson Dolomite and conformably overlying Devonian Grand View Dolomite and Devonian

Three Forks Formation. The dolostones are crystalline and medium-bedded, whereas the Three Forks Formation is thinly bedded shaly limestone that likely acted as a prominent detachment horizon farther to the northeast (Parker, 2021). Like to the south, these rocks are interpreted to have been deposited within a relatively shallow marine environment, such as upon an open-circulation continental shelf (Ross, 1947; Mapel et al., 1965).

Farther west, in the Pioneer, Boulder, and Smoky Mountains, age-correlative Ordovician to Devonian strata are considerably different. There, thinly bedded siltstones of the Silurian Trail Creek Formation conformably overlie the Phi Kappa Formation. The Trail Creek Formation is assumed to be Silurian in age because graptolites from the Wenlock epoch of the Silurian are found within 1 m of the bottom of the formation (Carter and Churkin, 1977; Dover, 1983). Like the Phi Kappa Formation below it, the thinly-bedded siltstone of the Silurian Trail Creek Formation has relatively little strength and may have been easily deformed during Mesozoic shortening, hosting décollements for thrust faults. Above the Trail Creek Formation in the Pioneer Mountains, two units are assumed to be Silurian to Devonian in age, because they sit between the Silurian Trail Creek Formation and a Devonian-aged unit above (Dover, 1983). These units are typically fine-grained and occasionally calcareous and are thought to occasionally interfinger with units they are in stratigraphic contact with, or are even equivalent to those units in places. Finally, the overlying Devonian Milligen Formation is a dark colored, fine-grained, siliceous and calcareous siltstone to shale (Dover, 1983). Conodont data suggests that the Milligen Formation is Middle to Upper Devonian in age (Sandberg et al., 1975). However, given the thickness of the unit (>1200m), the age is

most accurate toward the center of the formation and becomes increasingly uncertain toward the boundaries. The top of the Devonian Milligen Formation is in unconformable contact with the overlying Pennsylvanian to Permian Wood River Group (Dover, 1980; Mahoney et al., 1991). In total, early Paleozoic strata in the western Pioneer Mountains are estimated to be approximately 1850 m thick, although a complete section is not preserved intact in the area (Dover, 1980). These fine-grained rocks form prominent detachment-style folds within the study area.

Mississippian to Permian strata of the Lost River Range and White Knob Mountains

At the distal edge of the Copper Basin, the Mississippian McGowan Creek Formation lies unconformably atop the Devonian section of the Lost River Range (Link et al., 1996). The McGowan Creek Formation is >1000 m thick at its type section on the western flank of the northern Lost River Range but thins considerably toward the northeast (Skipp and Janecke, 2004). It consists of fine-grained siltstones, mudstones, micritic limestones, and rare pebble conglomerates (Link et al., 1996). It is commonly mapped as exhibiting a prominent pressure solution cleavage, and workers have suggested that the McGowan Creek Formation hosted a Mesozoic basal décollement above which short wavelength folds formed (Anastasio et al., 1997). Given the fine-grained character of the unit (and therefore relative lack of strength), it is sensible that detachments would exploit the McGowan Creek Formation. The unit is interpreted to represent the distal siliciclastic deposition synchronous with deposition of the Copper Basin Group farther west, and as such thickens to up to 4 km in thickness in the southern White Knob Mountains (Wilson et al., 1994). Above the McGowan Creek

Formation in the White Knob Mountains, the Mississippian White Knob Limestone rests conformably. The White Knob Limestone is characterized by a change in fossil assemblage and the introduction of siliciclastic sediment and chert when compared to the carbonate bank of the Lost River Range. Its type section at Cabin Creek, ID, was measured by Skipp (1961) to be approximately 2250 m thick (it was referred to as the Brazer Limestone at the time, but renamed the White Knob Limestone by Ross, 1962). The White Knob Limestone is divided into 3 informal members: the Lower White Knob Limestone, the Middle White Knob Limestone, and the Upper White Knob Limestone. The Lower White Knob Limestone is composed of lime mudstone and laminated limestone. The unit is abundantly fossiliferous, with ample bryozoans being a defining characteristic. The Middle White Knob Limestone is composed of fossiliferous lime packstones, grainstones, and boundstones. It has chert and quartzite pebble conglomerate interbeds that vary in thickness. The Upper White Knob Limestone is composed of interbedded limestone, sandstone, and conglomerate. It contains the most siliciclastic material of all three members. Like the McGowan Creek Formation below it, the White Knob Limestone is interpreted to have been deposited in the distal part of the Copper Basin, where water conditions were more suitable for the growth of lime-producing organisms than in the Copper Basin (Skipp, 1961; Link et al., 1996).

Northeast of the occurrence of the White Knob Limestone, the Mississippian to Permian carbonate bank of the Lost River Range consists of a thick package of limestones (~2600 m thick) and lies atop the Mississippian McGowan Creek Formation (Skipp et al., 1979a, 1979b). The base of the carbonate bank is the Mississippian Middle Canyon Formation, which is a dark, interbedded limestone and calcareous

siltstone, roughly 400 m thick. Above it sits the Mississippian Scott Peak Formation. The Scott Peak Formation is a massively bedded gray fossiliferous limestone that is approximately 700 m thick. Due to its thickness and resistance to weathering, it commonly crops out as cliffs and ledges within the Lost River Range and the White Knob Mountains. Fossils include brachiopods, crinoids, gastropods, bivalves, bryozoans, and rugose corals. Above the Scott Peak Formation, the Mississippian South Creek Formation presents as a thinly bedded, dark, clayey to silty limestone. Its thickness is approximately 100 m in the field area, and it weathers into slopes, making outcrops of the unit limited. Above the South Creek Formation is the Mississippian Surret Canyon Formation, an abundantly fossiliferous, light gray, cliff-weathering limestone. In the field area, it is approximately 250 m thick. These units of the carbonate bank make up the vast majority of outcrops within the field area, but two ridges north of Christian Gulch in the Lost River Range contain the remaining three units in the carbonate bank. The Mississippian Arco Hills Formation is a 75 m thick gray sandy limestone. Above it is the Mississippian Bluebird Mountain Formation, which is approximately 50 m thick in the field area. The Bluebird Mountain Formation is a silty limestone with interbeds of quartzose sandstone. It has been interpreted to represent a change in the long-stable carbonate bank depositional environment; the introduction of siliciclastic material into the carbonate bank suggests a possible decrease in sea level that would bring the bank and the shore closer together. Finally, the bottom of the Pennsylvanian to Permian Snaky Canyon Formation is exposed. This unit is more than 1000 m thick and laterally expansive; it spans the Lost River Range, the Lemhi Range, and the Beaverhead Mountains. The formation is variable in composition, but within the

field area it is primarily a thickly bedded, sandy, fossiliferous limestone (Ross, 1947; Huh, 1967; Skipp et al., 2009). The carbonate bank continues westward into the eastern White Knob Mountains and Pioneer Mountains, where it is thought to be truncated by the Copper Basin system. Limestones of the carbonate bank are mechanically weak and commonly deformed into short-wavelength detachment-style folds (Skipp et al., 2009).

Mississippian to Permian strata of the Pioneer, Boulder, and Smoky Mountains

Along the central and southwestern parts of the major transect, within the White Knob and Pioneer Mountains, the Mississippian Copper Basin Group is a thick (>4300 m at its thickest point) package of siliclastic rocks within the field area. The occurrence of these rocks within the Paleozoic “passive margin” succession in central Idaho has been used by prior workers to interpret that middle Paleozoic, “Antler” orogenesis affected the study area (e.g., Beranek et al., 2016). The major, margin-perpendicular changes in middle Paleozoic stratigraphy along the major transect has also been used to infer major, terrane-bounding thrust displacements within the study area. Because the potential for large-displacement thrusts along the transect is important for understanding the geometry, style, and magnitude of Mesozoic shortening, here I describe the prior work on these rocks to set the context for later structural interpretations.

The Copper Basin Group was initially described by Umpleby (1917) and mapped by Ross (1934) in the Pioneer Mountains. The rocks were given the Copper Basin formation designation by Ross (1962) and later promoted to group status by Paull et al. (1972). In 1975, Sandberg et al. proposed a corrected biostratigraphic correlation for

Paull et al.'s (1972) work and Nilsen (1977) mapped paleocurrent indicators that trended variably from the northwest to the east-southeast. Dover (1980, 1983) further mapped the Copper Basin Group within the heart of the Pioneer Mountains. Workers hypothesized that the Copper Basin Group was related to the Antler orogeny of Nevada, first described by Roberts et al. (1958). In this model, an eastward directed thrust placed an allochthonous terrane (the Roberts Mountain Allochthon) within central Idaho, creating a highland from which the Copper Basin Group sediment is sourced. However, as workers continued to refine observations about the Copper Basin Group, this solution did not seem consistent with the work done in Idaho. For example, tectonic modeling by Wilson et al. (1994) revealed that the crustal loading model of the Antler orogeny was incapable of producing the accommodation space as quickly as it was required to deposit the Copper Basin Group in Idaho. Finally, Link et al. (1996) reviewed prior work and defined a tight stratigraphic nomenclature to describe the group.

The Copper Basin Group is divided into three formations from bottom to top: the Little Copper Formation, the Drummond Mine Limestone, and the Argosy Creek Formation. The Argosy Creek Formation is further split into four members: the Scorpion Mountain Member, the Muldoon Canyon Member, the Brockie Lake Member, and the Iron Bog Creek Member. These units are variably mapped throughout east-central Idaho, but most of their type sections fall within the southern White Knob Mountains, ~45 km south of the major transect. Along the major transect of this investigation, only the Little Copper Formation, the Drummond Mine Limestone, and the Scorpion Mountain Member of the Argosy Creek Formation are observed. It is unknown if the upper members were originally deposited along the major transect and later eroded, or

if they were never deposited there at all. The Little Copper Formation is 1120 m thick at its type section and sits on the subjacent Devonian section. The formation comprises fine-grained sandstone and siltstone. Workers have interpreted the formation to have been deposited as a fine-grained turbidite lithofacies, transitioning toward channelized turbidite lithofacies toward the top of the formation. The Drummond Mine Limestone gradationally overlies the Little Copper Formation and is approximately 800 m thick at its type section. The rocks are primarily micritic and are interpreted to be calciclastic turbidite deposits. Like the Little Copper Formation, channelized turbidite lithofacies become more common towards the top. Finally, the Scorpion Mountain Member of the Argosy Creek Formation is 1100 m thick at its type section and ranges from conglomerate to the south to fine-grained flysch to the north near the major transect (Link et al., 1996). Paleocurrents within the member are primarily north-directed (Nilsen, 1977). The Little Copper Formation and the Scorpion Mountain formation are both fine-grained and therefore have likely little strength. In particular, the Little Copper Formation is commonly deformed into mesoscopic tight, east-vergent, chevron-style detachment folds (Wilson, 1994). It is possible that the short wavelength folds observed throughout the Copper Basin Group's modern exposure may form above a detachment that exploited these weak layers during Mesozoic shortening.

The accommodation space for the deposition of the Copper Basin Group has been interpreted to be based primarily in tectonics instead of eustasy (Link et al., 1996). This is because the section is particularly thick (>4300 m), far more than any fluctuation in sea level could account for (Link et al., 1996). Wilson et al. (1994) tested this hypothesis through subsidence modeling. These authors concluded that the subsidence

of the crust was too much over too little time to be the result of flexure after crustal loading. The required flexural rigidity of the crust (10^{22} Nm to 10^{23} Nm) is simply too weak to be realistic for the Paleozoic strata in the region. Instead, the authors proposed a sinistral transpressional model for the creation of the basin. In this model, a releasing bend basin is created just north of a restraining bend. Additionally, syndepositional normal faults within the basin formed, creating more accommodation space. The normal faults are hypothesized to have formed after the deposition of the Little Copper Formation due to the formation's observed submarine fan progradation as opposed to the abrupt shifts in facies in the higher units. These normal faults are mapped in the area around Muldoon Canyon, but are hypothesized to exist elsewhere in the Copper Basin Group at depth. This model envisioned a southern highland that shed sediment to the north, in agreement with paleocurrent indicators (Nilsen, 1977; Wilson et al., 1994).

Within the western Pioneer Mountains and the Smoky Mountains, Copper Basin Group strata are missing across an unconformity with underlying Devonian Milligen Formation and are overlain by the Pennsylvanian to Permian Wood River Formation (Mahoney et al., 1991). The Wood River Formation is over 3000 m thick and divided into 8 informal units within 3 members. At the scale of this study, we considered just the formation, and as such the 8 informal units and 3 members will not be described in detail here. The lower Wood River Formation consists primarily of limestone with some siliceous conglomerate focused near the bottom. Toward the middle of the formation, more siliciclastic material is introduced and micritic sandstones and quartz arenites become more common. Toward the top of the formation, the grain size decreases to silt, resulting in micritic siltstone. The unit is hypothesized to have been deposited within the

northwest-southeast trending Wood River Basin west of a paleotopographic Copper Basin high. This high is speculated to have formed after the deposition of the Copper Basin Group as a result of westward thrusting. The siliciclastic sediment found within the Wood River Formation was shed into the basin from this high (Mahoney et al., 1991).

Paleographic relationships between strata along the major transect

Because units within the western Pioneer and Smoky Mountains are of significantly different character than units within the eastern White Knob Mountains and Lost River Range, and are not known to lie in conformable contact with each other, workers have hypothesized transitions in the stratigraphy along the major transect. To explain the modern-day location of these sections, workers have interpreted there to be at least one thrust fault that accommodated significant horizontal displacement (see section: *Mesozoic crustal shortening*) and juxtaposed the two sections. Early workers believed that the western section was “allochthonous” based upon the facies interpretation of two different depositional environments (Carter and Churkin, 1977). Given that the primary conflicting observations are the difference between interpreted depositional environments and the graptolite ecology of the two sections, a change in the margin geometry may be able to explain the transition (see section: *Discussion*). It is critical that a plausible model for the relationship between these two sections is considered when testing the primary hypothesis. In the change in margin geometry model, the most significant “thin-skinned” structure in the region would be detached within the relatively weak rocks of the western section (e.g. Ordovician Phi Kappa

Formation and Silurian Trail Creek Formation), which would support the primary hypothesis of this study.

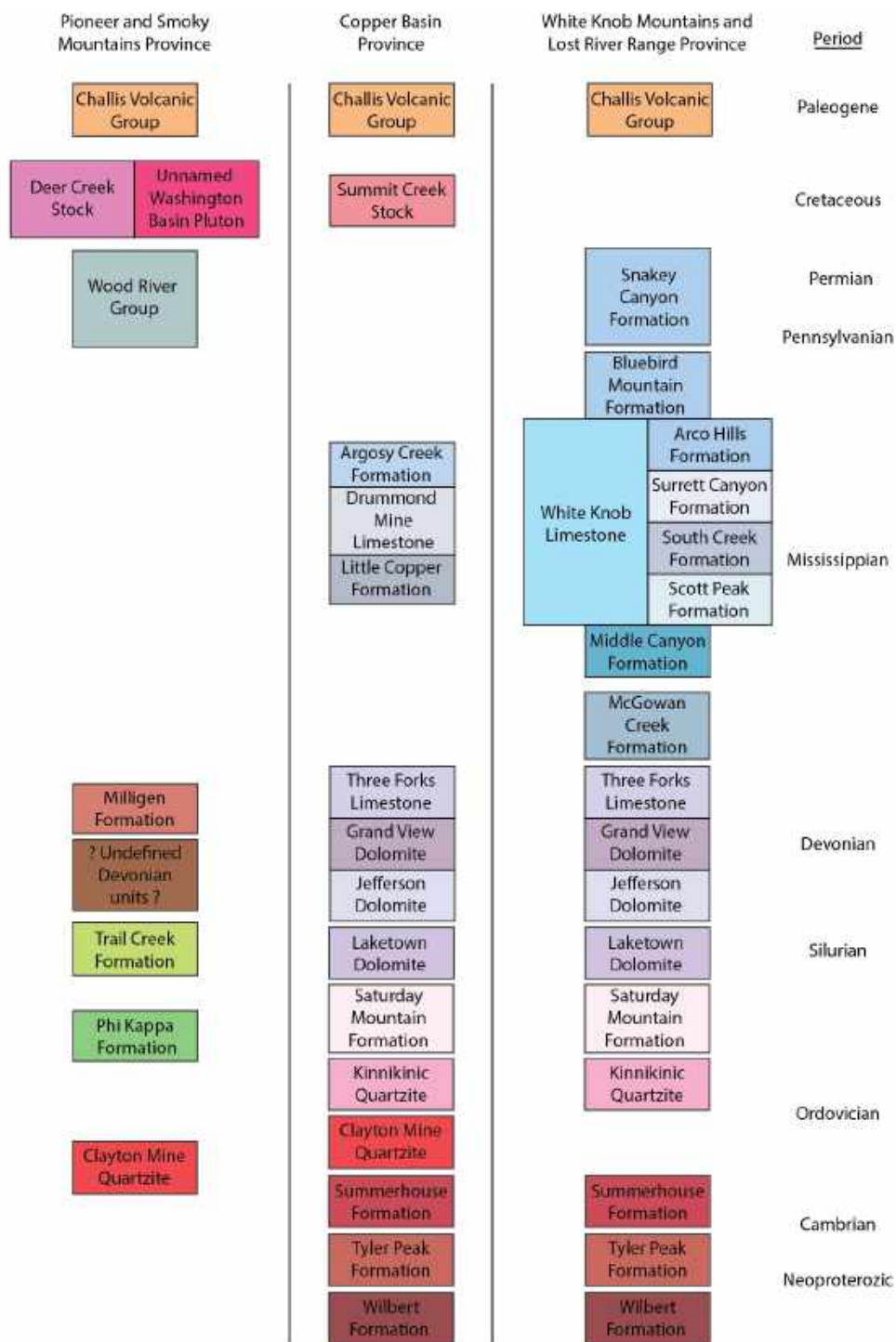


Figure 6 – Correlation of map units of east-central Idaho. Units are separated into three provinces based upon inferred depositional environment: the Pioneer and Smoky Mountains province, the Copper Basin province, and the White Knob Mountains and Lost River Range

Mesozoic crustal shortening

The field area is entirely contained within the physiographic province of the North American Cordillera. The Cordillera encompasses features produced from roughly 100 million years (~155-55 Ma) of contractional deformation (DeCelles, 2004). The current study is focused on the retroarc fold-thrust belt of the North American Cordillera, of which the Idaho-Montana fold-thrust belt is a part.

DeCelles (2004) described five distinct tectonomorphic zones within the Cordillera, two of which (the Sevier zone and the Laramide zone) are particularly relevant to the project and are hereafter described. The field area of the project defines the inboard part of the Sevier section of the Idaho-Montana fold-thrust belt. The Sevier fold-thrust belt is characterized by a thin-skinned structural style, with many short-wavelength folds. Generally, the Sevier belt is thought to have accommodated significant horizontal shortening and was active from approximately 165 Ma to 80 Ma. Laterally extensive mapped thrusts of this province in the study area include the Pioneer fault and the Copper Basin thrust fault. The Pioneer fault and the Copper Basin thrust fault both carried a thick package of Paleozoic rocks northeastward during horizontal shortening (Dover, 1983; Huerta, 1992; Rodgers et al., 1995).

The trace of the Pioneer fault is located within the Pioneer Mountains. The fault placed the Ordovician to Silurian Phi Kappa Formation and the Silurian Trail Creek Formation on top of the Scorpion Mountain Member of the Mississippian Copper Basin Group. Therefore, the fault juxtaposes the Copper Basin Group “province” and the Pioneer and Smoky Mountains “province” (Plate 1; Figure 6). Well-mapped fault exposures can be found in Little Fall Creek, Big Fall Creek, and the North Fork of the

Big Lost River (Palleiko, 2000). Per the older-on-younger relationship across the fault, the fault accommodated shortening in Mesozoic time by thrusting. Rock carried within the thrust sheet includes the Phi Kappa Formation, the Trail Creek Formation, the Milligen Formation, and the Wood River Group. Additionally, there are several short wavelength folds within the thrust sheet that can be found in all units of the sheet. Exposures of the fault are typified by the presence of heavily sheared and brecciated rock. Ample nearby thrust faults are considered by many to be part of the “Pioneer fault system” wherein a multitude of faults are rooted into one detachment and distribute shortening among them (Dover, 1949; Kim, 1986). West of the Pioneer fault, southwest of Hailey, ID, the Deer Creek thrust fault places the Lower Permian to Middle Pennsylvanian Dollarhide Formation on top of the Lower Permian to Middle Pennsylvanian Wood River Group (Skipt et al., 1994). The amount of slip is not well constrained for the fault, but authors have described it as a “minor” fault with little to no stratigraphic separation across the fault (Rodgers et al., 1995).

The trace of the Copper Basin thrust fault is mostly covered within the region, but exposures can be found near Fish Creek Reservoir and the eastern White Knob Mountains (Skipt and McIntyre, unpublished; Skipt and Brandt, 2012). The fault is interpreted to have accommodated shortening as a thrust during Mesozoic time. A second, older thrust fault is mapped at Fish Creek Reservoir that is thought to be Antler in age. This fault is said to have accommodated Mississippian shortening as part of the same fault system that formed the Antler orogeny in Nevada, creating an Antler-aged highland in Idaho through which the Copper Basin Group would have been deposited from (Roberts et al., 1958; Link et al., 1996; Skipt and Brandt, 2012). This Antler-aged

fault is not mapped elsewhere in central Idaho. The Copper Basin thrust fault placed Mississippian Copper Basin Group on top of Mississippian White Knob Limestone (Link et al., 1996). The chert in the White Knob Limestone may have had the same source as the Copper Basin Group (Link et al., 1996). Additionally, there is no stratigraphic separation across the fault; the rock is Mississippian in age on both sides of the fault (Rodgers and Janecke, 1992). As a result of this interpretation, the fault's maximum throw is limited to the thickness of the Copper Basin Group (a few kilometers). There are a number of short wavelength folds mapped within the thrust sheet of the Copper Basin thrust fault, which suggests a relatively shallow basal detachment.

Though the Laramide belt does not appear within the field area, it is important to summarize it as it plays an integral part in the formulation of the primary hypothesis. Northeast of the field area (toward southwestern Montana) "Laramide-style" (i.e. thick-skinned, basement involved) thrusts carried crystalline basement and Belt Supergroup rocks (Kulik and Schmidt, 1988; Skipp, 1988; Parker and Pearson, 2021). These basement-involved thrusts generally accommodated significantly less shortening than "Sevier-style" thrusts to the southwest (Montoya, 2019; Parker, 2021).

Critical Taper theory

Researchers have considered deformation within fold-thrust belts and accretionary wedges as conceptually analogous to snow in front of a snow plow (Elliott, 1976; Chapple, 1978; Davis et al., 1983; Dahlen, 1990). In the model that has become known as critical taper theory, a rectangular block of easily deformed material (such as sand) rests on top of a rigid slope that dips toward a rigid backstop. This weak material represents some flat-lying sedimentary rocks, such as a shale. The backstop pushes

into one side of the material, applying a compressive stress. This stress causes deformation to occur in the material above the basal décollement. The sloped material beneath this décollement remains undeformed. Deformation within the material takes the form of thrust faults, which accommodate shortening. The first thrust fault propagates near the rigid backstop. It allows the material to vertically thicken until the vertical stress (from thickened overburden) overcomes the applied compressive stress. At this point, it requires less work to shorten new material at the toe of the thrust fault than it does to thicken the material further. This results in a new thrust fault propagating outward from the previous thrust fault, away from the rigid backstop. This process is repeated cyclically, and causes the deforming material to take the shape of a wedge. This wedge is thickest near the applied stress and tapers away from it. The shape is defined by the dip angle of the basal decollement and the dip angle of the surface of the wedge. Combined, these angles define the critical taper. The critical taper is a function of the internal strength of the deformed material, the frictional resistance to sliding along the decollement, and the dip of the basal decollement. Therefore, the equilibrium angle of the critical taper will vary between different environments, such as between different fold-thrust belts (Davis et al., 1983).

Perturbations to a critically tapered wedge (one that grows self-similarly) are hypothesized to result in internal deformation (if the taper angle is lower than the critical angle) or further wedge propagation (if the taper angle is higher than the critical angle) in order to maintain its equilibrium critical taper angle (Davis et al., 1983; Dahlen, 1990).

Critical taper theory can be a useful tool for studying the kinematic evolution of continental fold-thrust belts even though orogenic belts have much more complicated

boundary conditions than the model. For example, the deforming strata in a fold-thrust belt will exhibit a mechanical stratigraphy, whereas grains of unconsolidated sand will not. There may be multiple detachments instead of just one basal detachment. However, numerical modeling shows that these variations do not cause disagreement with the critical taper model at the broad scale. It should be noted that at the sub-wedge scale, these variations do change the behavior of the model (Stockmal et al., 2007). For example, adding a relatively weak layer into the center of the model wedge will result in different behavior at that scale. This weak layer is easily exploited and forms a second décollement. This results in two different thrust sheets within one wedge, which together maintain critical taper (Stockmal et al., 2007). The same can be said for previously existing structures, which may be easier to reactivate instead of immediately propagating into unfractured rock. A further restriction in applying the model is that the model requires friction along a basal décollement, and therefore the model cannot be applied at or below the brittle-plastic transition. As the wedge grows, the basal décollement may achieve a depth below the brittle-ductile transition zone, especially in the interior of the fold-thrust belt. At these depths (350°C - 450°C ; 12-16 km for quartz-rich rocks), temperature increases cause basal friction to drop dramatically, and the surface slope will approach a dip angle of 0° (Davis et al., 1983). In spite of these limitations, critical taper theory is still useful for studying the upper crustal levels of fold-thrust belts.

Along the better-studied transects across the Sevier belt in southeastern Idaho-Wyoming and Nevada-Utah, critical taper theory is generally considered to be a good model for the development of the Sevier fold-thrust belt (DeCelles and Mitra, 1995); the

Sevier fold-thrust belt was generally wedge-shaped, propagated toward the foreland, and only involved strata above a basal décollement above crystalline basement rocks, which are all characteristics of deformation that are consistent with critical taper theory (Yonkee and Weil, 2015). This wedge propagated eastward over time. Like in the models of Stockmal et al. (2007), weak sedimentary layers encountered by the fold-thrust belt were easily exploitable and formed décollements for thrust fault propagation.

This relationship between critical taper theory and weak strata in the Sevier fold-thrust belt forms the basis for the central hypothesis of the grant this study contributes to (Figure 7). Along the major transect, in central Idaho, relatively weak Neoproterozoic and Cambrian strata occur at depth and were involved in thrusting (Brennan et al., 2020a). There, thrust faults could easily exploit those strata to form décollements, which created the broadly imbricated thrust pattern (“thin-skinned” deformation) observed in the area. However, these strata are not present toward (and northeast of) the Lemhi arch. At this point, a different weakness is hypothesized to have been exploited during continued deformation, such as the brittle-ductile transition. This newly formed, deeper décollement cut basement and involved it in thrusting, therefore explaining the transition in structural style (Montoya, 2019; Pearson NSF Grant).

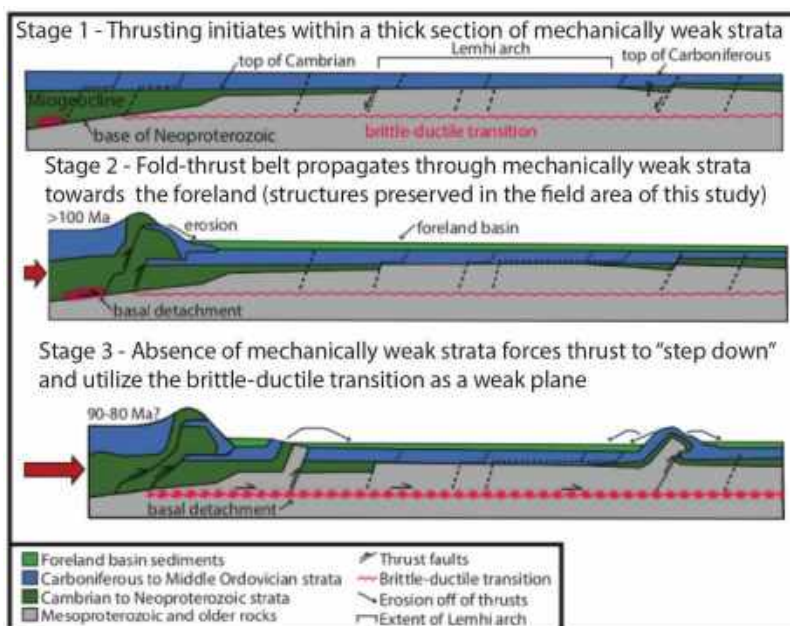


Figure 7- Schematic cross-sectional model illustrating the difference between "thin-skinned" and "thick-skinned" thrusts from east-central Idaho to southwestern Montana, as well as the evolution of structural style in the region. Characteristic "thin-skinned" thrusts are found on the left side of the diagram, while characteristic "thick-skinned" thrusts are found on the right side of the diagram. As the thrust belt propagates eastward, it first incorporates weak Cambrian and Neoproterozoic strata into the thrust-belt, creating thrusts similar to the "thin-skinned" end member. As that material disappears, the detachment steps down and utilizes the brittle-ductile transition zone as a detachment. This involves crystalline basement rock, and therefore creates structures more similar to the "thick-skinned" end member of structural style. The field area for this study preserves structures that formed during Stage 2. Modified from Montoya, 2019, originally modified from Pearson, personal communication.

Idaho batholith emplacement

The Idaho batholith is a series of large felsic intrusions that were emplaced primarily between 98 Ma and 53 Ma (Gaschnig et al., 2010). It is divided into two lobes: the Atlanta lobe of central Idaho (98-68 Ma) and the Bitterroot lobe of southwestern Montana (75-53 Ma). The Atlanta lobe is the more voluminous of the two. In general, western rocks are tonalitic to quartz-dioritic in composition, whereas eastern rocks are granitic or granodioritic in composition (Gaschnig et al., 2010). Researchers generally agree that the calc-alkaline Idaho batholith formed in response to east-dipping subduction under North America (Hyndman, 1983; Gaschnig, 2011).

Eocene volcanism and extension, and Miocene Basin and Range extension

After development of the fold-thrust belt, many structures in the area (e.g. normal faults and strike-slip faults) accommodated horizontal extension as a result of the initiation of the Basin and Range province. Northeast-striking faults north of the Snake River Plain formed during extension in Eocene time concurrent with many of the Challis Volcanic Group eruptive centers from 51 Ma – 43 Ma (Bennett, 1986). This includes normal reactivation of previous thrust faults, such as the Pioneer fault, as evidenced by slickenlines and structural analysis of paleo-stress direction (Palleiko, 2000). Eocene Challis Volcanic Group rocks conceal the surficial expression of many of the structures in the region (Gaschnig et al., 2010). Challis volcanic rock cover and extensional faulting makes interpretation of Mesozoic deformation within the region challenging. Rodgers and Janecke (1992) used paleogeologic mapping techniques to determine what the surface geology expression was at the initiation of Eocene sedimentation and volcanism, which aids in interpretation of pre-Cenozoic geology. This volcanic cover primarily erupted from 51 – 45 Ma, although its eruption continued until 40 Ma in the northern part of the Challis volcanic field. There are a variety of different lithologies that erupted during the Challis, such as andesites, dacites, and rhyodacites (Moye et al., 1988). Normal faults also initially accommodated WNW extension of the Pioneer metamorphic Core Complex (PCC) southwest of the field area from roughly >50-46 Ma. Further ENE extensional motion occurred from 38-33 Ma.

The Basin and Range province is an extensional region of western North America characterized by an alternating pattern of mountain ranges and basins. The Basin and Range formed during horizontal extension and exhumation of the region;

therefore, the faults that formed as a result are normal faults and strike-slip faults. Researchers have recorded exhumation of up to 8 km since Eocene time (Rodgers and Janecke, 1992). The Basin and Range province initiated in the early Miocene (17 Ma), and continues to evolve today (Dickinson, 2002). Normal faults produced by the Basin and Range are prevalent throughout east-central Idaho. While many of these fault traces are buried underneath Quaternary sediments, some are well exposed in the region. The Lost River Range fault dips SW on the western flank of the Lost River Range. It continues to accommodate extension today, with the historic Borah Peak earthquake of 1983 originating on the fault (Haller et al., 2010).

CHAPTER 3: METHODS

Field mapping was undertaken from June 2020 through September 2020 by Chase Porter with the help of Dr. David Pearson and Dr. Ryan Anderson. In June and early July of 2020, field mapping at the 1:24,000 scale was conducted northwest of Chilly, ID in the area surrounding Broken Wagon Creek and Mt. Anderson in the White Knob Mountains. The geology in this area primarily consists of folded Mississippian limestones, with occasional cover by Eocene Challis volcanic rocks. The field map was digitized in Adobe Illustrator. In July through September 2020, fieldwork was completed along the trace of a 126 km long cross-section transect within the Lost River Range, White Knob Mountains, and Pioneer Mountains along Trail Creek road and west of Ketchum, ID. This work was conducted to compile a transect map at 1:100,000-scale and consisted of confirming mapping by previous workers, sampling rocks of interest, and investigating the traces of Mesozoic thrust faults. Standard geologic procedures were utilized to identify geologic units, determine stratigraphic position, define stratigraphic relationships, and evaluate the geometry, kinematics, and style of deformation. Attitudes of geologic features were collected with a Brunton compass (set to 13 degrees east magnetic declination for central Idaho) and the FieldMOVE Clino app for iOS (Petroleum Experts, 2021). These attitudes included strikes and dips of bedding, cleavage planes, and foliations; they also included trends and plunges of slickenlines. Measurements were recorded in a field notebook and a rock hammer, hand lens, bottle of HCl, and scratch plate were used for fossil and mineral identification. Two igneous samples interpreted by other workers to cross cut contractional structures were collected for the purpose of obtaining a U-Pb zircon age of

crystallization. One sedimentary sample was collected for the purpose of U-Pb detrital zircon analysis.

Structural Analysis

Attitudes for geologic structures within the map area were plotted on stereonetts using the software Stereonet 10 (Allmendinger, 2018). Four stereonetts in total were produced: two for the area surrounding Broken Wagon Canyon (bedding and fold axes), and two for the entirety of the map area (bedding and cleavages). Kamb contour intervals and a cylindrical best fit for poles to planar features (or mean vector for poles to linear features) were calculated and applied to the stereonet. These best fit calculations are interpreted to define a mean fold axis, which was then used to interpret shortening direction within the region.

U-Pb zircon dating

Background

Uranium-Thorium-Lead (U-Th-Pb/U-Pb) zircon geochronology is a popular method for discerning a crystallization age for rock samples. This is because zircon incorporates U and Th into its crystalline structure (commonly up to thousands of parts-per-million) while simultaneously excluding Pb (Gehrels et al., 2008). Additionally, zircon is abundant and is resistant to alteration within the Earth's crust. This dating method utilizes three measured isotopic ratios to calculate a crystallization age: $^{206}\text{Pb}/^{207}\text{Pb}$, $^{206}\text{Pb}/^{238}\text{U}$, and $^{206}\text{Pb}/^{204}\text{Pb}$. Because of the low concentration of ^{235}U and the constant ratio of $^{238}\text{U}/^{235}\text{U}$ (137.818; Hiess et al., 2012), $^{207}\text{Pb}/^{235}\text{U}$ is not measured but instead calculated (Gehrels, 2012). This yields three isotopic systems ($^{206}\text{Pb}/^{207}\text{Pb}$, $^{206}\text{Pb}/^{238}\text{U}$, and $^{207}\text{Pb}/^{235}\text{U}$) that are independently used to calculate the crystallization age of the analyzed zircon crystal and plot a Wetherill Concordia diagram (Wetherill, 1956). A

Concordia diagram plots $^{206}\text{Pb}/^{238}\text{U}$ versus $^{207}\text{Pb}/^{235}\text{U}$ to draw a Concordia curve, which is a non-linear parametric curve as a result of differing half-lives for ^{235}U and ^{238}U . The curve is a set of solutions to the following equations (Schoene, 2014):

$$\frac{^{206}\text{Pb}}{^{238}\text{U}} = (e^{\lambda_{238}t} - 1)$$

$$\frac{^{207}\text{Pb}}{^{235}\text{U}} = (e^{\lambda_{235}t} - 1)$$

These equations produce a curve whose individual points should relate the $^{206}\text{Pb}/^{238}\text{U}$ and $^{207}\text{Pb}/^{235}\text{U}$ systems to the same analytical date. If all the produced points lie along this curve, then the system is said to be “concordant,” and the interpretation is that no external factor altered the isotopic ratios within the crystal. If points fall outside of the line, then the system is said to be “discordant” and indicates that the isotopic ratios were disturbed, such as during a lead loss event (Schoene, 2014). Depending upon the degree of uncertainty considered allowable by the researcher, analyses can be rejected if their discordancy is beyond a chosen threshold; for this study, analyses that are $\geq 10\%$ discordant were discarded. Finally, for samples that are considered satisfactorily concordant, a “best age” is selected from either the calculated $^{206}\text{Pb}/^{238}\text{U}$ or $^{207}\text{Pb}/^{235}\text{U}$ age. Generally, the former is more precise for relatively young (less than 1 Ga) grains whereas the latter is more precise for relatively old (greater than 1 Ga) grains (Gehrels et al., 2006).

Sample preparation and LA-ICP-MS

Two igneous rock samples were collected in the field (sample locations given in Figures 8 and 9) to acquire a crystallization age for the samples, which cut contractional

features. Therefore, it can be interpreted that the crystallization age of the samples is the minimum age for the end of Mesozoic shortening in their respective region, per the Law of Cross-Cutting Relations. The first sample (20CP14) collected was a granodiorite from the Deer Creek stock in the center of the Mahoney Butte quadrangle (Skipp et al., 1994). This sample was collected because it cuts the Deer Creek thrust, a fault which is interpreted by other workers to be a Mesozoic-aged contractional structure with ~1 km of stratigraphic separation (Skipp et al., 1994). Previous workers' unpublished analyses produced a hornblende $^{40}\text{Ar}/^{39}\text{Ar}$ cooling age of 94.4 ± 0.3 Ma (considered a maximum date due to the presence of excess argon) and a biotite $^{40}\text{Ar}/^{39}\text{Ar}$ cooling age 90.4 ± 0.2 Ma and (Snee, 1991 written communication cited in Skipp et al., 1994). The second sample (20CP16) was a biotite granodiorite in the Washington basin, north of Ketchum, ID; this sample was collected because it is previously undated and cuts through folds that are interpreted by other workers to be Mesozoic in age (Mahoney, 1995). A third (sedimentary) sample was collected from Cabin Creek, ID, with the intention of performing detrital zircon analysis, but ultimately failed to yield the required zircons. The two igneous samples were initially processed at Idaho State University, where they were crushed, powdered, and sieved through a 400 μm sieve. The samples were then fed onto a Wilfley table to isolate the denser mineral grains and were then further separated through traditional magnetic (Frantz barrier separator) and heavy liquid (methylene iodide) methods. Representative zircon grains were then handpicked, packaged, and sent to be imaged and analyzed at the Arizona LaserChron Center in Tuscon, Arizona. There, cathodoluminescence imagery was taken of the samples, U-Th-Pb and Lu-Hf isotopic analysis were performed, and rare earth element (REE)

analysis was performed.

Cathodoluminescence (CL) imagery is important for data interpretation in that it allows one to observe zones of compositional variation within a zircon crystal that would otherwise not be detected by plane-polarized or cross-polarized light. Specifically, cathodoluminescence imagery allows one to differentiate between the rims and the cores of the crystals, which allows for placement of the laser sampling sites in the area of interest on the crystal. This information also informs the interpretation of the origins of the zircon crystal (Gehrels et al., 2008).

Isotopic signatures from the zircon crystals were collected with a laser ablation inductively coupled plasma-mass spectrometer (LA-ICP-MS); laser spot locations were guided by the CL images. Within the machine, the zircon grain is shot with a laser, which vaporizes zircon material at the laser's impact site. The laser's parameters are typically ~30 μm in diameter, 7 Hz repetition rate, and have a fluence (the sum of particle energy per unit area) of 7 J/cm^2 (Gehrels et al., 2008). The zircon is ablated until a pit of ~20 μm depth is created, at which point the vaporized material is removed from the ablation chamber. This material is passed through the plasma of a single-collector Element2 ICP-MS and analyzed (Gehrels et al., 2008). See table 1 and table 2 for sampling information specific to 20CP14 and 20CP16 respectively.

20CP14 - Deer Creek Stock

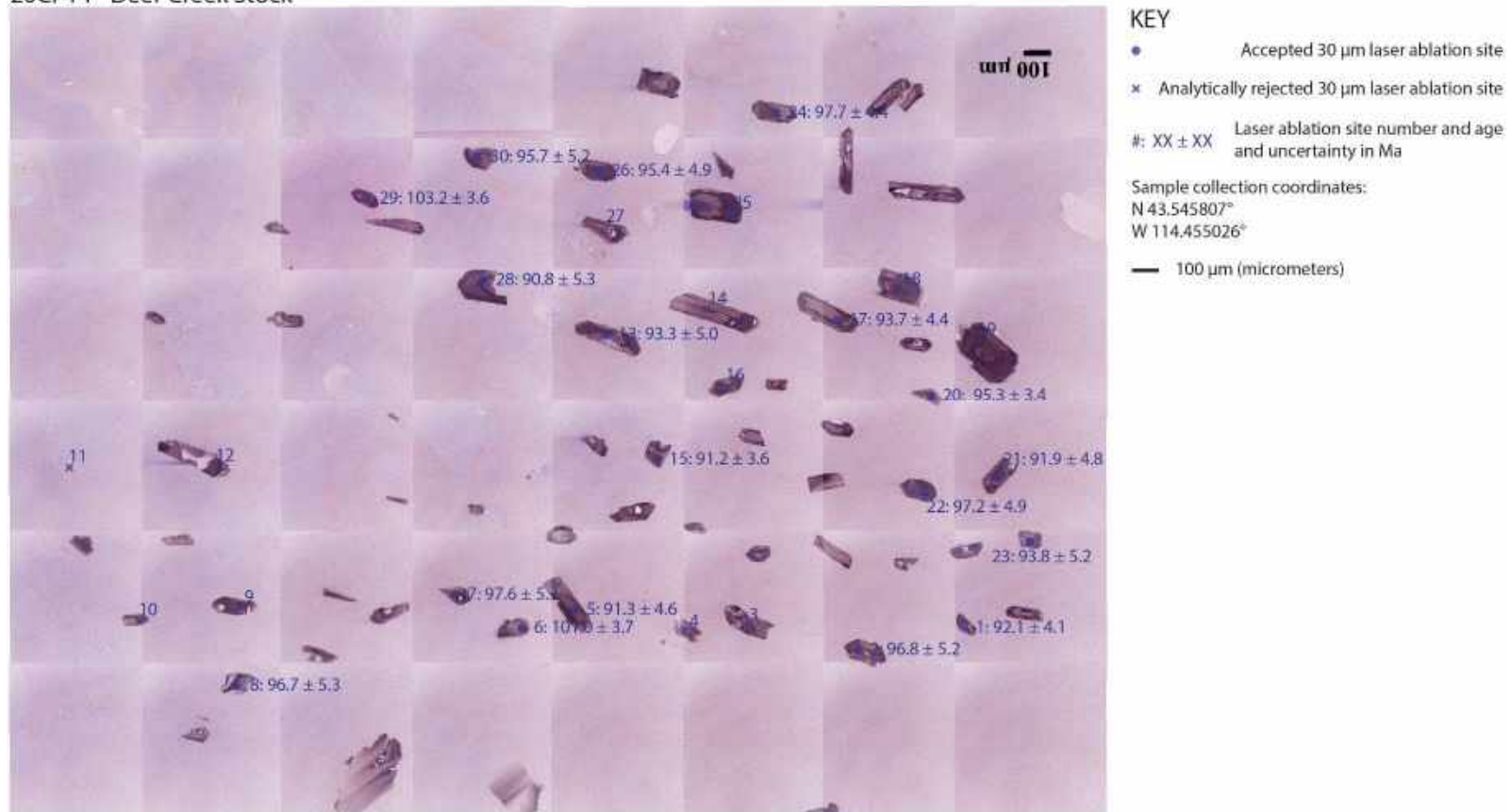


Figure 8 – Laser ablation targeting sites for 20CP14.

20CP16 - Unnamed Washington Basin Stock



Figure 9 – Laser ablation targeting spots for 20CP16.

Zircon sample data analysis

Analytical results from the LA-ICP-MS were imported into Isoplot (Ludwig, 2008), a Microsoft Excel plugin that is designed to calculate age and error of zircon samples that have undergone LA-ICP-MS. Zircon grains that yielded an age with greater than 10% measurement uncertainty were rejected. Some sources of uncertainty in these ages include variable initial U-Pb content, machine variability, systematic error (such as trace-element substitution), and analytical uncertainty. The remaining ages were used to create Concordia age diagrams for the samples. A weighted mean plot of the ages of the zircon grains was created to discern crystallization age.

ArcGIS map compilation

Geologic maps and accompanying cross-sections produced by previous workers (Mapel et al., 1965; Hall et al., 1978; Hays et al., 1978; Rember and Bennet, 1979; Dover, 1983; Hobbs et al., 1991; Worl et al., 1991; Fisher et al., 1992; Messina, 1993; Wilson, 1994; Skipp et al., 1994; Skipp and Wilson, 1994; Rodgers et al., 1995; Burton, unpublished; Pearson, unpublished; Porter, unpublished; Skipp and McIntyre, unpublished) along this investigation's cross-section transect were georeferenced in ArcGIS Pro and overlain together to create a mosaic that extends from the trace of the Deer Creek thrust southwest of Hailey, ID to the northeastern flank of the Lost River Range, ID. These maps were digitized to create polygons and line segments to connect identical geologic units and features across map boundaries in order to create a comprehensive map of the studied transect at 1:100,000-scale.

2D MOVE cross-section construction and balancing

A regional cross-section was constructed by compiling geologic mapping and field measurements within the map area along a transect that spans from southwest of

Hailey, ID to the northeastern flank of the Lost River Range, ID. The cross-section was drawn by hand with no vertical exaggeration, utilizing a topographic profile generated from a DEM created from SRTM data in MOVE 2019 (Petroleum Experts, 2021). After this initial draft was created, the cross-section was scanned and imported into MOVE 2019. MOVE 2019 is a modeling software that is capable of kinematic modeling in both two and three dimensions. It is useful for creating, balancing, and restoring geologic cross-sections at multiple scales. Within MOVE, two-dimensional area-balanced cross-section restorations were performed, and the cross-section was digitally edited whenever restoration made it apparent that the model was geologically unfeasible. Additionally, forward modeling of some structures was employed to test the viability of various mechanisms of deformation. Two algorithms were utilized for the cross-sectional modeling. The fault-parallel flow algorithm was utilized to model contractional structures, whereas the simple shear algorithm was used to model extensional structures.

The fault-parallel flow algorithm utilized by MOVE was designed to model geologic features in fault hanging walls, specifically within contractional settings (fold-thrust belts). The basis for this algorithm is the work of Egan et al. (1997). Particulate laminar flow over a fault ramp is modeled by dividing the fault into discrete dip domains, where dip bisectors differentiate between zones of changing dip magnitude. The algorithm joins various points along the dip bisectors that are equidistant from the fault plane. Then, particle movement is modeled along the lines created by joining the aforementioned points, which by definition are parallel to the fault plane (Petroleum Experts, 2021).

The simple shear algorithm utilized by MOVE was designed to model geologic features in the hanging walls of normal faults. The algorithm models the relationship between the fault geometry and the deformational structures that form within the hanging wall. Deformation is diffused throughout the entire hanging wall, rather than being focused along bedding planes. This property makes the algorithm useful for modeling syndepositional faults, where bedding thickness may vary with fault slip, as well as Cenozoic extensional faults (Petroleum Experts, 2021).

These two algorithms were used in conjunction with one another to test the feasibility of the subsurface geologic interpretations on the cross-sectional model. The model was restored to the predicted geometry along the transect prior to Mesozoic shortening (Plate 3). Once a feasible model was achieved, percent shortening was calculated by comparing the undeformed and deformed states.

CHAPTER 4: RESULTS

Reconnaissance mapping of type section of the White Knob Limestone, carbonate bank succession, and Copper Basin Group in central Idaho

Reconnaissance mapping was undertaken within various locations of interest near the major transect in accord with the primary goals of the project: to constrain the geometry, kinematics, magnitude of shortening, and timing of fold-thrust belt deformation. Particular attention was given to unit identifications within the field. Preliminary field investigation was undertaken near Jenson Spring, west of Darlington, ID. At this location, Skipp et al. (2009) mapped a well-preserved and accessible complete section of the carbonate bank of the Lost River Range. Field comparison between maps and outcrops improved confidence in unit identification.

Additional reconnaissance was undertaken in and around Broken Wagon Canyon, ID. Here, previous workers (Skipp and McIntyre, unpublished map of the Paint Pot, Horse Basin, Herd Lake, and Jerry Peak 1:24,000-scale quadrangles) mapped White Knob Limestone. This area is among the northeasternmost mapped exposures of the White Knob Limestone, which is considered to represent the eastern extent of siliciclastic sedimentation associated with the Mississippian Copper Basin Group system. The location of the Copper Basin thrust was also mapped at the poorly exposed contact between the White Knob Limestone and the Copper Basin Group; the thrust was considered to have juxtaposed the two units with a minimum of 20 km of displacement (Skipp and Hait, 1977). Given the uncertain relationship between the western, siliciclastic-bearing White Knob Limestone and chronostratigraphically equivalent eastern carbonate bank rock, it was critical to observe the transition from carbonate bank to White Knob Limestone. Following preliminary investigation of the unit

at Broken Wagon Canyon, mapping was undertaken at the type section within Cabin Creek, ID. There, all three members of the White Knob Limestone were observed. Both the White Knob Limestone and the carbonate bank typically deformed into detachment folds along the major transect, rather than thrust faults. Our observations found that significant parts of the White Knob Limestone are indistinguishable from the carbonate bank of the Lost River Range. For example, the upper White Knob Limestone contains siliceous interbeds that appear very similar to those found within the Arco Hills Formation at Jenson Spring. Similarly, the Lower White Knob Limestone was at some locations massively bedded like the Scott Peak Formation of the carbonate bank, and also contains a similar fossil assemblage. The primary differences between the carbonate bank and the White Knob Limestone was that the latter contains interbeds of sandstone and conglomerate with distinctive chert clasts. The White Knob Limestone also occasionally contained clasts of chert or bedded chert. These deposits were of variable thickness, and were often accompanied by a decrease in fossil content. Additionally, some parts of the White Knob Limestone section had abundances of bryozoan fossils that are not as common in rocks of the carbonate bank. These bryozoans were especially common near parts of the section that contained chert.

To finalize reconnaissance mapping of these units, the Copper Basin Group was explored within the western White Knob Mountains and the Pioneer Mountains. The primary exposure of the Copper Basin Group in those ranges are the two lowest formations, the Little Copper Formation and the Drummond Mine Limestone. Their character was similar to that described at their type sections. Higher on some ridges, the Scorpion Mountain member of the Argosy Creek Formation was found. It was

typically fine-grained and dark, similar to the description from its type section. Coarse conglomerates were rarely found within this area. In the southern White Knob Mountains, near Antelope Creek, the upper Argosy Creek Formation was observed. These members consisted primarily of distinctive coarse-grained chert pebble conglomerates. These units were not observed near the major transect.

Geologic Map of Broken Wagon Canyon, ID

Field mapping was undertaken at Broken Wagon Canyon, ID (refer to Plate 1 for full size, 1:24,000 scale geologic map of Broken Wagon Canyon, ID), with the intention of ascertaining the geometry and structural style of the central Idaho part of the Idaho-Montana fold-thrust belt, specifically within deformed rocks of the Mississippian carbonate bank. Previous workers at the location mapped thrust faults and abundant folds within the canyon (Skipp and McIntyre, unpublished). These thrust faults were interpreted to juxtapose the White Knob Limestone of the eastern Copper Basin province with carbonate bank rocks that dominate the late Paleozoic succession of east-central Idaho. Thus, Broken Wagon Canyon was an ideal location for investigating stratigraphic changes along the major transect.

Revised relationship between Mississippian strata at Broken Wagon Canyon, ID

Four weeks of fieldwork were undertaken near Skipp and McIntyre's (unpublished) proposed thrust contact between Mississippian Scott Peak Formation and Mississippian White Knob Limestone (see section: *Geologic background*) in an effort to determine the nature of the structure given that reconnaissance mapping showed that there was no stratigraphic separation across the fault (Figure 10). It was observed that there is no significant brecciation nor mylonitization at Skipp and McIntyre's

(unpublished) interpreted thrust contact. Further the orientation of bedding does not change across the contact, and that the contact is a gradational depositional contact between the two units. The primary change across the contact is the up-section appearance of chert pebbles and occasional bedded chert, with a minor increased abundance of bryozoan fossils above the proposed fault contact. The layers rich in chert pebbles have variable thickness where observed in Broken Wagon Canyon, varying from sub-meter scale to meter scale along strike.

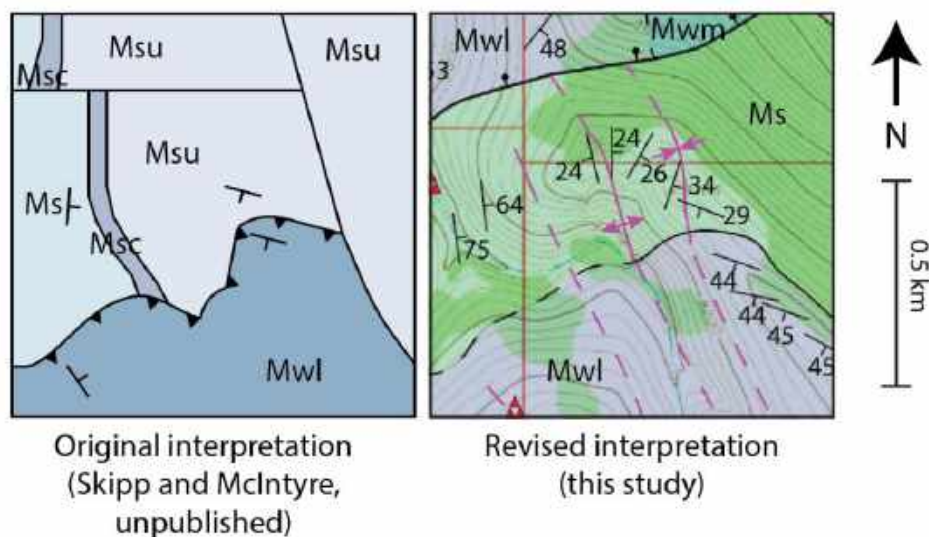


Figure 10 – Simplified snippet of Skipp and McIntyre’s original interpretation. Mwl is the Lower White Knob Limestone, which is age correlative to Msu (Surrett Canyon Formation), Msc (South Creek Formation), and Ms (Scott Peak Formation). Note that the the strike of bedding does not change across the mapped fault despite the Lower White Knob Limestone cutting across contacts here. Modified from Skipp and McIntyre (unpublished).

Structural Analysis within Broken Wagon Canyon, ID

Contractional Structures

On the western side of Broken Wagon Canyon, bedding generally dips $\sim 44^\circ$ to the northeast (Plate 1). On the eastern side of Broken Wagon Canyon, bedding generally dips to the southwest at $\sim 27^\circ$. This bedding pattern defines a regional-scale synclinorium with a wavelength of ~ 15 km that projects southward into the subsurface underneath the Big Lost River Valley. The fold axis of the synclinorium trends and slightly plunges to the SE. Throughout all of Broken Wagon Canyon, detachment folds trend northwest-southeast and have an average wavelength of approximately 450 m. These folds are concentrated in the southern half of the map area, but are present throughout. There is a minor ENE vergence to the folds. No thrust faults were observed to crop out within the map area.

Extensional Structures

Only one significant normal fault was identified within the Broken Wagon Canyon map area (Plate 1). The fault strikes southwest and dropped rocks down to the northwest. The fault cuts contractional structures, namely detachment folds and the Broken Wagon Canyon synclinorium, within the area. Throw along the normal fault is estimated to be approximately 250 m along the fault, based upon offset between stratigraphic units. The fault trace rarely appears at the surface, and most exposure is found within the lowest part of the central drainage. Where the fault crops out, jasperoidization and brecciation of the rock is common.

Stereonet Analysis at Broken Wagon area

Bedding and fold axis measurements were plotted onto two stereonet (Figure 11). A Kamb contour interval was calculated and applied to the poles to bedding measurements, which define a girdled fabric shape. Because the poles to bedding define a girdled fabric shape (Woodcock, 1977), a cylindrical best fit for the poles to bedding was calculated to constrain the orientation of folding. This pole trends 160° and plunges 11° to the southeast and represents an average fold axis for the bedding. A mean vector was also calculated for the measured fold axes within the area. This mean vector trends 158.8° and plunges 17.5° to the southeast.

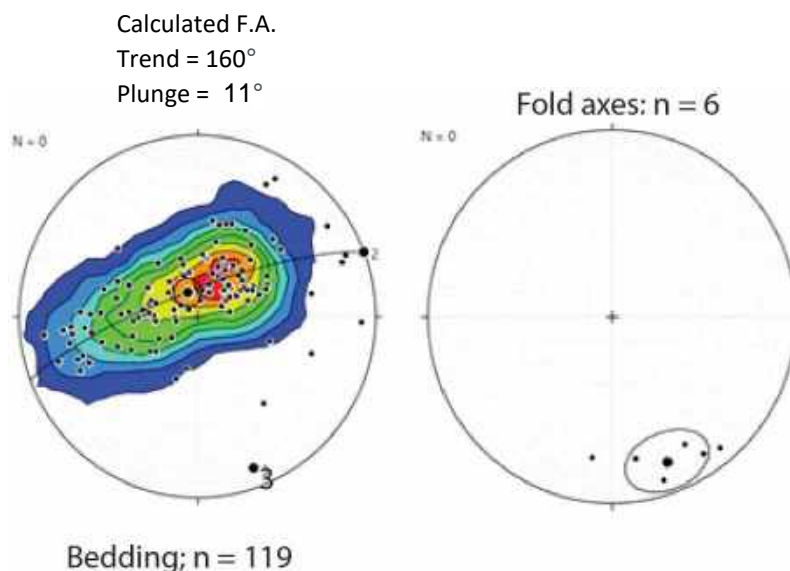


Figure 11 – Equal area lower hemisphere projection stereograms for orientations of bedding and fold axes within the Broken Wagon Canyon map area. The left plot is a plot of poles to bedding, with a cylindrical best fit fold axis labeled as “3,” which is a calculated fold axis that trends 160° and plunges 11° to the southeast. The right plot is a plot of detachment fold axes in the field area. The large black point is the mean vector, with an associated black ring of error. The mean vector trends 158.8° and plunges 17.5° to the southeast.

Jasperoidization

Jasperoid is prevalent throughout Broken Wagon Canyon, ID. Brecciation of variable clast size (cm scale) commonly accompanies jasperoid within the field area. This jasperoid is especially prevalent within the Mississippian Scott Peak Formation and the Mississippian White Knob Formation at this location. The jasperoid is most commonly found near fractures and faults in the field area. It is commonly observed within outcrops of limestone, where the boundary between jasperoid and limestone is unclear or gradational.

U-Pb zircon dating

Cathodoluminescence imaging (CL) of zircons from samples 20CP14 and 20CP16 (Figures 8 and 9) show that zircons typically display either sector zoning or oscillatory zoning. LA-ICP-MS analysis of two pluton samples sent to the Arizona LaserChron center yielded the following U-Pb zircon ages for the samples. Sample

20CP14, taken from the Deer Creek thrust-cutting Deer Creek stock southwest of Hailey, ID, yielded a weighted mean age (Figure 12) of 95.7 ± 2.7 Ma (2σ , including systematic and random errors here and henceforth).

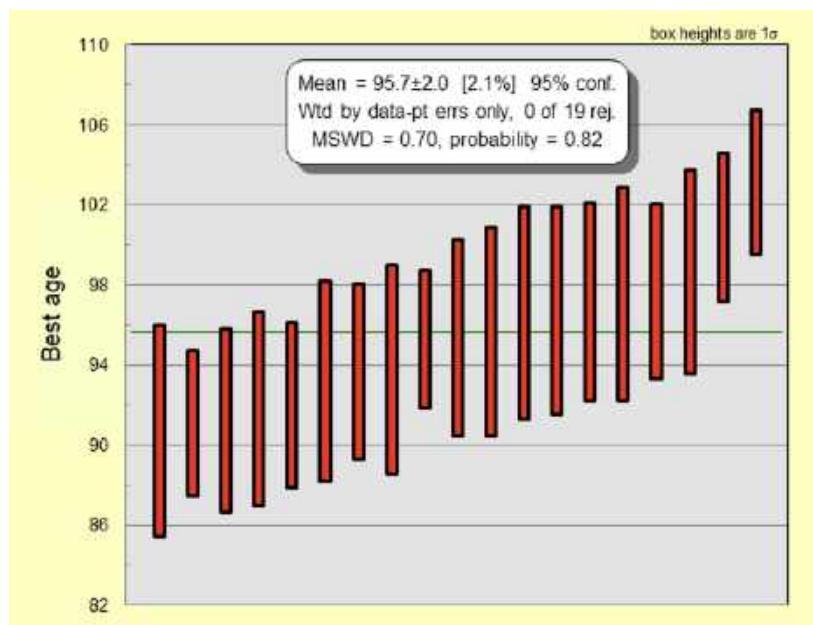


Figure 12 - Weighted mean age plot of sample 20CP14, taken from the Deer Creek stock, southwest of Hailey, ID. A Concordia plot was unable to be generated through Isoplot for this sample.

Sample 20CP16, taken from an unnamed stock within the Washington Basin, ID that crosscuts overturned folds within the Wood River Group, yielded a weighted mean age of 91.4 ± 1.4 Ma (2σ) (Figure 13).

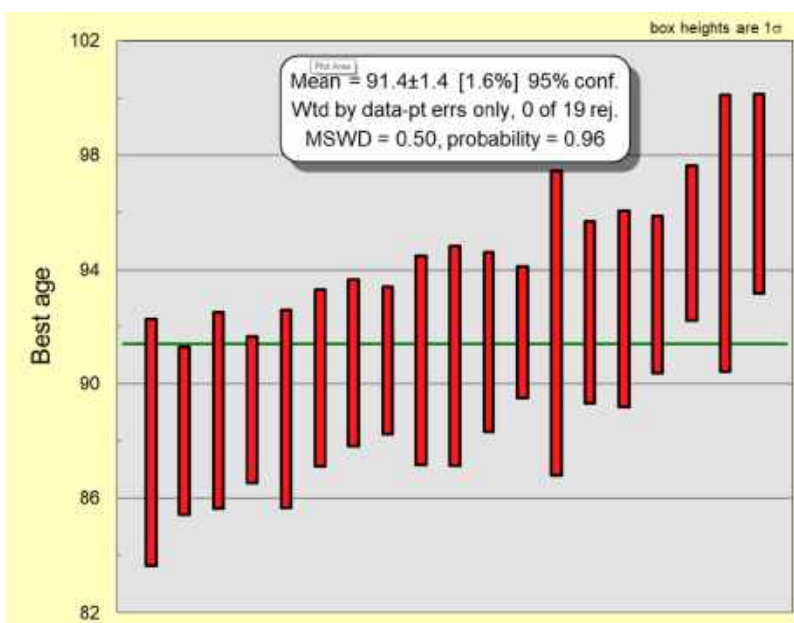


Figure 13 - Weighted mean age plot for U-Pb zircon results from sample 20CP16, taken from an unnamed stock within the Washington Basin, northwest of Ketchum, ID.

Compilation map and regional balanced cross section

Maps produced by previous workers were compiled in ArcGIS Pro at 1:100,000 scale to produce Plate 2. The total map area is ~ 980 km². The major transect is 126 km long and extends from southwest of Hailey, ID, through the northeastern flank of the Lost River Range, ID. Major features crossed by the transect include the Pioneer fault, the Copper Basin thrust, and the Lost River Range thrust fault and duplex. The transect is offset along the strike of bedding four different times in order to remain perpendicular to the mapped strike of planar structures along the length and to maximize sub-Eocene exposure levels of the fold-thrust belt. From west to east, A-A' begins near the southwestern edge of the Deer Creek stock, southwest of Hailey, ID, and continues to

just south of Keystone Gulch, in the Sawtooth National Forest, ID. A-A' has a total length of 27.5 km, and crosses the Deer Creek stock, folded Paleozoic strata, and the Wood River area. B-B' begins in the Sawtooth National Forest, ID, and continues to the mouth of Trail Creek Pass, near Chilly, ID. B-B' has a total length of 45.1 km, and crosses the Rock Roll Canyon area, the Pioneer fault, the Summit Creek stock, and folded Paleozoic strata. C-C' begins in the White Knob Mountains just north of Jerry Peak, and continues to the intersection of the White Knob Mountains and the Big Lost River Valley, ID. C-C' has a total length of 14.4 km, and crosses folded Paleozoic strata, the Copper Basin fault, and the Pecks Canyon area, ID. D-D' begins southwest of Anderson Peak, ID, and continues to the intersection between the Lost River Range, ID and the Little Lost River Valley, ID. D-D' has a total length of 39.3 km, and crosses the Broken Wagon Canyon area, Lost River Range fault, Lost River Range, ID, and folded Paleozoic strata.

The balanced cross-section reveals that structures that accommodated shortening within the region are detached within relatively weak sedimentary rocks. West of the Pioneer fault, kinematic modeling suggests that multiple bedding-parallel detachments occur within Devonian and Ordovician strata. In the Lost River Range and the White Knob Mountains, the primary upper detachment is within the McGowan Creek Formation. Across the entire transect, kinematic modeling suggests that the basal décollement occurs within Neoproterozoic strata. The basal detachment for the section is placed within the lower Neoproterozoic section at 7.5 km depth (relative to surface elevations in the Pioneer Mountains). The structures that utilized this detachment include the Copper Basin thrust fault and the Lost River Range thrust fault and duplex.

West of Little Fall Creek, ID, a shallower “middle” detachment is placed at approximately 3.8 km depth relative to surface elevations at the base of the Ordovician section. The Pioneer fault and duplex are both modeled to utilize this detachment, as well as a higher detachment within the basal Devonian section at approximately 3.3 km depth relative to surface elevations today above which small-wavelength folds (1-4 km) and conjectural blind thrusts within the Mahoney Butte quadrangle formed. In the model, this detachment also serves as the roof thrust for the Pioneer duplex. In the immediate footwall of the Lost River Range normal fault, the basal detachment is modeled at approximately 6 km depth. A second, higher detachment sits at variable depth at the base of the Mississippian McGowan Creek Formation. Short wavelength detachment folds within the region (approximately 1 to 3 km wavelength) utilized this detachment in the model.

An additional result from the balanced cross section is that structures that exhibit a large magnitude of structural relief formed at areas of pre-thrusting stratigraphy changes. For the Pioneer fault, this is at the boundary between Paleozoic rocks deposited on the continental shelf and continental slope. For the Copper Basin thrust fault, this is at the distal edge of the primary zone of Mississippian subsidence (i.e., eastern boundary of Copper Basin Group deposition) in central Idaho. Duplexes are interpreted to have formed at depth both on the western half and the eastern half of the major transect. These duplexes are interpreted to have utilized the same basal detachment as other structures. At Little Fall Creek, the roof thrust of this interpreted duplex (which is rooted in the overlying Devonian section) is often eroded, creating a window into imbricated thrusts in the roof thrust’s footwall. The duplex model was the

least complicated solution given that some ridges at Little Fall Creek contain sheets of Devonian rocks section sitting in angular fault contact with the thrust sheets below them. These “imbricated thrusts” carried Phi Kappa Formation and Trail Creek Formation in them. The western edge of the Lost River Range exposes the Silurian section at the surface in normal-faulted contact with Mississippian strata in the hanging wall of the Cenozoic Lost River fault system. The eastern edge of the Lost River Range exposes Cambrian strata at the surface. This relief was modeled to be generated by a thrust fault in the subsurface that created a synclinorium with a hinge zone within the Lost River Range. The eastern limb of this synclinorium is elevated further by a duplex in the Neoproterozoic section to better match mapped strata orientation observations. This synclinorium has a wavelength of approximately 20 km. Large wavelength folds are relatively rare and formed over deep detachments, modeled here as the regional basal detachment mentioned above. This produced synclinoria within the Lost River Range and the White Knob Mountains. On the western edge of the White Knob Mountains, the steeply overturned, northeast-vergent syncline that is found at Pecks Canyon is interpreted to have formed through fault propagation folding within the immediate footwall of the Copper Basin thrust fault. No “thick-skinned” structures are present within the field area, but may occur and be buried underneath sediment on the far eastern edge of the major transect.

In addition to the final, modern, deformed stage of the balanced cross section, Figure 13 highlights five modeled stages of progressive deformation into the hinterland of the fold-thrust belt along the major transect derived from the compilation map. Stage 1 displays the orientation of Paleozoic strata and structures prior to Mesozoic

shortening of the region and incorporates a possible pre-thrusting solution that seeks to explain regional stratigraphic problems along the transect (Huh, 1967; Mahoney et al., 1991; Link et al., 1996). Stage 2 displays the orientation of structures and strata following contraction along the Pioneer and associated faults. Stage 3 displays the orientations of structures and strata following contraction along the Copper Basin thrust fault. Stage 4 displays the orientations of structures and strata following contraction along the Lost River thrust fault and duplex system. Stage 5 displays the modern orientations of structures and strata following Cenozoic extension within the region.

Only three areas along the major transect exhibit significant structural relief (Plate 2): the Pioneer fault, the western edge of the Lost River Range, and the eastern edge of the Lost River Range. The rest of the major transect exposes Mississippian through lower Permian strata at the surface, which are often extensively folded but exhibit minimal stratigraphic separation across significant thrusts. The Pioneer fault placed the lower Ordovician Phi Kappa Formation section atop the Mississippian Copper Basin Group section, necessitating significant shortening. This section was thickened by the Pioneer duplex within the Ordovician and Silurian part of the section. Just 5 km west of the mapped trace of the Pioneer fault, a Cenozoic normal fault placed Mississippian through Permian strata in contact with the Ordovician section, reducing the structural relief again when compared to the footwall of the Pioneer fault. The total magnitude of shortening was approximately 54 km (Plate 3). The percent shortening was calculated based upon a final length of 130307 m and an initial length of 175297 m;

$$\left| \frac{\text{Length final} - \text{Length initial}}{\text{Length initial}} \right| * 100 = \% \text{ Shortening}$$

The result of this calculation was 26% shortening.

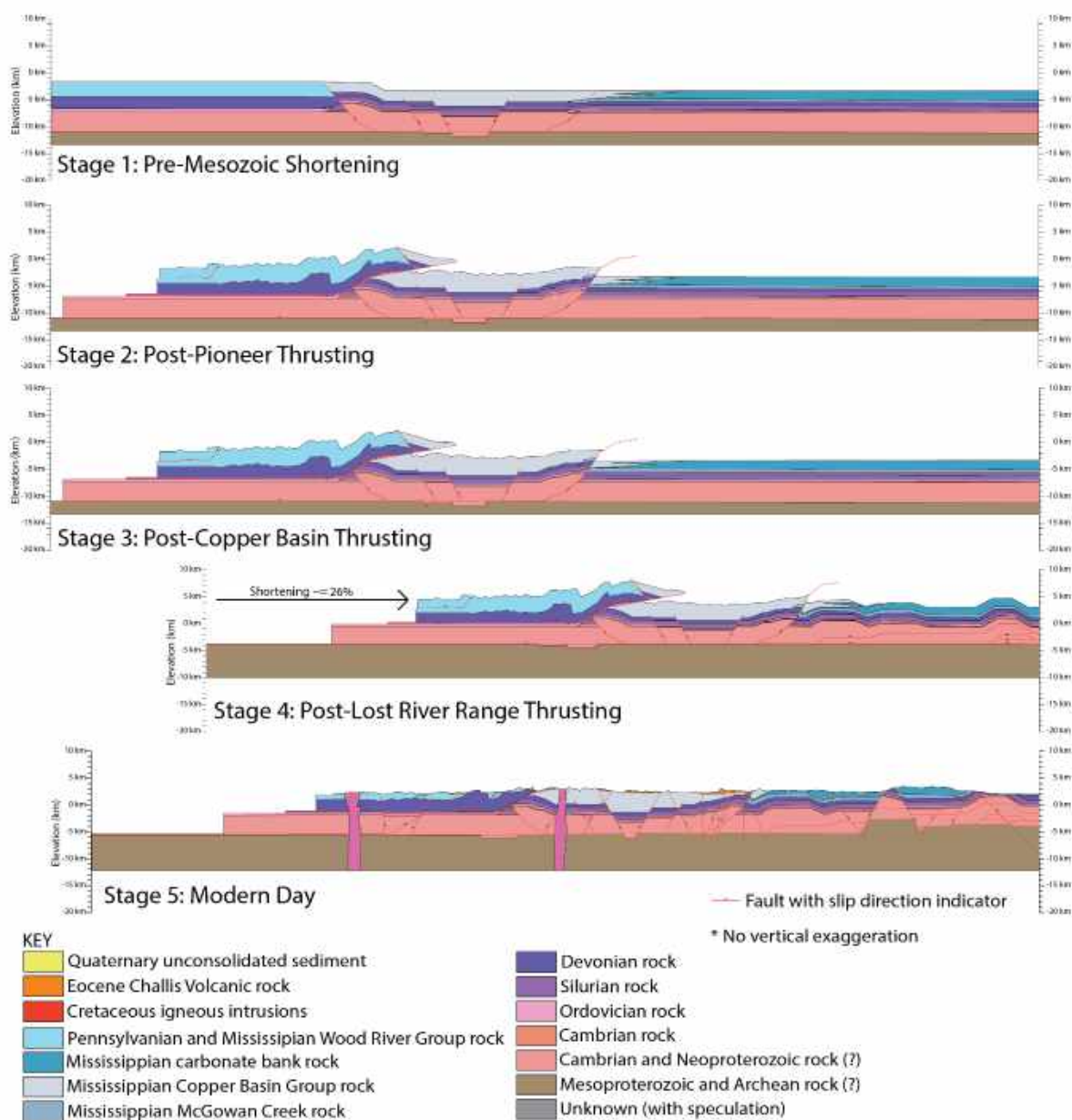


Figure 14— Simplified kinematic model of central Idaho portion of the Idaho-Montana fold-thrust belt. See Plate 3 for detailed regional balanced cross section.

Stereonet Analysis (Whole Section)

Bedding and cleavage measurements for the entire compiled regional cross section were plotted onto two stereonet (Figure 15). These measurements were collected in the field by Chase Porter, Dr. David Pearson, and Dr. Ryan Anderson. Additionally, attitudes were taken from maps published by previous authors and included within the data set. Kamb contour intervals were calculated and applied to the plots (Kamb, 1959). To approximate the orientation of regional folding along the transect, a cylindrical best fit to the poles to bedding was calculated using Stereonet 10 (Allmendinger, 2018), which represents an approximation of the average fold orientation along the transect. This pole represents an average fold axis for the bedding that trends 149.9° and plunges 3.9° to the southeast. A mean vector and cylindrical best fit were also calculated for the measured pressure-solution cleavages within the area because they may define a girdled fabric shape (Woodcock, 1977). The pole to this cylindrical best fit trends 150° and plunges 11° to the southeast.

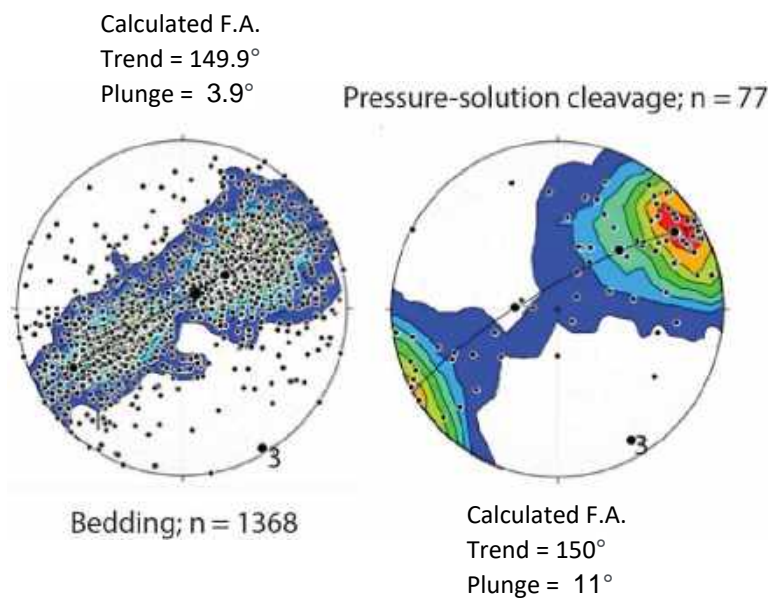


Figure 15 - Equal area lower hemisphere projection stereograms for orientations of bedding, pressure solution cleavage, and calculated fold axis within the map area. The left plot is a plot of poles to bedding. The point labeled "3" is the cylindrical best fit to the poles to bedding, which yields a calculated fold axis that trends 149.9° and plunges 3.9° to the southeast. The right plot is a plot of poles to measured pressure-solution cleavages in the field area. The point labeled "3" is cylindrical best fit to the poles to the cleavages, which yields a possible fold that trends 150° and plunges 11° to the southeast.

CHAPTER 5: DISCUSSION

Revised stratigraphy and structure of Broken Wagon Canyon, ID

Revised stratigraphic relationship between Mississippian White Knob Limestone and Mississippian carbonate bank of the Lost River Range, ID

The Copper Basin thrust fault was originally proposed to explain the change in facies observed between the Copper Basin Group of the Pioneer Mountains and the carbonate bank of the Lost River Range. There is limited surface expression of the fault within central Idaho. The best mapped exposure is described by Skipp and Hait (1977) to occur in the southern White Knob Mountains near Fish Creek Reservoir, roughly 60 km south of the major transect of this study (Skipp and Brandt, 2012). However, the fault mapped there carried rock found west of the Pioneer fault and placed it atop Copper Basin Group in the footwall, similar to the behavior of the Pioneer fault as opposed to the Copper Basin thrust. Other mapped exposures of the Copper Basin thrust fault, such as in the eastern White Knob Mountains, are poorly exposed, making it difficult to perform structural analysis. There are also locations where workers had previously mapped the Copper Basin thrust fault system that today can be explained through other solutions in light of new evidence, such as at Broken Wagon Canyon. Here, I propose that earlier workers' proposed thrust on the basis of facies juxtaposition is not necessary and instead I propose that only minor shortening was accommodated by the Copper Basin thrust. The justification for my new interpretation is described herein.

First, the type section of White Knob Limestone at Cabin Creek, ID (Skipp, 1961;

Ross, 1962; Neely, 1981) is age-correlative (Skipp and Mamet, 1970; Neely, 1981; Link et al., 1996) with the Middle Canyon Formation through the Arco Hills Formation of the Lost River Range carbonate bank as defined by Huh (1967). This indicates that there is no stratigraphic separation between lower White Knob Limestone of the proposed thrust hanging wall and the footwall Scott Peak Formation. Though a major thrust could still accommodate significant horizontal shortening, it would be highly unlikely to juxtapose two different units without any stratigraphic separation across it. This is because thrust faults cut up section in the direction of transport and therefore juxtapose older, deeper hanging wall rocks against younger, shallower footwall rocks (Dahlstrom, 1970). In the case of the Copper Basin thrust, age-equivalent rocks were proposed to occur on both sides of the fault (Skipp and Hait, 1977). Rodgers and Janecke's (1992) paleogeologic map at the base of the Eocene Challis Volcanic Group unconformity also indicates a lack of stratigraphic separation across the Copper Basin thrust.

Second, the conglomerate interbeds within the White Knob Limestone, which include chert clasts, are of variable thickness and geographical extent, suggesting that the conglomerates represent distal tongues of submarine fans that intermittently infiltrated the carbonate bank succession. These submarine fans were interpreted by Wilson (1994) and Wilson et al. (1994) to have been sourced from highlands to the south and southwest. These conglomeratic beds within the White Knob Limestone were hypothesized by Link et al. (1996) to represent the same Chesterian-age conglomeratic intervals of the Iron Bog Creek Member of the Copper Basin Group. This proposed correlation is bolstered by the presence of distinctive chert clasts within the White Knob Limestone conglomerates that is similar to age-correlative chert clasts found within the

Copper Basin Group a few kilometers to the southwest based upon similar appearance. This bolsters the interpretation that the White Knob Limestone is similar to the carbonate bank succession to the east/northeast but with occasional conglomerate tongues derived from the south/southwest.

Third, within the Broken Wagon map area, our investigation of Skipp and McIntyre's (unpublished) interpreted thrust with hanging wall White Knob Limestone and footwall Scott Peak Formation suggests that the contact is not a thrust fault. Our recent mapping of this contact indicates that there is no evidence (e.g., brecciation, a strain gradient, etc.) of faulting; instead, we interpret the contact as a bedding-parallel, gradational, depositional contact. Though a proposed thrust fault could occur as a hanging-wall flat on a footwall-flat and therefore the bedding could be concordant in dip across the contact, this possibility seems unlikely because the White Knob Limestone and the Scott Peak Formation are both extensively folded in detachment folds in the field area.

Fourth, the presence of identical fossil assemblages in both units—in addition to the inferred contemporaneous deposition as described above—suggests a similar depositional environment. Though bryozoan fossils become more common and rugose corals become less common up-section, the fossil assemblage is very similar for both units, also including brachiopods, bivalves, crinoids, and gastropods. I speculate that the up-section increase in bryozoa may reflect the introduction of chert by the Copper Basin Group: Mississippian bryozoans tended to prefer muddy environments (McKinney and Gault, 1980) whereas Mississippian rugose corals tended to prefer warm, shallow water characteristic of a carbonate bank (Aretz, 2010). It seems plausible that the

introduction of chert and increased depth from Copper Basin subsidence would have expanded the ecological niche for bryozoans and limited the resources available to rugose corals.

Given the above, we interpret that the Mississippian White Knob Limestone represents a gradational change within the Mississippian carbonate bank as a result of the introduction of siliciclastic sediment from the deposition of the Copper Basin Group to the south and west. The resulting depositional environment is that of an east-prograding fan of Copper Basin Group interfingering with the west-prograding carbonate bank of the Lost River Range (Wilson et al., 1994; Link et al., 1996). This idea has been proposed by other workers (Skipp et al., 2009), but has never been mapped within the field until this study. This revision has significant implications for the existence of and amount of slip required by the Copper Basin thrust fault could have accommodated (see subsection: **Contractional structures**).

Thus, previous workers' interpretations that the White Knob Limestone sits in thrust fault contact with the carbonate bank of east-central Idaho is not justified by current results. The preferred interpretation here is instead that the conglomerate-bearing, but largely carbonate White Knob Limestone represents deposition within the transitional region between submarine fans and turbidite deposits that were interpreted to form the Copper Basin Group and the age-equivalent carbonate bank succession of east-central Idaho.

Jasperoid at Broken Wagon Canyon, ID

Because the jasperoid found at Broken Wagon Canyon shares characteristics with hydrothermal alteration of rock, the jasperoid is hypothesized to have been formed

by the secondary replacement of calcite with silica within the limestone during Cenozoic time, likely through the introduction of hydrothermal fluids in the area (Soulliere et al., 1989).

Structure of Broken Wagon Canyon, ID

Mapping and structural analysis of the region near Broken Wagon Canyon reveals that earlier contractional structures were crosscut by a later normal fault. Short-wavelength folds have fold axes that trend NW-SE and are interpreted here as detachment folds. Significant shearing and cleavage present within the McGowan Creek Formation at its type section in the Lost River Range and fold wavelengths suggests that these folds were formed above a bedding-parallel detachment that is rooted at the base of the Mississippian McGowan Creek Formation. This unit is known as a regional detachment horizon (e.g., Anastasio et al., 1997) within the Lost River Range, which is only a few km from the Broken Wagon Canyon map area. There is also a long-wavelength fold that forms a syncline that encompasses the entire area of Broken Wagon Canyon. Because of the difference in wavelength between the two kinds of folds at Broken Wagon Canyon, we interpret that the synclinorium formed above a thrust fault rooted within a primary detachment that is utilized by many structures in the area and is relatively deep within the section (~7 km depth). Kinematic modeling indicates that this thrust fault is likely the same thrust fault that produced the Lost River Range synclinorium ~6 km to the northeast (see subsection: *Contractional structures*).

These contractional structures are interpreted to have been offset by a west-southwest-striking normal fault within the field area that dropped rocks down in its hanging wall to the northwest. This fault's strike is roughly perpendicular to the Basin

and Range normal faults in the region, which strike SE-NW. Similarly oriented normal faults that strike WSW-ENE can be found throughout east-central Idaho, such as those that bound the Borah Peak horst. Based upon these orientation differences, I interpret that the fault at Broken Wagon Canyon formed around the same times as faults of similar orientation in the region as opposed to during Basin and Range extension; specifically, around 48-49 Ma (Janecke, 1992).

Shortening direction in Broken Wagon Canyon

Stereonet analysis of structures within Broken Wagon Canyon produced an average fold axis that trends 159° for the area (Figure 12). Assuming that shortening direction is perpendicular to the fold axis, shortening in Broken Wagon Canyon was southwest-northeast (249° to 69°). In comparison to the major transect, which yields a shortening orientation of $240^\circ/60^\circ$ (perpendicular to calculated fold axis); the slightly different orientation (9°) from the overall shortening direction may be associated with the major fold that is detached relatively deeply when compared to the depth of detachment for the minor folds. Together, these folds produced a synclinorium whose fold axis has approximately the same trend and plunge of the northern part of the Lost River Range, ID. Elsewhere along the transect, detachment folds are not bound within a synclinorium and their fold axes trend more akin to the regional average.

Structure and stratigraphy along the major cross-section transect Additional support for revised stratigraphic relationships across the Pioneer fault

Early workers (Skipp and Hait, 1977) in the region originally described the Pioneer fault as transporting “allochthonous” rock up to 50 km (see section: *Geologic Background*). However, workers now consider the rocks found in the hanging wall of the

Pioneer thrust to be of the same “terrane” but of a different depositional environment as its footwall (Link et al., 1988). I modeled the extreme end-member of this more recent idea: that the Pioneer thrust ramp exists at the location of a paleo-continental rise. This model proposes that the Paleozoic section found in the modern-day hanging wall of the Pioneer fault was deposited in contact with the Paleozoic section east of the modern-day Pioneer fault. As a result, the Ordovician Phi Kappa Formation is in contact with the Ordovician Kinnikinic Quartzite at depth (see Plate 3). The decision to pursue this model was made in an effort to produce a minimum shortening model. Given that the cross-sectional model is balanced and sequentially restorable, this supports the more recent idea that the lower Paleozoic rocks in the hanging wall of the Pioneer fault are not “allochthonous.” I go further to propose that the main fault surface of the Pioneer fault is only required to have accommodated a minimum of roughly 12 km of shortening.

Contractional structures

There is a wide variety of contractional structures along the major transect. Here, I detail primarily three of these major structures: the Pioneer fault, the Copper Basin fault, and the Lost River thrust fault. The Pioneer fault is exposed in the Pioneer Mountains and placed Ordovician Phi Kappa Formation on top of Mississippian Copper Basin Group. I interpret that the Pioneer fault was rooted in a detachment at the base of rheologically weak, fine-grained rocks of the Ordovician Phi Kappa Formation. In the eastern part of the regional cross section, there is no detachment in the Ordovician part of the section, which is interpreted to be a consequence of the eastward coarsening grain size of the lower Paleozoic strata. Additionally, given that there are several imbricate thrust faults exposed in the immediate hanging wall of the Pioneer fault that

duplicate the Phi Kapp and overlying Trail Creek strata, the Pioneer fault is interpreted to represent the floor thrust of a duplex whose roof thrust is rooted in a detachment at the top of the Silurian Trail Creek Formation/base of the Devonian section. This duplex is interpreted to have initially formed at depth and was brought up the Pioneer fault ramp through later shortening. These observations and associated hypotheses explain the repeated pattern of Phi Kappa Formation and Trail Creek Formation within thrust sheets at Little Fall Creek, ID. The Devonian roof thrust is exposed at the peak bounding the southwestern side of Little Fall Creek, as well as within the drainage southwest of the peak. There is also some evidence for out-of-sequence thrusting at the front of the Pioneer duplex, because one thrust sheet is missing the Trail Creek part of the section that we see repeated in the other thrusts here. This solution is the one I chose to model, but I recognize that there is some uncertainty associated with this. In the hanging wall of the Pioneer fault, I suspect that short-wavelength folds and blind thrusts in the Rock Roll Canyon quadrangle utilized the relatively shallow upper detachment of the roof thrust at the base of the Devonian section. The lower Paleozoic part of the section differs across the Pioneer fault (see subsection: *Additional support for revised stratigraphic relationships across the Pioneer fault*). I speculate that it is not a coincidence that the Pioneer fault occurs at this location: I suspect that the shelf-slope break, and change in stratigraphy formed from the postulated former continental rise here between the relatively weak Ordovician Phi Kappa Formation and the relatively strong Kinnikinic Quartzite were exploited by the Pioneer fault.

The Copper Basin thrust fault was hypothesized to occur along the central part of the regional transect though its trace is thought to be nearly entirely buried beneath the

Challis Volcanic Group. Occurrence of the Copper Basin Group west of the carbonate bank of east-central Idaho has been interpreted by previous workers to imply a major spatial transition in depositional environment associated with increased proximity to tectonism during the Antler orogeny to the south and west (Link et al., 1996). During our field investigation of the only hypothesized exposure of the Copper Basin fault, we were unable to identify high quality outcrop of the rocks in the hanging wall or footwall of the Copper Basin thrust. However, reconnaissance mapping northwest of Peck's Canyon in the hypothesized footwall of the Copper Basin fault led to identification of a major north-northwest-trending, east-northeast verging overturned syncline whose overturned western limb is overlain unconformably by the Challis Volcanic Group <2 km across-strike from the mapped location of the Copper Basin thrust; we tentatively interpret this major fold as an overturned footwall syncline associated with the Copper Basin thrust but more work is needed. Notwithstanding future independent structural investigations of the Copper Basin thrust, the thrust was mapped by Skipp and McIntyre (unpublished) to juxtapose the Little Copper Formation of the Copper Basin Group against age-equivalent (Link et al., 1996) McGowan Creek Formation. Given that the eastward thickness change of Copper Basin Group rocks is poorly known, we adopt Wilson et al.'s (1994) hypothesis that it was deposited syn-kinematically within the hanging walls of normal and/or oblique slip faults east of the modern location of the Pioneer fault (see Figure 13).

Our investigations of the stratigraphic and structural relationships at Broken Wagon Canyon in the context of our reconnaissance investigation of other Mississippian strata in central Idaho suggests that distal tongues of Copper Basin Group submarine

fans are interbedded in carbonate bank limestones; this suggests that the source of sediment for the Copper Basin Group was within “reasonable range” of the carbonate bank. There is some uncertainty here in how far it would be possible to transport clasts, so for my minimum shortening cross-sectional model I limited slip along the fault to a few kilometers. Therefore, I interpret the Copper Basin thrust fault to be a steeply-dipping thrust reactivation of a Paleozoic normal fault; this hypothesized older normal fault formed in tandem with the deposition of the Copper Basin Group. Like the Pioneer fault, I believe it is no coincidence that the ramp of the fault is located at a change in stratigraphy. It seems likely that it was easier for the Copper Basin thrust fault to reactivate a previous normal fault than to propagate into the relatively strong dolostones of the lower carbonate bank. Additionally, I modeled the Copper Basin thrust fault as being rooted in a regional detachment found at approximately 7 km depth. It is uncertain which rocks are present at this depth. I rooted the thrust in this detachment because there is no evidence for a detachment within the Ordovician part of the section here as there is in the hanging wall of the Pioneer thrust. However, there is some evidence that I interpret to be indicative of a detachment of that depth to the east in the Lost River Range. There is also a detachment of uncertain depth that forms short wavelength folds in the Copper Basin Group, but I failed to find any exposure of this detachment. This detachment likely lies well above the detachment for the Copper Basin thrust fault given the wavelength of the associated folds.

The final major contractional structure in the region is a modeled thrust fault that underlies the eastern White Knob Mountains and the Lost River Range. This fault is interpreted to have produced significant structural relief, exposing Silurian rocks on the

western side of the Lost River Range and Cambrian (and possibly older) rocks on the eastern side of the range. This fault is modeled to produce the Broken Wagon Canyon and the Lost River Range synclinoria through a series of thrust ramps and flats. Additionally, I modeled a duplex to be present at depth on the eastern side of the Lost River Range. This duplex explains why the eastern flank of the Lost River Range is steeply dipping ($\sim 60^\circ$ to the west) while the western flank only dips shallowly ($\sim 30^\circ$). I believe that the eastern flank initially dipped more shallowly, but a duplex formed later and steepened the eastern limb of the synclinorium. Both the Lost River thrust fault and the duplex utilized the common 7 km deep detachment. I determined this because that amount of stratigraphy (discerned through measured sections by other works) is required to be carried in the hanging wall of the fault, given that Cambrian (or possibly older) rocks are exposed at the surface and do not have a detachment exposed within those units. Like the Copper Basin thrust, the age of the rocks that host this detachment is uncertain. There is some uncertainty in this model, however, because no fault trace is exposed at the surface. The short-wavelength folds that dominate the Mississippian part of the section here are likely formed above the Mississippian McGowan Creek Formation detachment that I believe formed the detachment folds at Broken Wagon Canyon.

These three major structures are all interpreted to have bedding-parallel detachments, accommodate relatively high shortening magnitudes, and do not require any basement involvement; thus, their structural style seems to fall more closely to the “thin-skinned” end-member of thrusting. Within and northeast of the Lemhi Range into southwestern Montana, to the east of the current study, “thick-skinned” structures

carried silica-cemented Mesoproterozoic quartzites and crystalline basement rocks (Parker and Pearson, 2021).

Shortening direction in east-central Idaho

Stereonet analysis of structures along the transect produced an average fold axis for the region that trends 150° (Figure 14). We assumed that shortening direction is perpendicular to the fold axis, and therefore shortening in east-central Idaho was SW-NE (240° to 60°) and progressively propagated into the hinterland of the thrust belt to the northeast. This result is 9° different from the shortening direction inferred at Broken Wagon Canyon. This suggests that shortening direction in east-central Idaho underwent limited variation as shortening progressed. This variation has been captured by other workers. In the Bayhorse region of Idaho, Brennan (2018) calculated an average fold axis that trends 349° , implying a more W-E shortening direction under the same assumption as before. Montoya (2019) calculated a fold axis that trends 155° in the northern Lost River Range, near Leaton Gulch. This result is similar to the result calculated in this study, and similarly implies a SW-NE shortening direction.

Age constraints on shortening

As a result of field-checking various maps throughout the region, I confirmed that contractional structures within the field area are cut by various igneous bodies. Per Steno's Law of Cross Cutting Relations, the uncut igneous bodies must have been emplaced after the end of shortening on the structure they cut. This allows me to use dating results of the igneous rocks as a maximum age for the end of shortening on the structure. First, the Deer Creek thrust and folds southwest of Hailey, ID, are cut by the Deer Creek stock in the Mahoney Butte quadrangle, which yielded a new U-Pb zircon

age of 95.7 ± 2.7 Ma. This new age is in agreement with unpublished hornblende (maximum) and biotite (cooling) $^{40}\text{Ar}/^{39}\text{Ar}$ dates of 94.4 ± 0.3 Ma and 90.4 ± 0.2 Ma, respectively (Snee, written communication cited in Skipp et al., 1994). Based on this new age, we assert that major folding and thrusting in this region occurred in Early Cretaceous time, prior to ca. 96 Ma. The similarity between U-Pb zircon crystallization and $^{40}\text{Ar}/^{39}\text{Ar}$ cooling ages suggests that the pluton cooled relatively rapidly.

Approximately 30 km along-strike to the north of the regional transect in Washington Basin, the White Cloud Mountains expose folds cut by an unnamed and undated quartz diorite pluton (Mahoney, 1995). Our U-Pb zircon date of 91.4 ± 2.4 Ma indicates that major folding was complete by this time. The crosscutting relationship is outside of the current transect, but is extrapolated along-strike and interpreted to be representative of similar structures in the current transect and therefore constrains a minimum shortening age for the White Cloud Mountains and western Pioneer Mountains. Finally, the Pioneer thrust is cut by the Idaho batholith to the west and the Summit Creek stock to the east. Pearson (personal communication) obtained a U-Pb zircon age of emplacement for the Summit Creek stock—which cuts the Pioneer thrust near Trail Creek—to be 48.5 ± 0.8 Ma. Given that the Summit Creek stock was likely emplaced concurrently with extensional reactivation of the Pioneer fault (Pearson, personal communication), this suggests that Early Cretaceous shortening was followed by extensional reactivation during regional Eocene extension.

All of these ages are similar to recent U-Pb zircon ages of plutons of the eastern Idaho batholith. For example, Montoya (2019) and Krohe (2016) reported identical 96.9 ± 0.8 Ma U-Pb zircon ages from two separate plutons ~25 km apart exposed between

Challis and Stanley Idaho: the western pluton was interpreted by prior workers to cut the Pioneer thrust (see discussion in Montoya, 2019) and the eastern pluton was emplaced into the Bayhorse anticline (Krohe, 2016 and Brennan et al., 2020b). Ma et al. (2021) also obtained U-Pb zircon ages between 85-100 Ma from several granitoids in the Sawtooth metamorphic complex, approximately 30 km west-northwest of Washington basin. All of these ages suggest a Lower Cretaceous age of thrusting and major folding in the western part of the regional cross section; timing constraints on contractional structures in the eastern part of the transect are not available. Detrital zircon results derived from the Early Cretaceous Kootenai Formation of southwestern Montana suggest that foreland basin rocks were receiving sediment from recycling of lower and middle Paleozoic strata in central Idaho (Rosenblume et al., 2021). Thus, active thrusting and erosion was likely occurring along the major transect (this study) during the time of Kootenai Formation deposition (~135-110 Ma; Rosenblume et al., 2021). Contractional structures along the transect were then crosscut by 97-91 Ma plutons.

Current results in the context of other workers' ongoing studies in the Idaho-Montana fold-thrust belt regarding the transition in structural style

Because the cross-sectional model produced by this investigation serves to provide a regional perspective on structural style, it is critical to extend the results to neighboring regions to place these results in context. By comparing the timing of deformation and the structural style of deformation between this investigation and neighboring regions, we are able to observe the fold-thrust belt as a whole, which increases the size of our dataset and our confidence in observed trends within the data.

The cross-sectional model's focus on the geology within the area west of the transition in structural style within the Idaho-Montana fold thrust belt allows us to

evaluate the control on the northeastward change in structural style with more confidence. The major transect of this investigation contains a thick package of Neoproterozoic and Cambrian rocks at depth. Conversely, the major transect of Parker (2021) lacks this thick package of rocks; instead, its western edge crosses the Lemhi arch, where Ordovician Kinnikinic Quartzite sits directly atop Mesoproterozoic quartzite. The shortening style of deeper structures along Parker's (2021) transect is more aptly described as being close to the "thick-skinned" end member of structural style. Conversely, the structural style of this investigation is more similar to the "thin-skinned" end member of structural style. This follows the geographical distribution of the two major deformational zones of Mesozoic shortening in Laurentia. The western hinterland of the fold-thrust belt is more Sevier in character, whereas the eastern foreland is more Laramide in character.

The coincidence between differences in stratigraphy and differences in structural style between the two major transects lends credence to a possible relationship between structural style and pre-orogenic stratigraphy. If the two transects are combined to create a model that spans the full Idaho-Montana thrust belt, it becomes apparent that, while no discrete transition between structural style can be discerned, the broad zone over which structural style changes directly overlaps with the zone of stratigraphy change within the fold-thrust belt. Therefore, the evidence supports the model that proposes that changes in pre-orogenic stratigraphic architecture controlled the transition between structural styles in the Idaho-Montana fold-thrust belt. This solution is satisfying in that it reduces the inherent conflict that existed between field

observations in Idaho and Montana and the flat-slab subduction model employed to the southwest.

Extensional structures

This investigation was primarily focused on the Mesozoic history of the region, and as such Cenozoic extensional structures were not analyzed in detail. However, there are a few details and uncertainties worth mentioning. First, the Lost River fault was modeled to drop everything west of the fault down in its hanging wall. Because there was no evidence observed to suggest any other normal faults made significant regional changes to structural level, the modeled slip on the Lost River thrust fault is the least complicated solution. Additionally, the Pioneer fault has indicators of normal slip, suggesting normal reactivation of a previous thrust fault. There is no published evidence to ascertain the quantitative magnitude of slip on the fault, so I did not model the normal slip in my minimum shortening cross-sectional model, and this slip is ignored. This is a major source of uncertainty within the model, as the Pioneer fault generates the most structural relief of any structure along the major transect and likely slipped further than modeled here.

CHAPTER 6: CONCLUSIONS

This study contributes to a body of evidence concerning the pre-Mesozoic stratigraphy and geometry, kinematics, timing, and style of Mesozoic contractional structures of central Idaho. The cross-sectional model produced in this study proposes a depth for various detachments in the region. Additionally, this study presents new evidence that refines the relationship between the White Knob Limestone and the Mississippian carbonate bank of the Lost River Range, ID. The results of this study are summarized as follows:

1. The Mississippian White Knob Limestone of the Copper Basin Group system is not a distinct geologic unit. Instead, it represents a transition zone between distal fans of the Copper Basin Group and the Mississippian carbonate bank of the Lost River Range. Evidence of this relationship is preserved at Broken Wagon Canyon, ID. The implication of this is that it is unnecessary that a large magnitude of shortening be accommodated by the Copper Basin fault.
2. Major mapped thrusts in the region occur near pre-thrusting changes in stratigraphy. The Pioneer fault propagated through a Paleozoic continental rise, while the Copper Basin thrust fault formed where a thick package of conglomerates and flysch meets a thick package of limestones. Therefore, previous workers' interpretations that suggest major thrusts bound exotic terranes are not supported by the current results.
3. The cross-sectional model suggests that structures that accommodated horizontal shortening within the region were rooted into detachments within relatively weak and easily deformed rocks.

4. The cross-sectional model results suggest that major thrusts in the region are rooted to a detachment that sits at approximately 7 km depth today for most of the transect. It is assumed that this is within Neoproterozoic rocks.
5. Several higher detachments exist in shallower rocks than the regional detachment mentioned above. West of the Pioneer fault, two detachments exist at approximately 3 km depth today, whereas east of the Copper Basin thrust fault a higher detachment sits at approximately 1.5 km depth today.
6. The cross-sectional model predicts the existence of a third large thrust in the region that underlies Pecks Canyon through the Lost River Range. This thrust does not crop out on the surface anywhere.
7. Shortening-related structures in the region are cut by two plutons with the following U-Pb zircon ages: the Deer Creek Stock (95.7 ± 2.7 Ma) and an unnamed pluton in the Washington Basin (91.4 ± 2.4 Ma). Additional results from Lower to mid Cretaceous foreland basin strata in southwestern Montana corroborate that this portion of the fold-thrust belt was active in Early Cretaceous time. Therefore, crustal shortening along the transect is constrained to Early Cretaceous time (prior to approximately 96 Ma).
8. Shortening direction inferred from structures within the region was primarily WSW-ENE. Shortening magnitude was approximately 26% shortening.

WORKS CITED

- Allmendinger, R.W., Ramos, V.A., Jordan, T.E., Palma, M., and Isacks, B.L., 1983, Paleogeography and Andean structural geometry, northwest Argentina: *Tectonics*, v. 2, no. 1, p. 1-16, doi:10.1029/TC002i001p00001
- Allmendinger, R., 2018, Stereonet 10. Cornell University, Ithaca, NY.
- Anastasio, D.J., Fisher, D.M., Messina, T.A. and Holl, J.E., 1997, Kinematics of décollement folding in the Lost River Range, Idaho: *Journal of Structural Geology*, v. 19(3-4), p. 355-368.
- Aretz, M., 2010, Habitats of colonial rugose corals: the Mississippian of western Europe as example for a general classification: *Lethaia*, v. 43(4), p. 558-572.
- Armstrong, F. C., and Oriel, S.S., 1965, Tectonic development of Idaho-Wyoming thrust belt: *AAPG Bulletin* 49, no. 11, p. 1847-1866, doi:10.1306/A663386E-16C0-11D7-8645000102C1865D
- Armstrong, R.L., 1968. Sevier orogenic belt in Nevada and Utah. *Geological Society of America Bulletin*, v. 79, no. 4, p. 429-458.
- Armstrong, R.L., 1974, Magmatism, Orogenic timing and orogenic diachronism in the Cordillera from Mexico to Canada: *Nature*, v. 247, p. 348-351.
- Axen, G.J., van Wijk, J.W., and Currie, C.A., 2018, Basal continental mantle lithosphere displaced by flat-slab subduction: *Nature Geoscience*, v. 11, n. 12, p. 961-964.
- Beranek, L.P., Link, P.K., and Fanning, C.M., 2016, Detrital zircon record of mid-Paleozoic convergent margin activity in the northern U.S. Rocky Mountains: Implications for the Antler orogeny and early evolution of the North American Cordillera: *Lithosphere*, v. 8, p. 533–550, doi:10.1130/L1557.1131.
- Bird, P., 1984, Laramide crustal thickening event in the Rocky Mountain foreland and Great Plains. *Tectonics*, v. 3, no. 7, p. 741-758.
- Burchfiel, B.C., and Davis, G.A., 1972, Structural framework and evolution of the southern part of the Cordilleran orogen, western United States: *American Journal of Science*, v. 272, no. 2, p. 97-118, doi:10.2475/ajs.272.2.97
- Burton, B., and Link, P.K., personal comm., Unpublished geologic map of Little Fall Creek and vicinity, Custer and Blaine counties, Idaho: scale 1:24,000.
- Brennan, D.T., 2018, Geologic mapping and detrital zircon provenance of the Bayhorse anticline, Custer County, Idaho: Revised Neoproterozoic to lower Paleozoic stratigraphy [M.S. Thesis]: Pocatello, Idaho State University, 149 p., 1 plate.
- Brennan, D.T., Pearson, D.M., Link, P.K. and Chamberlain, K.R., 2020a, Neoproterozoic Windermere Supergroup near Bayhorse, Idaho: Late-stage Rodinian rifting was deflected west around the Belt basin: *Tectonics*, v. 39, no. 8, p.e2020TC006145.

- Brennan, D.T., Pearson, D.M., Link, P.K. and Chamberlain, K.R., 2020b, Geologic map of the Bayhorse anticline, Custer County, Idaho: Idaho Geological Survey Technical Report, #T-20-01, 1:24,000-scale.
- Brennan, D.T., Pearson, D.M., Link, P.K., Milton, J., in review, Connecting the northern sector of the U.S. western Laurentian rift margin: An emerging Neoproterozoic to early Paleozoic tectono-stratigraphic framework for central Idaho: GSA Memoir.
- Carter, C. and Churkin, M., 1977, Ordovician and Silurian graptolite succession in the Trail Creek area, central Idaho--a graptolite zone reference section v. 1020, US Government Printing Office.
- Chapple, W.M., 1978, Mechanics of thin-skinned fold-and-thrust belts: Geological Society of America Bulletin 89, no. 8, p.1189-1198.
- Churkin Jr, M., 1963, Graptolite beds in thrust plates of central Idaho and their correlation with sequence in Nevada: AAPG Bulletin, v. 47, no. 8, p. 1611-1623.
- Coney, P.J. and Reynolds, S.J., 1977, Cordilleran Benioff zones: Nature, v. 270, p. 403-406.
- Coney, P.J., Jones, D.L. and Monger, J.W., 1980, Cordilleran suspect terranes: Nature, v. 288, no. 5789, p. 329-333.
- Coogan, J.C. and Royse Jr, F., 1990, Overview of recent developments in thrust belt interpretation. Geologic field tours of western Wyoming and adjacent Idaho, Montana, and Utah: Geological Survey of Wyoming Public Information circular, v. 29, p. 89-124.
- Copeland, P., Currie, C.A., Lawton, T.F., and Murphy, M.A., 2017, Location, location, location: The variable lifespan of the Laramide orogeny: Geology, v. 45, no. 3, p. 223-226, doi:10.1130/G38810.1
- Dahlen, F.A., 1990, Critical taper model of fold-and-thrust belts and accretionary wedges: Annual Review of Earth and Planetary Sciences, v. 18, no. 1, p. 55-99.
- Dahlstrom, C.D.A., 1970, Structural geology in the eastern margin of the Canadian Rocky Mountains: Bulletin of Canadian Petroleum Geology, v. 18, p. 332-406.
- Davis, D., Suppe, J., Dahlen, F.A., 1983, Mechanics of fold-and-thrust belts and accretionary wedges: Journal of Geophysical Research: Solid Earth, v. 88, no. B2, p. 1153-1172.
- Decelles, P.G., 1986, Sedimentation in a tectonically partitioned, nonmarine foreland basin: The Lower Cretaceous Kootenai Formation, southwestern Montana: Geological Society of America Bulletin, v. 97(8), p. 911-931.
- DeCelles, P.G. and Mitra, G., 1995, History of the Sevier orogenic wedge in terms of critical taper models, northeast Utah and southwest Wyoming: Geological Society of America Bulletin, v. 107, no. 4, p. 454-462.

- DeCelles, P.G., 2004, Late Jurassic to Eocene evolution of the Cordilleran thrust belt and foreland basin system, western U.S.A.: *American Journal of Science*, v. 304, no. 2, p. 105-168, doi:10.2475/ajs.304.2.105
- Dickinson, W.R., 1970. Relations of andesites, granites, and derivative sandstones to arc-trench tectonics: *Reviews of Geophysics*, v. 8, no. 4, p. 813-860.
- Dickinson, W.R., and Snyder, W.S., 1978, Plate tectonics of the Laramide orogeny, *in* Matthews III, V., ed., *Laramide Folding Associated with Basement Block Faulting in the Western United States: Geological Society of America Memoir 151*, p. 355-366, doi:10.1130/MEM151-p355.
- Dickinson, W.R., 2002, The Basin and Range Province as a composite extensional domain: *International Geology Review*, v. 44, no. 1, p.1-38.
- Doughty, P.T. and Chamberlain, K.R., 1996, Salmon River Arch revisited: new evidence for 1370 Ma rifting near the end of deposition in the Middle Proterozoic Belt basin: *Canadian Journal of Earth Sciences*, v. 33, no. 7, p.1037-1052.
- Dover, J.H., 1949, Geology of the Boulder-Pioneer wilderness study area, Blaine and Custer counties, Idaho: *Geological Survey Bulletin*, v. 1497, p.15.
- Dover, J.H., 1980, Status of the Antler orogeny in central Idaho—clarifications and constraints from the Pioneer Mountains, *in* Fouch, T.D., and Magathan, E., eds., *Paleozoic paleogeography of the west-central United States: Rocky Mountain Section (SEPM) of Society of Economic Paleontologists and Mineralogists Paleogeography Symposium I*, p. 371–385.
- Dover, J.H., 1983, Geologic map and sections of the central Pioneer Mountains, Blaine and Custer Counties, central Idaho: U.S. Geological Survey, *Miscellaneous Investigations Series Map I-1319*, scale 1:48,000, 1 sheet.
- Ducea, M. and Saleeby, J., 1998, A case for delamination of the deep batholithic crust beneath the Sierra Nevada, California. *International Geology Review*, v. 40, no. 1, p. 78-93.
- Dumitru, T.A., Gans, P.B., Foster, D.A. and Miller, E.L., 1991, Refrigeration of the western Cordilleran lithosphere during Laramide shallow-angle subduction: *Geology*, v. 19, n. 11, p.1145-1148.
- Egan, S.S., Buddin, T.S., Kane, S.J. and Williams, G.D., 1997, Three-dimensional modelling and visualisation in structural geology: new techniques for the restoration and balancing of volumes. *in* *Proceedings of the 1996 geoscience information group conference on geological visualization. Electronic Geology Special Volume v. 1*, p. 67-82.
- Elliott, D., 1976, A discussion on natural strain and geological structure—the energy balance and deformation mechanisms of thrust sheets: *Philosophical Transactions of the Royal Society of London Series A, Mathematical and Physical Sciences*, v. 283, no. 1312, p.289-312.

- Erslev, E.A., 1993, Thrusts, back-thrusts and detachment of Rocky Mountain foreland arches, *in* Schmidt, C. J., Chase, R. B., and Erslev, E. A., eds., Laramide Basement Deformation in the Rocky Mountain Foreland of the Western United States: Geological Society of America Special Paper, v. 280, p. 339–339.
- Finzel, E.S. and Rosenblume, J.A., 2021, Dating lacustrine carbonate strata with detrital zircon U-Pb geochronology. *Geology*, v. 49(3), p.294-298.
- Foster, D.A., Mueller, P.A., Mogk, D.W., Wooden, J.L., Vogl, J.J., 2006, Proterozoic evolution of the western margin of the Wyoming craton: Implications for the tectonic and magmatic evolution of the northern Rocky Mountains: *Canadian Journal of Earth Sciences*, v. 43, no. 10, p. 1601-1619.
- Fisher, F.S., McIntyre, D.H., and Johnson, K.M., 1992, Geologic map of the Challis 1 degree x 2 degrees quadrangle, Idaho: U.S. Geological Survey, Miscellaneous Investigations Series Map I-1819, scale 1:250,000
- Garber, K.L., Finzel, E.S., Pearson, D.M., 2020, Provenance of synorogenic foreland basin strata in southwestern Montana requires revision of existing models for Laramide tectonism: *North American Cordillera: Tectonics*, v. 39, no. 2, p. e2019TC005944, doi:10.1029/2019TC005944
- Gardner, Cole T., 2021, New insights into the provenance and regional tectonics of a middle Cretaceous retroforeland basin, Southwestern Montana, USA [M.S. Thesis]: Iowa City, University of Iowa.
- Gaschnig, R.M., Vervoort, J.D., Lewis, R.S., McClelland, W.C., 2010, Migrating magmatism in the northern US Cordillera: in situ U–Pb geochronology of the Idaho batholith: *Contributions to Mineralogy and Petrology* 159, p. 863–883, doi:10.1007/s00410-009-0459-5
- Gaschnig, R.M., Vervoort, J.D., Lewis, R.S., Tikoff, B., 2011. Isotopic evolution of the Idaho Batholith and Challis Intrusive Province, Northern US Cordillera. *J.Petrol.* 52, 2397–2429
- Gaschnig, R.M., Vervoort, J.D., Lewis, R.S., and Tikoff, B., 2013, Probing for Proterozoic and Archean crust in the northern U.S. Cordillera with inherited zircon from the Idaho batholith: *Bulletin of the Geological Society of America*, v. 125, p. 73–88, doi: 10.1130/B30583.1
- Gehrels, G.E., Valencia, V.A., and Ruiz, J., 2008, Enhanced precision, accuracy, efficiency, and spatial resolution of U-Pb ages by laser ablation-multicollector-inductively coupled plasma-mass spectrometry: *Geochemistry and Geophysics*, v. 9.
- Gehrels, G., 2012, Detrital Zircon U-Pb Geochronology: Current Methods and New Opportunities, *in* *Tectonics of Sedimentary Basins: Recent Advances*, C. Busby and A. Azor, eds.: Wiley-Blackwell Publishing, p. 47-62.

- Hall, W. E., Batchelder, J. H., and Tschanz, C. M., 1978, Geologic map of the Sun Valley 7.5-minute quadrangle, Blaine County Idaho: U. S. Geological Survey Open-File Report 78- 1058. Scale 1:24,000.
- Haller, K.M., Wheeler, R.L., Adema, G.W., 2010, Quaternary fault and fold database of the United States. US Geol. Surv. [Available at <http://earthquakes.usgs.gov/hazards/qfaults.>].
- Hamilton, W., 1969. Mesozoic California and the underflow of Pacific mantle: Geological Society of America Bulletin, v. 80, no. 12, p. 2409-2430.
- Hays, W.H., McIntyre, D.H., and Hobbs, S.W., 1978, Geologic map of the Lone Pine Peak quadrangle, Custer County, Idaho: U.S. Geological Survey, Open-File Report OF-78-1060, scale 1:62,500.
- Hiess, J., Condon, D.J., McLean, N. and Noble, S.R., 2011, 238U/235U systematics in terrestrial uranium-bearing minerals: Science, v. 335(6076), p. 1610-1614.
- Hobbs, S.W., Hays, W.H., and McIntyre, D.H., 1991, Geologic map of the Bayhorse area, central Custer County, Idaho: U.S. Geological Survey, Miscellaneous Investigations Series Map I-1882, scale 1:62,500.
- Huerta, A.D., 1992, Lake Creek fault: evidence of pre-Challis shear within south-central Idaho. [M.S. Thesis] Pocatello, Idaho State University, 57 p., 5 plates.
- Huh, O.K., 1967, The Mississippian system across the Wasatch line, east-central Idaho, extreme south-western Montana: Montana Geol. Soc. 18th Ann. Field Conf. Guidebook, p. 31-62.
- Hyndman, D. W., 1983, The Idaho batholith and associated plutons, Idaho and western Montana, in Roddick, J. A., ed., Circum-Pacific plutonic terranes: Geological Society of America Memoir 159, p. 213-240.
- James, W.C. and Oaks, R.Q., 1977, Petrology of the Kinnikinic Quartzite (Middle Ordovician), east-central Idaho: Journal of Sedimentary Research, v. 47, no. 4, p.1491-1511.
- Janecke, S.U., 1992, Kinematics and timing of three superposed extensional systems, east central Idaho: Evidence for an Eocene tectonic transition: Tectonics, v. 11, no. 6, p. 1121-1138.
- Kaempfer, J.M., Guenther, W.R., Pearson, D.M., 2021, Proterozoic to Phanerozoic tectonisms in southwestern Montana basement ranges constrained by low temperature thermochronometric data: Tectonics, doi: 10.1029/2021TC006744
- Kamb, W.B., 1959, Petrofabric observations from Blue Glacier, Washington, in relation to theory and experiment: J. Geophys. Res., v. 64, p. 1908-1909.
- Kim, A.Y.H., 1986, The kinematics of brittle polyphase deformation within the Pioneer metamorphic core complex, Pioneer Mountains, Idaho (Master's thesis, Lehigh University).

- Kley, J., Monaldi, C.R. and Salfity, J.A., 1999, Along-strike segmentation of the Andean foreland: causes and consequences: *Tectonophysics*, v. 301(1-2), p.75-94.
- Krohe, N., 2016, Structural framework and detrital zircon provenance of the southern portion of the Clayton quadrangle, Custer County, Idaho [M.S. Thesis]: Pocatello, Idaho, Idaho State University, 107 p., 1 plate.
- Kulik, D.M., Schmidt, C.J. and Perry, W.J., 1988, Region of overlap and styles of interaction of Cordilleran thrust belt and Rocky Mountain foreland, *in* Schmidt, C.J., and Perry, W.J., Jr., editors, *Interaction of the Rocky Mountain foreland and the Cordilleran thrust belt: Geological Society of America Memoir*, v. 171, p. 75-98.
- Lacombe, O., and Bellahsen, N., 2016, Thick-skinned tectonics and basement-involved fold–thrust belts: insights from selected Cenozoic orogens: *Geological Magazine*, v. 153, no. 5-6, p. 763-810, doi:10.1017/S0016756816000078
- Lewis, R.S., Link, P.K., Stanford, L., and Long, S.P., 2012, Geologic map of Idaho: Idaho Geological Survey Map M-9, scale 1:750,000.
- Li, Z.X., Bogdanova, S.V., Collins, A.S., Davidson, A., De Waele, B., Ernst, R.E., Fitzsimons, I.C.W., Fuck, R.A., Gladkochub, D.P., Jacobs, J., Karlstrom, K.E., Lu, S., Natapov, L.M., Pease, V., Pisarevsky, S.A., Thrane, K., and Vernikovsky, V., 2008, Assembly, configuration, and break-up history of Rodinia: A synthesis: *Precambrian Research*, v. 160, no. 1–2, p. 179–210, doi:10.1016/j.precamres.2007.04.021.
- Link, P.K., Skipp, B., Hait Jr, M.H., Janecke, S. and Burton, B.R., 1988, Structural and stratigraphic transect of south-central Idaho: a field guide to the Lost River, White Knob, Pioneer, Boulder, and Smoky Mountains. *Guidebook to the geology of central and southern Idaho: Idaho Geological Survey Bulletin*, v. 27, p. 5-42.
- Link, P.K., Warren, I., Preacher, J.M., and Skipp, B., 1996, Stratigraphic analysis and interpretation of the Mississippian Copper Basin Group, McGowan Creek Formation, and White Knob Limestone, south-central Idaho, in Longman, M.W., Sonnenfield, M.D., eds., *Paleozoic Systems of the Rocky Mountain Region: Rocky Mountain Section, SEPM (Society for Sedimentary Geology)*, p. 117-144.
- Link, P.K. and Lewis, R.S. eds., 2007, *Proterozoic geology of western North America and Siberia: SEPM (Society for Sedimentary Geology) Special Publication 86*, p. 101-128
- Link, P.K., Autenrieth-Durk, K.M., Cameron, A., Fanning, C.M., Vogl, J.J., Foster, D.A., 2017a, U-Pb zircon ages of the Wildhorse gneiss, Pioneer Mountains, south-central Idaho, and tectonic implications: *Geosphere*, v. 13, no. 3, p.681-698.
- Link, P.K., Todt, M.K., Pearson, D.M., and Thomas, C., 2017, 500–490 Ma detrital zircons in Upper Cambrian Worm Creek and correlative sandstones, Idaho, Montana, and Wyoming: Magmatism and tectonism within the passive margin: *Lithosphere*, v. 9, p. 910–926, <https://doi.org/10.1130/L671.1>.

- Liu, S. and Currie, C.A., 2016, Farallon plate dynamics prior to the Laramide orogeny: Numerical models of flat subduction: *Tectonophysics*, v. 666, p. 33-47, doi:10.1016/j.tecto.2015.10.010
- Livaccari, R.F., Burke, and K. Şengör, A.M.C., 1981, Was the Laramide orogeny related to subduction of an oceanic plateau?: *Nature*, v. 289, p. 276-278.
- Ludwig, K., 2008, Isoplot version 4.15: a geochronological toolkit for microsoft Excel. Berkeley Geochronology Center, Special Publication, v. 4, p.247-270.
- Mahoney, J.B., Link, P.K., Burton, B.R., Geslin, J.K., and O'Brien, J.P., 1991, Pennsylvanian and Permian Sun Valley Group, Wood River basin, south-central Idaho, *in* Cooper, J.D., and Stevens, C.H., eds., *Paleozoic paleogeography of the western United States, Volume II: Los Angeles, Pacific Section, SEPM (Society for Sedimentary Geology)*, p. 551–579. Los Angeles, Pacific Section, SEPM (Society for Sedimentary Geology), p. 551–579
- Mahoney, J.B., 1995, Geologic setting of mineral deposits in the Washington Basin Area, Custer County, south-central Idaho: *U.S. Geological Survey Bulletin*, p. G1–G12.
- Ma, C., Foster, D.A., Mueller, P.A., Dutrow, B.L. and Marsh, J., 2021. Mesozoic crustal melting and metamorphism in the US Cordilleran hinterland: Insights from the Sawtooth metamorphic complex, central Idaho. *GSA Bulletin*, v. 133, no. 9-10, p. 2031-2050.
- Maletz, J., Steiner, M. and Fatka, O., 2005, Middle Cambrian pterobranchs and the question: What is a graptolite?: *Lethaia*, v. 38, no. 1, p. 73-85.
- Mapel, W.J., Read, W.H., and Smith, R.K., 1965, Geologic map and sections of the Doublespring quadrangle, Custer and Lemhi Counties, Idaho: *U.S. Geological Survey, Geologic Quadrangle Map GQ-464*, scale 1:62,500.
- McCandless, D.O., 1982, A reevaluation of Cambrian through Middle Ordovician stratigraphic of southern Lemhi Range [M.S. Thesis]: University Park, The Pennsylvania State University, 235 p.
- McClelland, W.C., and Oldow, J.S., 2004, Displacement transfer between thick- and thin-skinned décollement systems in the central North American Cordillera: *Geological Society, London, Special Publications*, v. 227, no. 1, p. 177–195.
- McDowell, R. J., 1997, Evidence for synchronous thin-skinned and basement deformation in the Cordilleran fold-thrust belt: the Tendoy Mountains, southwestern Montana: *Journal of Structural Geology*, v. 19, no. 1, p. 77-87, doi:10.1016/S0191-8141(96)00044-2.
- McKinney, F.K. and Gault, H.W., 1980, Paleoenvironment of Late Mississippian fenestrate bryozoans, eastern United States: *Lethaia*, v. 13(2), p. 127-146.
- Messina, T. A. (1993) The geometry and kinematics of intra-thrust sheet decollement folding: Lost River Range, Idaho. [M.S. Thesis]: Bethlehem, Lehigh University. 45 p.

- Milton, J., 2020, Geologic mapping, stratigraphy, and detrital zircon geochronology of the southeastern Borah Peak horst, Custer County, Idaho: Age reassignment and correlation of Neoproterozoic to Lower Paleozoic strata, [M.S. Thesis]: Pocatello, Idaho State University. 145 p, 1 plate.
- Montoya, L., 2019, Investigation of structural style within the Sevier fold-thrust belt along the southwester boundary of the Lemhi arch, central Idaho, [M.S. Thesis]: Pocatello, Idaho State University. 80 p, 4 plates.
- Moye, F.J., Hackett, W.R., Blakey, J.D., and Snider, L.G., 1988, Regional geologic setting and volcanic stratigraphy of the Challis volcanic field, central Idaho, *in* Link, P. K., and Hackett, W. R., eds, Guidebook to the Geology of Central and Southern Idaho: Idaho Geological Survey Bulletin 27, p. 87-97.
- Mueller, P.A., Wooden, J.L., Mogk, D.W. and Foster, D.A., 2011, Paleoproterozoic evolution of the Farmington zone: Implications for terrane accretion in southwestern Laurentia: *Lithosphere*, v. 3, no. 6, p. 401-408.
- Neely, K.W., 1981, Stratigraphy and paleoenvironments of the Late Mississippian White Knob Formation and equivalent rocks in the White Knob Mountains, south-central Idaho: [M.S. Thesis]: Moscow, University of Idaho. p. 142.
- Nichols, D.J., Perry Jr, W.J. and Haley Johns, J.C., 1985, Reinterpretation of the palynology and age of Laramide syntectonic deposits, southwestern Montana, and revision of the Beaverhead Group: *Geology*, v. 13(2), p. 149-153.
- Nilsen, T.H., 1977, Paleogeography of Mississippian turbidites in south-central Idaho, *in* J.H. Stewart, C.H. Stevens, and A.E. Fritsche, eds., Paleozoic paleogeography of the western United States: Pacific Coast Paleogeography Symposium I, SEPM, Pacific Section, Los Angeles, California, p. 275-299.
- Palleiko, D.M., 2000, Structural analysis of the Pioneer thrust fault, Big and Little Fall Creek drainages, Pioneer Mountains, Blaine and Custer counties, Idaho.
- Parker, S. D., 2021, Stratigraphic control on the transition from thin- to thick-skinned thrusting in the Idaho-Montana fold-thrust belt, [Ph.D. Dissertation]: Pocatello, Idaho State University, 234 p., 2 plates.
- Parker, S. D., and Pearson, D. M., 2021, Pre-thrusting stratigraphic control on the transition from a thin-skinned to thick-skinned structural style: An example from the double-decker Idaho-Montana fold-thrust belt: *Tectonics*, v. 40, e2020TC006429, <https://doi.org/10.1029/2020TC006429>.
- Paull, R.A., M. A. Wolbrink, R.G. Volkman, and R.L. Grover, 1972, Stratigraphy of Copper Basin Group, Pioneer Mountains, south-central Idaho: *AAPG Bulletin*, v. 56, p. 1370-1401.
- Pearson, D.M., Kapp, P., DeCelles, P.G., Reiners, P.W., Gehrels, G.E., Ducea, M.N., and Pullen, A., 2013, Influence of pre-Andean crustal structure on Cenozoic thrust belt kinematics and shortening magnitude: Northwestern Argentina: *Geosphere*, v. 9, no. 6, p. 1766-1782, doi:10.1130/GES00923.1

- Pearson, D.M., and Link, P.K., 2017, Field guide to the Lemhi arch and Mesozoic-Early Cenozoic faults and folds in east-central Idaho: Beaverhead Mountains: Northwest Geology, v. 46, p. 101-112
- Pfiffner, O.A., 2017, Thick-skinned and thin-skinned tectonics: a global perspective: Geosciences, v. 7, no. 3, p. 71, doi:10.3390/geosciences7030071
- Rember W.C., and E.H. Bennett, 1979, Geologic map of the Pullman quadrangle, Idaho: Idaho Bureau of Mines and Geology, scale 1:250,000.
- Roberts, R.J., Hotz, P.E., Gilluly, J. and Ferguson, H.G., 1958, Paleozoic rocks of north-central Nevada: AAPG Bulletin, v. 42(12), p. 2813-2857.
- Rodgers, D.W., and Janecke, S.U., 1992, Tertiary paleogeologic maps of the western Idaho-Wyoming-Montana thrust belt, *in* Link, P. K., Kuntz, M. A., and Platt, L. B., eds., Regional Geology of Eastern Idaho and Western Wyoming: Geological Society of America Memoir 179, p. 83–94.
- Rodgers, D.W., Link, P.K., and Huerta, A.D., 1995, Structural framework of mineral deposits hosted by Paleozoic rocks in the northeastern part of the Hailey 1°x 2° quadrangle, south-central Idaho, *in* Worl, R.G., Link, P.K., Winkler, G.R., and Johnson, K.M., eds., Geology and Mineral Resources of the Hailey 1°x2° Quadrangle and the Western Part of the Idaho Falls 1°x2° Quadrangle, Idaho: United States Geological Survey Bulletin 2064-B, p. B-1–15.
- Rosenblume, J.A., Finzel, E.S. and Pearson, D.M., 2021, Early Cretaceous provenance, sediment dispersal, and foreland basin development in southwestern Montana, North American Cordillera: Tectonics, v. 40, no. 4, p.e2020TC006561.
- Ross, C.P., 1934, Correlation and interpretation of Paleozoic stratigraphy in south-central Idaho: Geological Society of America Bulletin, v. 45, p. 937–1000, doi:10.1130/gsab-45-937.
- Ross, C.P., 1947, Geology of the Borah Peak quadrangle, Idaho. Geological Society of America Bulletin, v. 58(12), p. 1085-1160.
- Ross, C.P., 1962, Upper Paleozoic rocks in central Idaho: AAPG Bulletin, v. 46, no. 3, p. 384-405.
- Royse, F., Warner, M.A., and Reese, D.L., 1975, Thrust belt structural geometry and related stratigraphic problems, Wyoming-Idaho-Northern Utah: Rocky Mountain Association of Geologists 1975 Symposium, p. 41-54.
- Ruppel, E.T., 1986, The Lemhi arch: a late Proterozoic and early Paleozoic landmass in central Idaho, *in* Peterson, J.A., ed., Paleotectonics and sedimentation in the Rocky Mountain region, United States: American Association of Petroleum Geologists Memoir 41, p. 119– 130, doi: 10 .1306 /M41456C6.
- Saleeby, J., 2003, Segmentation of the Laramide Slab – evidence from the southern Sierra Nevada region: Geological Society of America Bulletin, v. 115, no. 6, p. 655-668.

- Sandberg, C.A., Geological survey (Estados Unidos) and government printing office, 1975, McGowan Creek Formation, new name for lower Mississippian flysch sequence in east-central Idaho. US Government Printing Office.
- Schoene B. 2014. U-Th-Pb geochronology. In *The Crust*, ed. RL Rudnick, p. 341–78. Treatise Geochem. 4. Amsterdam: Elsevier. 2nd ed.
- Scholten, R., 1957, Paleozoic evolution of the geosynclinal margin north of the Snake River Plain, Idaho-Montana: Geological Society of America Bulletin, v. 68, no. 2, p. 151-170.
- Skipp, B.A., 1961, Interpretation of sedimentary features in Brazer Limestone (Mississippian) near Mackay, Custer County, Idaho: AAPG Bulletin, v. 45, no. 3, p. 376-389.
- Skipp, B. and Mamet, B.L., 1970, Stratigraphic micropaleontology of the type locality of the White Knob Limestone (Mississippian), Custer County, Idaho: US Geological Survey Professional Paper, v. 700, p. B118-B123.
- Skipp, B. and Hait Jr, M.H., 1977, Allochthons along the northeast margin of the Snake River Plain: Wyoming Geological Association 29th Annual Field Conference Guidebook, v. 29, p. 499-515.
- Skipp, B., Hoggan, R. D., Schleicher, A. & Douglas, R. C. 1979a. Upper Paleozoic carbonate bank in east-central Idaho---Snaky Canyon, Bluebird Mountain, and Arco Hills Formations and their paleotectonic significance. Bull. U.S. geol. Surv. 1486.
- Skipp, B., Sando, W.J., and Hall, W.E., 1979b, Mississippian and Pennsylvanian (Carboniferous) systems in the United States-Idaho: U.S. Geological Survey Prof. Paper 1110-AA.
- Skipp, B., 1988, Cordilleran thrust belt and faulted foreland in the Beaverhead Mountains, Idaho and Montana, *in* Schmidt, C.J., and Perry, W.J., Jr., eds., Interaction of the Rocky Mountain foreland and the Cordilleran thrust belt: Geological Society of America Memoir 171, p. 237-266.
- Skipp, B., and Link, P. K., 1992, Middle and Late Proterozoic rocks and Late Proterozoic tectonics in the southern Beaverhead Mountains, Idaho and Montana: A preliminary report, *in* Link, P.K., Kuntz, M.A., and Platt, L.B. eds., Regional Geology of Eastern Idaho and Western Wyoming: Geological Society of America Memoirs, v. 179, p. 141-154.
- Skipp, A., Wilson., B., 1994, Geologic map of the eastern part of the Challis National Forest and vicinity, Idaho. USGS miscellaneous investigations series map I-2395, Denver, CO, scale 1:250,000.
- Skipp, B., Hall, W.E. and Link, P.K., 1994, Geologic Map of the Mahoney Butte Quadrangle, Blaine County, Idaho. USGS geologic quadrangle map GQ-1742, scale 1:24,000.

- Skipp, B., and Janecke, S.U., 2004, Geologic map of the Montana part of the Dubois 30' × 60' quadrangle, southwest Montana: Montana Bureau of Mines and Geology open-file report MBMG 490, scale 1:100,000, 1 sheet, 13 p. text.
- Skipp, B., Snider, L.G., Janecke, S.U. and Kuntz, M.A., 2009, Geologic map of the Arco 30× 60 minute quadrangle, south-central Idaho. Moscow, Idaho, Idaho Geological Survey, scale 1:100,000.
- Skipp, B., and Brandt, T.R., 2012, Geologic map of the Fish Creek Reservoir 7.5' quadrangle, Blaine County, Idaho: U.S. Geological Survey Scientific Investigations Map 3191, 1 sheet, scale 1:24,000, pamphlet, 15 p.
- Skipp, B., and McIntyre, unpublished, Geologic map of the Horse Basin Quadrangle, Jerry Peak quadrangle, Herd Lake quadrangle, and The Paint Pot quadrangle, Custer County, Idaho: Personal communication, scale 1:24,000.
- Sloss, L.L., 1950, Paleozoic sedimentation in Montana area: AAPG Bulletin, v. 34(3), p. 423-451.
- Soulliere, S.J., Worl, R.G. and Johnson, K.M., 1989, Geology and mineral deposits of the Hailey and western Idaho Falls 1 degree x 2 degrees quadrangles, Idaho (No. 89-639): US Geological Survey open-file report 89-639, v. ii, 140 p.
- Stewart, J.H., 1972, Initial Deposits in the Cordilleran Geosyncline: Evidence of a Late Precambrian (<850 m.y.) Continental Separation: Geological Society of America Bulletin, v. 83, p. 1345–1360.
- Stockmal, G.S., Beaumont, C., Nguyen, M., and Lee, B., 2007, Mechanics of thin-skinned fold-and-thrust belts: Insights from numerical models *in* Sears, J.W., Harms, T.A., and Evenchick, C.A., eds., *Whence the Mountains? Inquiries into the evolution of orogenic systems: A volume in Honor of Raymond A. Price*: Geological Society of America Special Paper 433, p. 63–98.
- Strickland, A., Miller, E.L., Wooden, J.L., 2011, The timing of Tertiary metamorphism and deformation in the Albion–Raft River–Grouse Creek metamorphic core complex, Utah and Idaho: *The Journal of Geology*, v. 119, no. 2, p. 185-206.
- Umpleby, J.B., 1917, *Geology and ore deposits of the Mackay region, Idaho*, v. 97, US Government Printing Office.
- Vervoort, J.D., Lewis, R.S., Fisher, C., Gaschnig, R.M., Jansen, A.C. and Brewer, R., 2016, Neoproterozoic and Paleoproterozoic crystalline basement rocks of north-central Idaho: Constraints on the formation of western Laurentia: *GSA Bulletin*, v. 128, no. 1-2, p. 94-109.
- Vogl, J., Borel, M., McFadden, R., Ortiz-Guerrero, C., 2021, A tale of two detachments: structural relationships and strain along the northwest margin of the Pioneer Mountains metamorphic core complex: *Northwest Geology*, v. 50, p. 69-77.
- Wilson, E., 1994, Demise of the Glide Mountain thrust fault, Pioneer Mountains, Blaine and Custer counties, south-central Idaho. [M.S. Thesis]: Pocatello, Idaho State University. 188 p., 2 plates.

- Wilson, E., Preacher, J. M., and Link, P. K., 1994, New constraints on the nature of the Early Mississippian Antler sedimentary basin in Idaho, *in* Embry, A. F., Beauchamp, B., and Glass, D.J., eds., *Pangea: Global environments and resources: Canadian Society of Petroleum Geologists Memoir 17*, p. 155–174
- Wetherill, G.W., 1956. Discordant uranium-lead ages, I. *Eos, Transactions American Geophysical Union*, v. 37, no. 3, p. 320-326.chall
- Woodcock, N.H., 1977, Specification of fabric shapes using an eigenvalue method: *Geological Society of America Bulletin*, v. 88(9), p. 1231-1236.
- Worl, R.G., Kiilsgaard, T.H., Bennett, E.H., Link, P.K., Lewis, R.S., Mitchell, V.E., Johnson, K.M., and Snyder, L.D., 1991, Geologic map of the Hailey 1°x 2° Quadrangle, Idaho: U.S. Geological Survey Open-File Report 91-340, scale 1:250,000.
- Yonkee, W.A., Dehler, C.D., Link, P.K., Balgord, E.A., Keeley, J.A., Hayes, D.S., Wells, M.L., Fanning, C.M., and Johnston, S.M., 2014, Tectono-stratigraphic framework of Neoproterozoic to Cambrian strata, west-central US: Protracted rifting, glaciation, and evolution of the North American Cordilleran margin: *Earth-Science Reviews*, v. 136, p. 59-95, doi:10.1016/j.earscirev.2014.05.004
- Yonkee, W.A., and Weil, A.B., 2015, Tectonic evolution of the Sevier and Laramide belts within the North American Cordillera orogenic system: *Earth-Science Reviews*, v. 150, p. 531-593, doi:10.1016/j.earscirev.2015.08.001.

Figure 16: 20CP14 U-Pb geochronologic analyses							Isotope ratios					Apparent ages (Ma)							
Analysis	U	206Pb	U/Th	206Pb*	±	207Pb*	±	206Pb*	±	error	206Pb*	±	207Pb*	±	206Pb*	±	Best age	±	Conc
	(ppm)	204Pb		207Pb*	(%)	235U*	(%)	238U	(%)	corr.	238U*	(Ma)	235U	(Ma)	207Pb*	(Ma)	(Ma)	(Ma)	(%)
20CP14 -Spot 28	99	588	1.4	32.7449	20.5	0.0597	21.3	0.0142	5.8	0.27	90.8	5.3	58.9	12.2	NA	NA	90.8	5.3	NA
20CP14 -Spot 15	237	2578	2.7	19.5579	5.0	0.1004	6.4	0.0142	4.0	0.63	91.2	3.6	97.1	6.0	245.7	115.6	91.2	3.6	NA
20CP14 -Spot 5	119	866	0.9	29.3090	12.5	0.0671	13.5	0.0143	5.0	0.37	91.3	4.6	65.9	8.6	NA	NA	91.3	4.6	NA
20CP14 -Spot 21	273	4312	2.2	19.0449	4.7	0.1039	7.1	0.0144	5.3	0.75	91.9	4.8	100.3	6.8	306.6	107.4	91.9	4.8	NA
20CP14 -Spot 1	660	89478	1.1	19.9288	2.6	0.0995	5.2	0.0144	4.5	0.87	92.1	4.1	96.3	4.8	202.3	59.5	92.1	4.1	NA
20CP14 -Spot 13	249	1753	2.2	20.7153	5.4	0.0970	7.7	0.0146	5.4	0.71	93.3	5.0	94.0	6.9	111.7	128.3	93.3	5.0	NA
20CP14 -Spot 17	208	959	2.1	25.8664	6.6	0.0781	8.1	0.0146	4.7	0.58	93.7	4.4	76.3	6.0	NA	NA	93.7	4.4	NA
20CP14 -Spot 23	240	811	2.5	30.5394	9.8	0.0662	11.3	0.0147	5.6	0.49	93.8	5.2	65.1	7.1	NA	NA	93.8	5.2	NA
20CP14 -Spot 20	257	6370	3.8	13.6762	9.5	0.1502	10.2	0.0149	3.6	0.36	95.3	3.4	142.1	13.5	1016.4	193.5	95.3	3.4	NA
20CP14 -Spot 26	252	9872	2.7	10.2819	11.5	0.1999	12.7	0.0149	5.2	0.41	95.4	4.9	185.0	21.4	1571.4	217.0	95.4	4.9	NA
20CP14 -Spot 30	214	1413	2.1	21.5776	7.3	0.0956	9.2	0.0150	5.5	0.60	95.7	5.2	92.7	8.1	14.5	176.6	95.7	5.2	NA
20CP14 -Spot 8	144	2448	2.7	20.3345	5.6	0.1024	7.8	0.0151	5.5	0.70	96.7	5.3	99.0	7.4	155.3	130.4	96.7	5.3	NA
20CP14 -Spot 2	227	1076	2.7	24.8971	18.7	0.0837	19.4	0.0151	5.4	0.28	96.8	5.2	81.6	15.3	NA	NA	96.8	5.2	NA
20CP14 -Spot 22	241	172200	2.5	16.8156	5.7	0.1245	7.6	0.0152	5.1	0.67	97.2	4.9	119.2	8.6	583.3	123.6	97.2	4.9	NA
20CP14 -Spot 7	297	12489	1.7	19.9953	3.5	0.1052	6.5	0.0153	5.5	0.84	97.6	5.3	101.5	6.3	194.5	81.8	97.6	5.3	NA
20CP14 -Spot 24	148	1150	2.4	28.3017	20.3	0.0744	20.8	0.0153	4.5	0.22	97.7	4.4	72.9	14.6	NA	NA	97.7	4.4	NA
20CP14 -Spot 11	162	1664	2.2	21.2594	6.3	0.1000	8.2	0.0154	5.2	0.64	98.7	5.1	96.8	7.6	50.1	150.8	98.7	5.1	NA
20CP14 -Spot 6	304	20286	1.3	19.9723	3.4	0.1089	5.0	0.0158	3.7	0.74	101.0	3.7	105.0	5.0	197.2	78.5	101.0	3.7	NA
20CP14 -Spot 29	297	37196	1.9	14.5597	5.8	0.1527	6.8	0.0161	3.5	0.52	103.2	3.6	144.3	9.1	888.3	120.0	103.2	3.6	NA

Figure 17: 20CP16 U-Pb geochronologic analyses																			
							Isotope ratios						Apparent ages (Ma)						
Analysis	U	206Pb	U/Th	206Pb*	±	207Pb*	±	206Pb*	±	error	206Pb*	±	207Pb*	±	206Pb*	±	Best age	±	Conc
	(ppm)	204Pb		207Pb*	(%)	235U*	(%)	238U	(%)	corr.	238U*	(Ma)	235U	(Ma)	207Pb*	(Ma)	(Ma)	(Ma)	(%)
20CP16 -Spot 9	54	106	1.2	2.5439	25.4	1.3517	34.1	0.0250	22.8	0.67	158.9	35.8	868.3	201.7	3882.2	389.5	158.9	35.8	NA
20CP16 -Spot 8	1462	14917	4.2	19.7382	2.5	0.0998	4.3	0.0143	3.5	0.81	91.5	3.1	96.6	3.9	224.5	58.3	91.5	3.1	NA
20CP16 -Spot 6	2207	56282	3.5	19.9552	1.7	0.1043	4.0	0.0151	3.6	0.91	96.7	3.5	100.8	3.8	199.2	38.7	96.7	3.5	NA
20CP16 -Spot 5	1411	8006	3.8	20.5989	1.8	0.0949	3.4	0.0142	2.8	0.84	90.8	2.6	92.1	3.0	124.9	42.7	90.8	2.6	NA
20CP16 -Spot 4	1579	26532	3.4	20.0575	1.6	0.0956	4.2	0.0139	3.9	0.93	89.1	3.4	92.7	3.7	187.3	36.5	89.1	3.4	NA
20CP16 -Spot 30	449	7593	5.3	20.5709	4.3	0.0933	5.8	0.0139	3.9	0.67	89.2	3.5	90.6	5.1	128.2	102.3	89.2	3.5	NA
20CP16 -Spot 3	1245	4186	2.4	20.0129	3.1	0.0988	4.0	0.0143	2.5	0.63	91.8	2.3	95.7	3.7	192.5	72.2	91.8	2.3	NA
20CP16 -Spot 29	1248	14851	2.4	19.8501	2.1	0.0999	6.2	0.0144	5.8	0.94	92.1	5.3	96.7	5.7	211.4	48.4	92.1	5.3	NA
20CP16 -Spot 26	1759	7770	5.1	20.6847	2.7	0.0928	3.9	0.0139	2.9	0.74	89.1	2.6	90.1	3.4	115.2	62.5	89.1	2.6	NA
20CP16 -Spot 25	2382	20139	2.8	20.1606	1.6	0.1018	5.4	0.0149	5.1	0.95	95.3	4.8	98.4	5.0	175.3	38.4	95.3	4.8	NA
20CP16 -Spot 22	1429	36083	3.5	19.4790	2.0	0.1050	3.5	0.0148	2.9	0.82	94.9	2.7	101.4	3.4	255.0	46.3	94.9	2.7	NA
20CP16 -Spot 21	1064	1763	2.0	18.3396	5.6	0.1067	6.9	0.0142	4.0	0.58	90.8	3.7	102.9	6.8	391.9	126.7	90.8	3.7	NA
20CP16 -Spot 19	1672	5991	3.5	21.5152	3.1	0.0926	4.6	0.0145	3.4	0.75	92.5	3.2	89.9	4.0	21.5	73.6	92.5	3.2	NA
20CP16 -Spot 18	810	33629	3.5	19.3885	2.5	0.1011	4.9	0.0142	4.3	0.86	91.0	3.8	97.8	4.6	265.7	57.4	91.0	3.8	NA
20CP16 -Spot 17	1424	4457	4.2	20.8059	2.6	0.0934	4.3	0.0141	3.4	0.80	90.2	3.1	90.6	3.7	101.3	61.8	90.2	3.1	NA
20CP16 -Spot 16	1052	37456	4.1	19.3851	2.1	0.1035	3.7	0.0146	3.0	0.81	93.1	2.7	100.0	3.5	266.1	49.2	93.1	2.7	NA
20CP16 -Spot 15	821	7960	3.8	20.5766	3.4	0.0970	5.0	0.0145	3.7	0.74	92.6	3.4	94.0	4.5	127.5	79.0	92.6	3.4	NA
20CP16 -Spot 14	561	38243	1.5	19.0853	3.5	0.0992	6.1	0.0137	4.9	0.82	88.0	4.3	96.1	5.6	301.7	80.0	88.0	4.3	NA
20CP16 -Spot 13	2560	47239	2.4	20.6798	1.7	0.1129	4.3	0.0169	3.9	0.92	108.3	4.2	108.6	4.4	115.7	39.0	108.3	4.2	NA
20CP16 -Spot 11	436	7502	3.6	18.8622	3.9	0.1009	5.1	0.0138	3.3	0.65	88.4	2.9	97.6	4.8	328.5	88.8	88.4	2.9	NA
20CP16 -Spot 1	877	7175	3.3	18.5210	3.8	0.1055	5.0	0.0142	3.2	0.65	90.8	2.9	101.8	4.8	369.7	85.9	90.8	2.9	NA

GEOLOGIC MAP OF THE NORTHEASTERN PART OF THE HORSE BASIN QUADRANGLE, BROKEN WAGON CANYON, CUSTER COUNTY, IDAHO

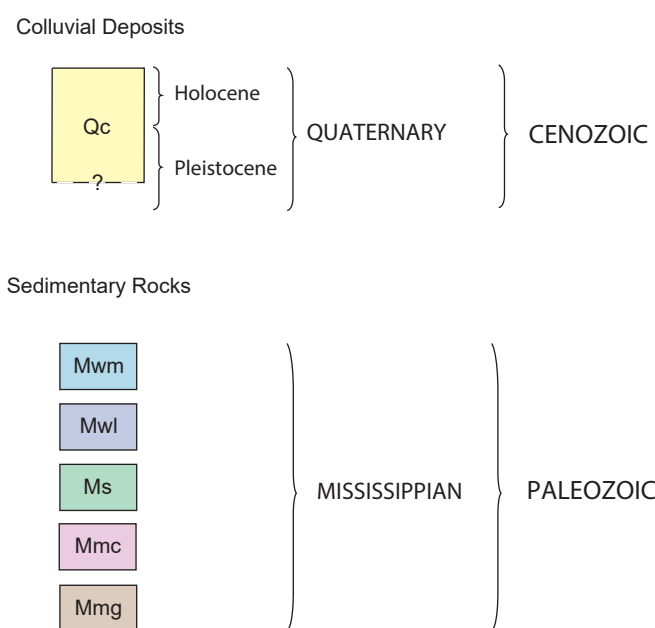
Edwin C. Porter

Idaho State University, Department of Geosciences
Plate 1 in Porter, 2021 ISU M.S. Thesis

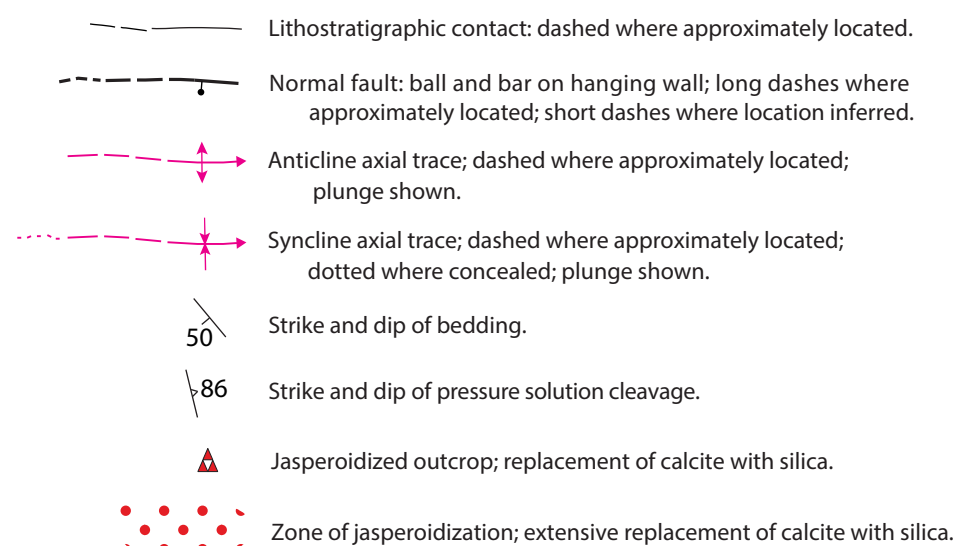
DESCRIPTION OF MAP UNITS

Grain size classification of unconsolidated and consolidated sediment is based on the Wentworth scale (Lane, 1947). Carbonate rocks are described using Dunham's (1962) classification. Unit thicknesses and map distances are listed in metric units.

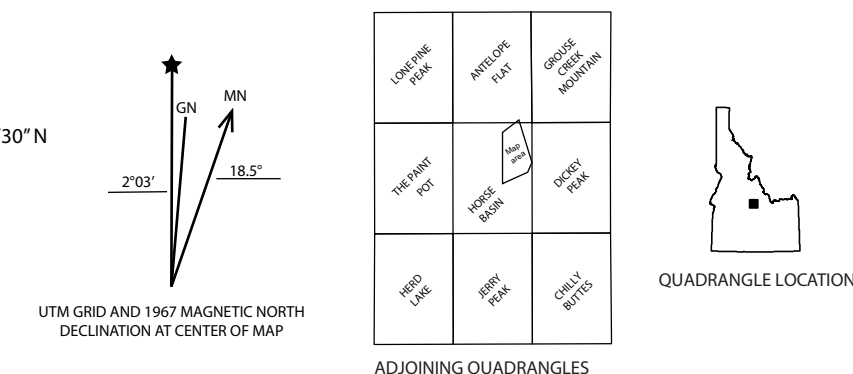
CORRELATION OF MAP UNITS



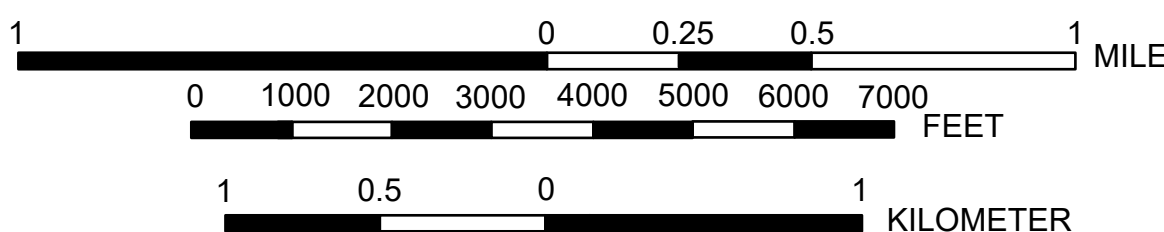
SYMBOLS



QUADRANGLE LOCATION



SCALE 1:24,000



Contour interval 40 feet

Base Map Credit

Mapped, edited, and published by the Geological Survey Control by USGS and USC&GS.

Topography by photogrammetric methods from aerial photographs taken in 1966. Field checked 1967.

Polyconic projection, 1927 North American datum 10,000-foot grid based on Idaho coordinate system, central zone, 1000-meter Universal Transverse Mercator grid ticks, zone 11.

Field work conducted in the summer of 2020. Funding for this research was provided by NSF-Tectonics EAR-1728563. Map version 12-8-2021.

COLLUVIAL DEPOSITS

Qc Colluvium (Holocene)—Sub-rounded to angular unconsolidated colluvium ranging between clay and cobble-sized grains. Sorting ranges from poor to moderate. Thickness varies throughout field area, ranging between ~1-3 m thick, with increased thickness in drainages.

PALEOZOIC STRATA

Mwm Middle White Knob Limestone (Mississippian)—Dark gray to medium gray-weathering limestone with interbedded medium gray to tan-brown chert and quartz pebble conglomerate, as well as brown weathering yellow-tan sandstone. Limestone ranges from lime (micritic) mudstone to packstone. Beds are planar with gradational (between lime beds) and sharp (between lime and siliceous beds) contacts and range between 0.5 m to 3 m thick. Total thickness in the field area is minimally 80 m thick (upper contact not preserved in field area). Dominantly ledge forming. Gradational contact below with Lower White Knob Limestone. Contact above is not exposed in the field area. Fossils in lime beds include crinoid fragments (common; 1 mm to 2 cm diameter), brachiopods (occasional; 5 mm to 1 cm diameter), and bryozoans (occasional; 4 mm to 5 cm in length). Chronostratigraphically correlative to uppermost Scott Peak Formation, South Creek Formation, and Surret Canyon Formation in the Lost River Range (Skipton and Mamet, 1970; Link et al., 1996).

Mwl Lower White Knob Limestone (Mississippian)—Dark gray to medium-gray-weathering limestone. Lime (micritic) mudstone to packstone, with interbeds of brown to tan weathering mudstone and siltstone near base of formation. Very rare beds of lime-clast conglomerate (clasts range between 5 mm and 5 cm in size) near upper part of unit. Occasional beds contain nodular black chert or bedded chert. Toward the upper part of the Lower White Knob Limestone, the unit becomes a locally-cherty, abundantly-fossiliferous wackestone to grainstone with diverse fauna. Limestone beds are planar with gradational contact between and range from 2 cm to 2 m thick. Siliceous beds are planar with sharp contacts between and range between 5 mm and 3 cm thick. Total thickness in the field area is approximately 400 m thick. Dominantly ledge-forming. Gradational contact below with Scott Peak Formation, marked by appearance of fine-grained marker bed. Gradational contact above with Middle White Knob Limestone, marked by first appearance of siliceous conglomerate bed. Fossils include crinoid fragments (common; 1 mm to 2 cm diameter), bryozoans (common, especially near top of unit; fan and fenestrate; 4 mm to 7 cm in length), rugose corals (occasional; 1 cm to 18+ cm in length rarely), colonial corals (rare; 4 cm to 25 cm diameter), brachiopods (occasional; <1 cm in length, rarely 10+ cm in length), bivalves (rare; 1 cm to 3 cm in length), and gastropods (rare; 1 cm to 2.5 cm diameter). Beds commonly deformed into detachment folds (~25 m wavelength), with rare cleavage. Unit is commonly fetid. Temporally correlative to Middle Canyon Formation and the Scott Peak Formation in the White Knob Mountains (Link et al., 1996). A lower marker bed is dark gray to medium-dark-gray-weathering limestone. Dominantly lime (micritic) mudstone with rare wackestone. Bed is planar and roughly 2 m thick. Fossil content includes crinoid fragments (uncommon; 1 mm to 3 mm diameter) and brachiopods (3 mm to 6 mm diameter).

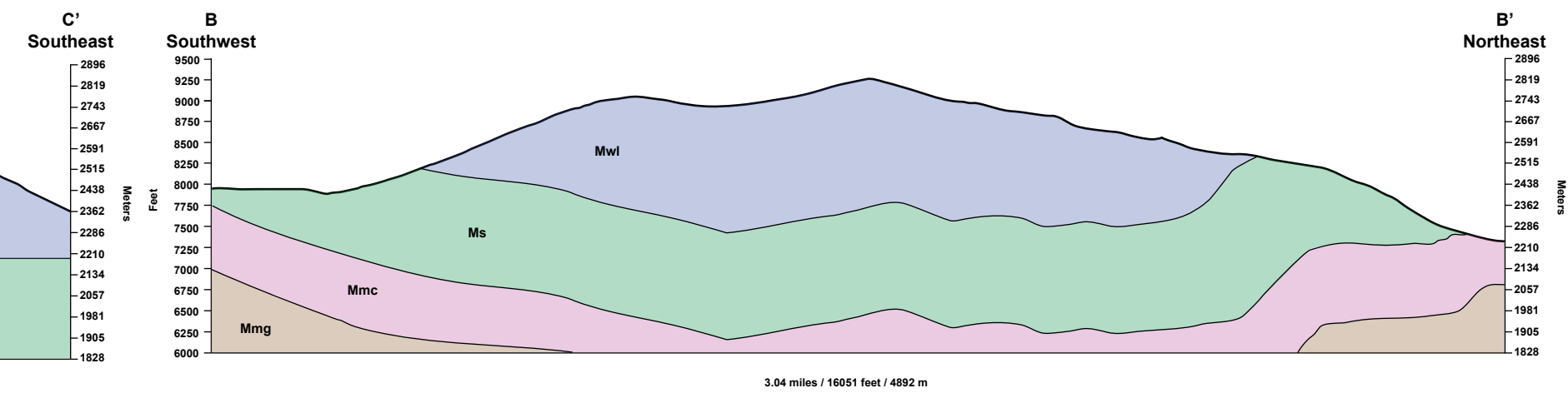
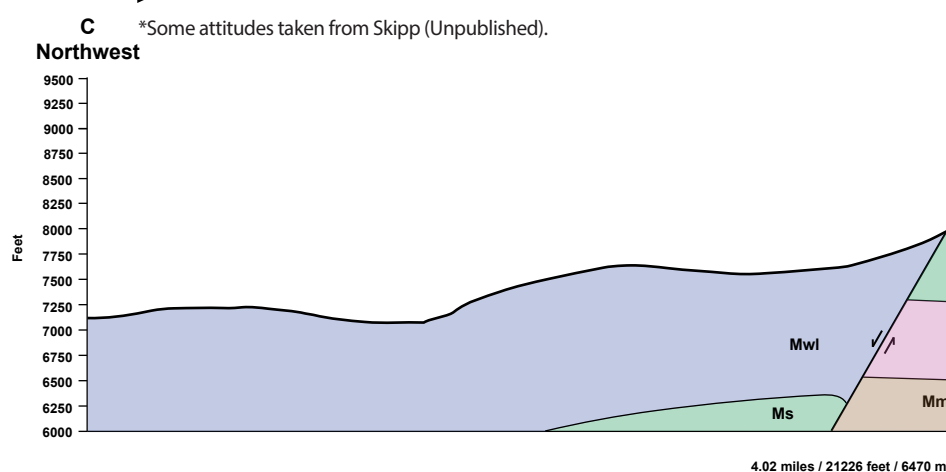
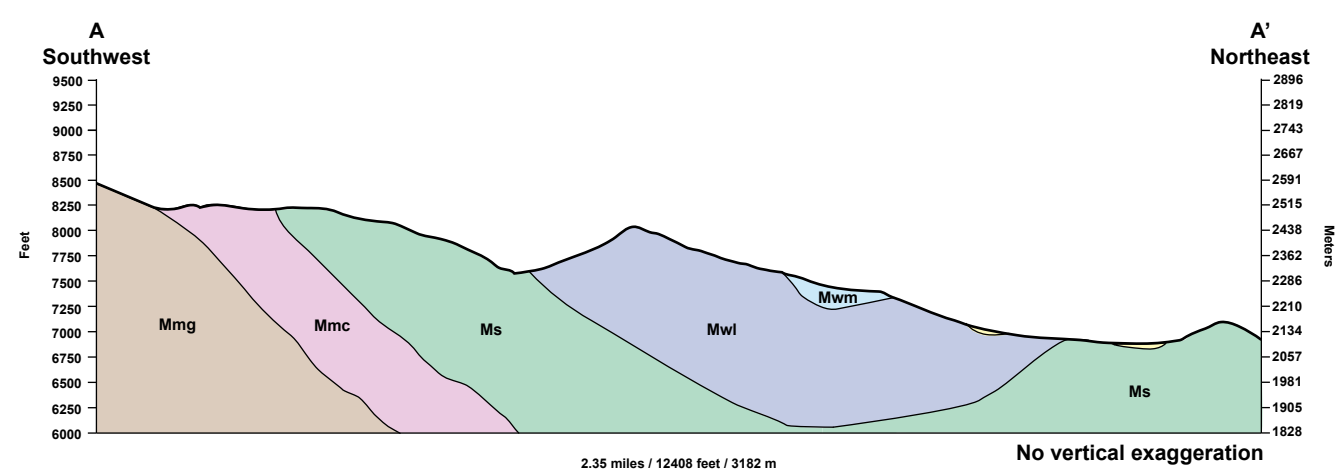
Ms Scott Peak Formation (Mississippian)—Dark to light-gray weathering limestone. Fossiliferous lime wackestone to lime packstone, with occasional beds of lime siltstone to lime (micritic) mudstone. Grains are dominantly silt-sized particles, but range from sand to clay-sized. Occasional beds contain nodular black chert, and rarely contain bedding-parallel chert. Massive, tabular beds with gradational contacts between range from 1 to 3 m in thickness; total unit thickness exceeds 400 m in the field area. Cliff-forming weathering pattern. Cross-bedding rare. Gradational contact below with Middle Canyon Formation marked by first appearance of massive limestone beds. Gradational contact above with Lower White Knob Limestone, marked by appearance of fetid fine-grained marker bed. Fossils include crinoid fragments (common; <5 mm diameter, often 1 mm diameter), rugose corals (occasional; typically <2 cm length, rarely 15+ cm length), brachiopods (common; <1 cm length typically; rarely 9+ cm length), and bryozoans (occasional; typically fenestrate, rarely fan; ~1 cm width). Beds rarely exhibit cleavage and are deformed into detachment folds (~55 m wavelength). Chronostratigraphically correlative to the Lower White Knob Limestone in the White Knob Mountains (Link et al., 1996).

Mmc Middle Canyon Formation (Mississippian)—Medium gray weathering to light gray and tan silty limestone to lime mudstone with interbedded tan and yellow siltstone particularly near base of formation. Beds are planar and range in thickness between 3 mm and 5 cm. Interbedded siltstone ranges between 1 mm and 5 mm thick. Total unit thickness in field area exceeds 230 m. Unit is slope forming, with interbedded siltstone weathering in a fissile manner. Sharp contact below with McGowan Creek Formation and gradational contact above with Scott Peak Formation marked by first appearance of massive limestone beds. Fossil content is primarily crinoid fragments (<5 mm diameter, often 1 mm diameter). Folding common at outcrop scale (~25 cm wavelength) (Link et al., 1996).

Mmg McGowan Creek Formation (Mississippian)—Dark gray weathering to dark brown, dark gray, and deep burgundy shale to argillaceous siltstone, with rare interbedded light-gray silty lime mudstone weathering tan to lavender in the middle to upper part of the section. Beds are planar with sharp contacts between beds and range in thickness between 1 mm and 1 cm; total unit thickness in the field area exceeds 1100 m thick. Fissile weathering behavior, with slope-forming weathering pattern. Upper part of section has common bioturbation of unknown species in lime section. Rare beds of increased thickness (~15 cm thick) consisting of sand-sized siliceous material uncommon but present in upper part of section. Contact below is not exposed in field area. Sharp contact above with Middle Canyon Formation, sparsely exposed in field area. Pencil cleavage is common throughout unit.

REFERENCES

- Link, P.K., Warren, I., Preacher, J.M., and Skipp, B., 1996, Stratigraphic analysis and interpretation of the Mississippian Copper Basin Group, McGowan Creek Formation, and White Knob Limestone, south-central Idaho, in Longman, M.W., Sonnenfeld, M.D., eds., Paleozoic systems of the Rocky Mountain Region: Rocky Mountain Section, SEPM (Society for Sedimentary Geology), p. 117-144.
- Skipp, B., and McIntyre, Unpublished field map of the Horse Basin quadrangle, Jerry Peak quadrangle, Herd Lake quadrangle, and The Paint Pot quadrangle, 1:24,000, Idaho.



*Some attitudes taken from Skipp (Unpublished).

COMPILED GEOLOGIC MAP ALONG A TRANSECT IN CUSTER AND BLAINE COUNTIES, CENTRAL IDAHO

Edwin C. Porter
 Idaho State University, Department of Geosciences
 Plate 2 in Porter, 2021 ISU M.S. Thesis

MAP UNITS

Quaternary surficial deposits		Paleozoic sedimentary rocks north of 44° N	
Q	Quaternary deposits, undivided	Mwu	Upper White Knob Limestone (Mississippian)
Eocene units		Mwm	Middle White Knob Limestone (Mississippian)
Tc	Challis Volcanic Group	Mwl	Lower White Knob Limestone (Mississippian)
Tsc	Smiley Creek conglomerate	Mu	Undifferentiated carbonate bank units (Mississippian)
Tei	Quartz monzonite of Summit Creek stock	PMu	Snaky Canyon Formation, Bluebird Mountain Formation, and Arco Hills Formation (Lower Permian to Upper Mississippian)
Cretaceous intrusive rocks		Msu	Surrett Canyon Formation (Upper Mississippian)
Kdcq	Biotite granodiorite of Deer Creek stock	Msc	South Creek Formation (Upper Mississippian)
Copper Basin Group		Ms	Scott Peak Formation (Mississippian)
Mcb	Undifferentiated Copper Basin Group (Mississippian)	Mmc	Middle Canyon Formation (Mississippian)
Mca	Muldoon Canyon Member of the Copper Basin Group (Mississippian)	Mmg	McGowan Creek Formation (Lower Mississippian)
Msm	Scorpion Mountain Member of the Copper Basin Group (Mississippian)	Dt	Three Forks Limestone (Devonian)
Mcd	Drummond Mine Limestone of the Copper Basin Group (Mississippian)	Dg	Grand View Dolomite (Devonian)
Mcl	Little Copper Formation of the Copper Basin Group (Mississippian)	Dj	Jefferson Dolomite (Devonian)
Paleozoic sedimentary rocks south of 44° N		Sl	Laketown Dolomite (Silurian)
Pdm	Dollarhide Formation (Lower Permian to Middle Pennsylvanian)	SOs	Saturday Mountain Formation (Ordovician)
Pww	Wood River Formation (Lower Permian to Middle Pennsylvanian)	Ok	Kinnikinic Quartzite (Ordovician)
Dm	Milligen Formation (Devonian)		
Dca	Unnamed argillite (Devonian)		
Dss	Unnamed siltstone (Devonian)		
St	Trail Creek Formation (Silurian)		
SOp	Upper Phi Kappa Formation (Silurian to Ordovician)		
Op	Phi Kappa Formation (Ordovician)		

SYMBOLS

	Bedding (with dip)		Normal fault
	Cleavage (with dip)		Thrust fault
	Overturned bedding (with dip)		Low-angle normal fault
	20CP14 Sample location		Strike-slip fault
	Anticline		Fault (Sense of slip undetermined)
	Syncline		Well-located
	Overturned anticline		Inferred
	Overturned syncline		Concealed
	X-X' Cross Section Transect		

SOURCES OF GEOLOGIC DATA

- 1 Burton, B., and Link, P.K., personal comm., Unpublished geologic map of Little Fall Creek and vicinity, Custer and Blaine counties, Idaho: Personal communication, scale 1:24,000.
- 2 Dover, J.H., 1983, Geologic map and sections of the central Pioneer Mountains, Blaine and Custer counties, central Idaho: U.S. Geological Survey, Miscellaneous Investigations Series Map I-1319, scale 1:48,000.
- 3 Hobbs, S.W., Hays, W.H., and McIntyre, D.H., 1991, Geologic map of the Bayhorse area, central Custer County, Idaho: U.S. Geological Survey, Miscellaneous Investigations Series Map I-1882, scale 1:62,500.
- 4 Link, P.K., and Rodgers, D.W., 1995, Geologic map of the northeastern part of the Hailey 1x2 quadrangle, south-central Idaho: US Geological Survey Bulletin 2064-B, plate 1, scale 1:100,000.
- 5 Mapel, W.J., Read, W.H., and Smith, R.K., 1965, Geologic map and sections of the Doublespring quadrangle, Custer and Lemhi counties, Idaho: U.S. Geological Survey, Geologic Quadrangle Map GQ-464, scale 1:62,500.
- 6 Messina, T.A., 1993, The geometry and kinematics of intra-thrust sheet decollement folding: Lost River Range, Idaho: [M.S. Thesis] Bethlehem, Lehigh University, 49 p.
- 7 Mapping from current study
- 8 Skipp, B., and McIntyre, unpublished, Geologic map of the Horse Basin quadrangle, Jerry Peak quadrangle, Herd Lake quadrangle, and The Paint Pot quadrangle, Custer county, Idaho: Personal communication, scale 1:24,000.
- 9 Skipp, B., Hall, W.E., and Link, P.K., 1994, Geologic map of the Mahoney Butte quadrangle, Blaine County, Idaho: U.S. Geological Survey, Geologic Quadrangle Map GQ-1742, scale 1:24,000.
- 10 Wilson, A.B., and Skipp, B., 1994, Geologic map of the eastern part of the Challis National Forest and vicinity, Idaho: U.S. Geological Survey, Miscellaneous Investigations Series Map I-2395, Scale 1:250,000.
- 11 Wilson, E., 1994, Demise of the Glide Mountain thrust fault, Pioneer Mountains, Blaine and Custer Counties, south central Idaho: [M.S. Thesis] Pocatello, Idaho State University, 188 p, 2 plates.

INDEX MAP SHOWING SOURCES OF GEOLOGIC DATA

